Oleosome

Natürliche Emulgatoren und deren Verhalten an lebensmittelrelevanten Grenzflächen

Kumulative Dissertation zur Erlangung des Grades „Doktor der Naturwissenschaften“

am

Fachbereich Chemie, Pharmazie und Geowissenschaften

der Johannes Gutenberg-Universität Mainz

von

Gustav Maximilian Waschatko

2013

Tag der mündlichen Prüfung: 13. Mai 2013

Dekan: Prof. Dr. Holger Frey

1. Berichterstatter: Prof. Dr. Thomas A. Vilgis

2. Berichterstatter: Prof. Dr. Gerald Gimpl

VORWORT

Die vorliegende Arbeit wurde in der Zeit vom Januar 2010 bis April 2013 in der Arbeitsgruppe von Prof. Dr. Thomas A. Vilgis am Max-Planck-Institut für Polymerforschung angefertigt. Die Ergebnisse der Arbeit, sowie deren Diskussion, sind in den folgenden drei Veröffentlichungen beschrieben:

1 Waschatko, G.; Schiedt, B.; Vilgis, T. A.; Junghans, A., Soybean Oleosomes Behavior at the Air–Water Interface. *The Journal of Physical Chemistry B* 2012, 116 (35), 10832-10841

2 Waschatko, G.; Junghans, A.; Vilgis, T. A., Soy milk oleosome behaviour at the air-water interface. *Faraday Discussion* 2012, 158 (0), 157-169.

3 Maurer, S.; Waschatko, G.; Schach, D.; Schiedt, B.; Dahl, J.; Weidner, T.; Bonn, M.; Vilgis, T. A., The role of intact oleosin for the stabilization of oleosomes. *The Journal of Physical Chemistry B, submitted*

Es folgt eine zusammenfassende Einleitung der drei Veröffentlichungen dieser kumulativen Dissertation. Es wird darin beschrieben und untersucht: das Vorkommen, die Extraktion, Zusammensetzung und das Verhalten von Soja-Oleosomen an lebensmittelrelevanten Grenzflächen. Dies wird in den Kontext anderer Lipidkörperchen und Emulgatoren gestellt. Es wurden gezielt Soja-Oleosome untersucht, welche zu den kleinsten Oleosome gehören und damit verbunden einen hohen Gehalt an Oleosinen aufweisen. Es konnte gezeigt werden, dass nach erfolgreicher Reinigung der Oleosome allein von diesen schirmförmigen Proteinen die Ladung, Aggregation und das Grenzflächenverhalten der Oleosome bestimmt wird, denn unerwünschte Allergene und Speicherproteine konnten effektiv entfernt werden. Die Oleosine sind mit der spektroskopisch nachgewiesenen α-helicalen Haarnadelstruktur (3) und längsten bekannten hydrophoben Peptidsequenz im Öl der Oleosome verankert. Der durchgeführte enzymatische Verdau der äußeren Oleosin-Domänen führte zum Verlust der sterischen und elektrostatischen Abschirmung der Lipide. (2, 3)

Die wichtigste Erkenntnis dieser Arbeit ist jedoch, dass Oleosome analog zu LDL-Partikeln an der Luft-Wasser-Grenzfläche aufplatzen und somit eine Möglichkeit zum schnellen Transport von grenzflächenaktiven Substanzen darstellen. Die nach dem Aufspreiten der Oleosomenkomponenten gebildete Monolage ist exemplarisch, um das faszinierende Verhalten von Phospholipiden, Triglyceriden und grenzflächenaktiven Proteinen, sowie deren Wechselwirkungen, zu untersuchen. Zweidimensionale Aggregat- und Domänbildungen in Abhängigkeit des pH-Wertes, der Ionenstärke und der Oberflächenbelegung sowie zeitabhängige Netzwerkbildung und Phasenseparation sind dabei innerhalb dieses Dreikomponentensystems gezielt steuerbar. (1)

Mainz, April 2013

INHALTSVERZEICHNIS

ABKÜRZUNGSVERZEICHNIS

Abkürzung	Bedeutung
BAM	Brewster Angle Microscope/ Brewster-Winkel-Mikroskop
CARS	Coherent anti-Stokes Raman (scattering) spectroscopy
DAG	Diacylglyceride
FA/ FS	Fatty acid/ Fettsäure
HDL	High-density lipoprotein (Lipoprotein hoher Dichte)
LDL	Low-density lipoprotein (Lipoprotein niedriger Dichte)
MAG	Monoacylglyceride
NBD-DPPE	1,2-dipalmitoyl-sn-glycero-3-phosphoethanolamine-N-(7-nitro-2-1,3-benzoxadiazol-4-yl)
pI	Isoelektrischer Punkt
PL	Phospholipide
TAG	Triacylglyceride

Drei- und Einbuchstabencodes der kanonischen Aminosäuren

Aminosäure	Dreibuchstabencode	Einbuchstabencode
Alanin	Ala	A
Arginin	Arg	R
Asparagin	Asn	N
Asparaginsäure	Asp	D
Cystein	Cys	C
Glutamin	Gln	Q
Glutaminsäure	Glu	E
Glycin	Gly	G
Histidin	His	H
Isoleucin	Ile	I
Leucin	Leu	L
Lysin	Lys	K
Methionin	Met	M
Phenylalanin	Phe	F
Prolin	Pro	P
Serin	Ser	S
Threonin	Thr	T
Tryptophan	Trp	W
Tyrosin	Tyr	Y
Valin	Val	V

1. ZUSAMMENFASSENDE EINLEITUNG

1.1. OLEOSOME ODER ÖLKÖRPERCHEN

Eukaryoten und Prokaryoten speichern Neutralfette (Triacylglyceride, TAG) in subzellulären Tröpfchen als Reservestoff. Am bekanntesten sind die Oleosome als Lipidreservoire der pflanzlichen Zellen. Sie treten insbesondere in den Samengeweben von Pflanzen auf. (*1*) Samen oder Saaten werden durch die Lebensmittelindustrie verarbeitet und von Menschen und Tieren konsumiert. Des Weiteren sind sie eine natürliche Emulsion und beinhalten neben Ölen extrahierbare Emulgatoren.

Oleosome sind 0,2 bis 2 µm große Öltröpfchen, welche von einer Monolage Phospholipide und speziellen Strukturproteinen, den sogenannten Oleosinen umgeben sind (Abb. 1). Oleosine sind alkalische 15-30 kDa große Proteine, die während der Samenbildung exprimiert werden und hauptverantwortlich für die Stabilität der Oleosome sind. Ihrer Faltung wegen werden sie in drei Domänen eingeteilt. Ihre mittlere hydrophobe Domäne formt ein Haarnadelmotiv verbunden durch einen Prolinknopf und ist in der TAG-Matrix verankert, die hydrophilen und geladenen N- und C-terminalen Bereiche ragen in die wässrige Phase und schirmen somit die Phospholipide nach außen hin ab. Nur die mittlere Domäne ist stark konserviert unter den verschiedenen Pflanzenspezies und mit etwa 70 Aminosäuren die längste bekannte hydrophobe Sequenz. (*2*)

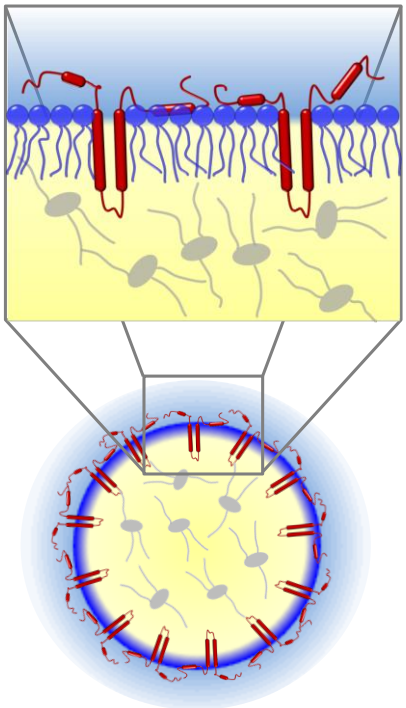

Abb. 1: Modell eines Oleosoms mit Vergrößerung der Grenzschicht aus Triacylglyceriden (grau), Phospholipiden (blau) und Oleosinen (rot), erstellt mit Denise Schach (siehe Publikation 2).

Diese mit Phospholipiden und Proteinen stabilisierten Öltröpfchen zeigen Gemeinsamkeiten und Unterschiede zu anderen natürlichen Lipidtröpfchen, welche u.a. in Milch, Eigelb oder Blut zu finden sind und erheblich zur Struktur von verarbeiteten Lebensmitteln beitragen.

Ziel dieser Doktorarbeit ist es, die außerordentliche Stabilität von Oleosomen als natürliche Emulsion, sowie deren Verhalten an „künstlichen“ nahrungsmittelrelevanten Grenzflächen (Schäume, Emulsionen, Sojaprodukte) zu verstehen. Dabei werden an diesem Dreikomponentensystems die Wechselwirkungen zwischen Triacylglyceriden (Fetten), Phospholipiden und den speziellen grenzflächenaktiven Proteinen namens Oleosinen untersucht. Diese Wechselwirkungen sind ladungsabhängig und werden deswegen über den pH-Wert und die Ionenstärke des umgebenden Mediums beeinflusst (Publikation 1). Eine weitere Triebkraft für die Zustandsänderungen der Komponenten und deren Wechselwirkungen ist die Grenzfläche selbst. Dabei spielen bekannte Phänomene der Einzelkomponenten, wie Phasenübergänge der Phospholipide und Denaturierung, Umfaltung oder Aggregation von Proteinen an der Grenzfläche eine Rolle. Die dritte angewendete Manipulation der Oleosomen-Komponenten ist der Verdau, genauer die Hydrolyse durch Enzyme. Insbesondere die Abtrennung der äußeren Proteinschicht der Oleosomen verändert ihre Stabilität, Ladung und ihr Grenzflächenverhalten und zeigt die Wechselwirkungen zwischen Proteinen und Lipiden auf (Publikation 2 und 2). Dies hat allgemeine Relevanz für das Verständnis von Emulsionen und Schäumen in Lebensmitteln, denn diese werden in den meisten Fällen durch Phospholipide und Proteine stabilisiert.

1.2. BIOLOGISCHE BEDEUTUNG VON OLEOSOMEN IN PFLANZEN

Oleosome sind die einzigartigen subzellulären Lipidreservoire aller Samen. Innerhalb eines Samens sind sie sowohl in den Keimblättern (Kotyledonen) als auch in der Embryonalachse zu finden. (*3*) Außerhalb von Samen treten Oleosome noch in dem fettreichen Fruchtfleisch von z.B. Oliven oder Avocados auf. Dort enthalten sie jedoch weniger bis keine Oleosine und sind größer. (*4*) Dies führte zu der Annahme, dass die Oleosinkonzentration umgekehrt proportional zur Größe der Oleosome ist. (*5*) Außerdem sind Oleosome Bestandteil der Tapetosome im Tapetum und werden dort nach dem gleichen Mechanismus, wie in dem sich entwickelnden Embryo (1.2.1 Samenbildung), am rauen ER synthetisiert. (*6*)

Bei einem hohen Ölgehalt eines Samens steigt auch der Anteil der Oleosine am Gesamtproteingehalt des Samens. *Arabidopsis thaliana* Samen enthalten mehr als 40% Öl und deshalb sind auch 10% ihrer Proteine Oleosine. (*2*)

Von der Samenbildung und Samenreifung über die anschließende Keimruhe (Dormanz) bis zur Keimung bleibt der geringe Durchmesser (d) der Oleosome und somit im Verhältnis zum Volumen die große Kugeloberfläche ($A_O = \pi d^2$) erhalten (und somit eine größere Oberfläche pro TAG-Einheit). Es kommt kaum zur Koaleszenz in dieser Zeit. In welcher Größe Oleosome im Samen gebildet werden wird über das Verhältnis von Öl zu Oleosinen (Matrix/ Monolage an der Oberfläche) kontrolliert, wobei ein höheres Öl zu Oleosin Verhältnis zu größeren Oleosomen führt (*7*). Wird die gleiche Masse von Oleosinen im Samen synthetisiert, führt eine geringere Ölmenge zu kleinen und eine große Ölmenge zu großen Oleosomen. (*8*) Zusätzlich verursacht eine Reduktion der Oleosin-Expression durch RNA-Interferenz (RNA-Silencing) unphysiologische, größere Oleosome. (*9, 10*)

Einen Größenvergleich verschiedener Ölsaaten und ihre prozentuale chemische Zusammensetzung zeigt Tab. 1. Besonders große Oleosome sind in Erdnuss, Sesam und Kakaobohnen zu finden. Die Oleosome aus Sojabohnen zählen mit zu den kleinsten (*11*) unter den Ölsaaten. Ihre Größe und chemische Zusammensetzung wird genauer in Kapitel 1.5 erläutert.

Tab. 1: Mittlerer Durchmesser in µm und chemische Zusammensetzung in Prozent (w/w) von Oleosomen isoliert aus den Samen verschiedener Pflanzen:

	Soja (siehe 1.5)	Raps (*5*)	Senf (*5*)	Baum wolle (*5*)	Lein samen (*5*)	Mais (*5*)	Erd nuss (*5*)	Sesam (*5*)	Mandel (*12*)	Kakao bohne (*13*)
Mittlerer Durchmesser in µm	0,26		0,73	0,97	1,34	1,45	1,95	2,00	2,60	≤ 7 µm
Neutralfette in % (w/w)		94,21	94,64	96,99	97,65	97,58	98,17	97,37	94,40	
Proteine in % (w/w)	4,40	3,46	3,25	1,70	1,34	1,43	0,94	0,59	1,40	
PL in % (w/w)		1,97	1,6	1,18	0,90	0,91	0,80	0,57	1,00	
Freie Fettsäuren in % (w/w)		0,36	0,17	0,13	0,11	0,09	0,09	0,13	0,80	

Oleosome liegen im Cytoplasma der Samenzellen vor (Abb. 2). Sie zeigen eine Affinität zum Plasmalemma, Proteinkörpern (protein bodies) und dem endoplasmatischen Retikulum. (*14*) Ihre intrazelluläre Moblisierung und die Verbindung zu den katabolischen Organellen (Peroxisomen, Glyoxysomen) bei der Keimung und der anschließenden Umwandlung in den Sämling ist nur bruchstückhaft verstanden (siehe Kap. 1.2.2).

Besonders die räumliche Nähe zu den mit Speicherproteinen (Glycinin und β-Conglycinin) gefüllten Proteinkörpern oder Proteinspeichervakuolen (siehe Abb. 2) erhöht den Aufwand bei der Oleosomenreinigung, da diese durch die Zentrifugationsschritte abgetrennt werden müssen.

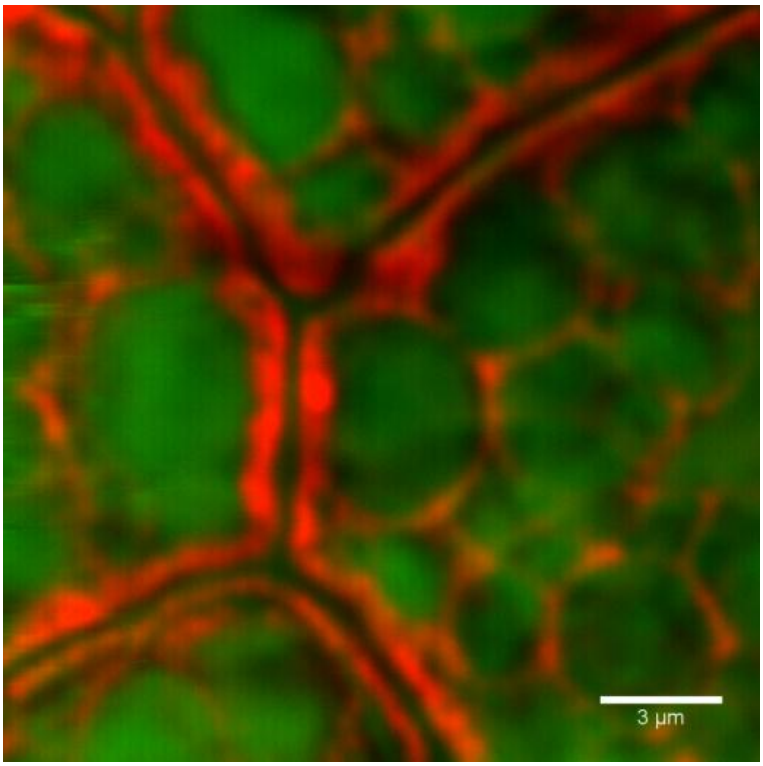

Abb. 2: Visualisierung von Oleosomen (rot, 2880 cm^{-1}) und Proteinkörper (grün, 3000 cm^{-1}) durch CARS (Coherent anti-Stokes Raman scattering spectroscopy) Mikroskopie in Sojabohnenschnitten. Die Aufnahme wurde von Nils Billecke und Henriette Jaurich mit dem Leica TCS CARS Mikroskop der Arbeitsgruppe Sapun Parekh am MPI für Polymerforschung aufgenommen.

1.2.1. SAMENBILDUNG

Während der Samenreifung werden TAG im ER synthetisiert und innerhalb der ER-Membran gesammelt. Dies führt zum Ausknospen (Abb. 3) der neuen Oleosome aus der ER-Membran (*15*), welche durch die Einlagerung von Oleosinen an deren Oberfläche stabilisiert werden. Die Adressierung der am Ribosom synthetisierten Oleosine erfolgt ohne spezielle (N-terminale) Signalsequenz. Allein die hohe Hydrophobizität der langen mittleren Aminosäurensequenz ist entscheidend für die Adressierung. Auch ein Austausch der Proline des Prolinknopf-Motivs verändert nicht die Adressierung der Oleosine in die ER-Membran. (*16*)

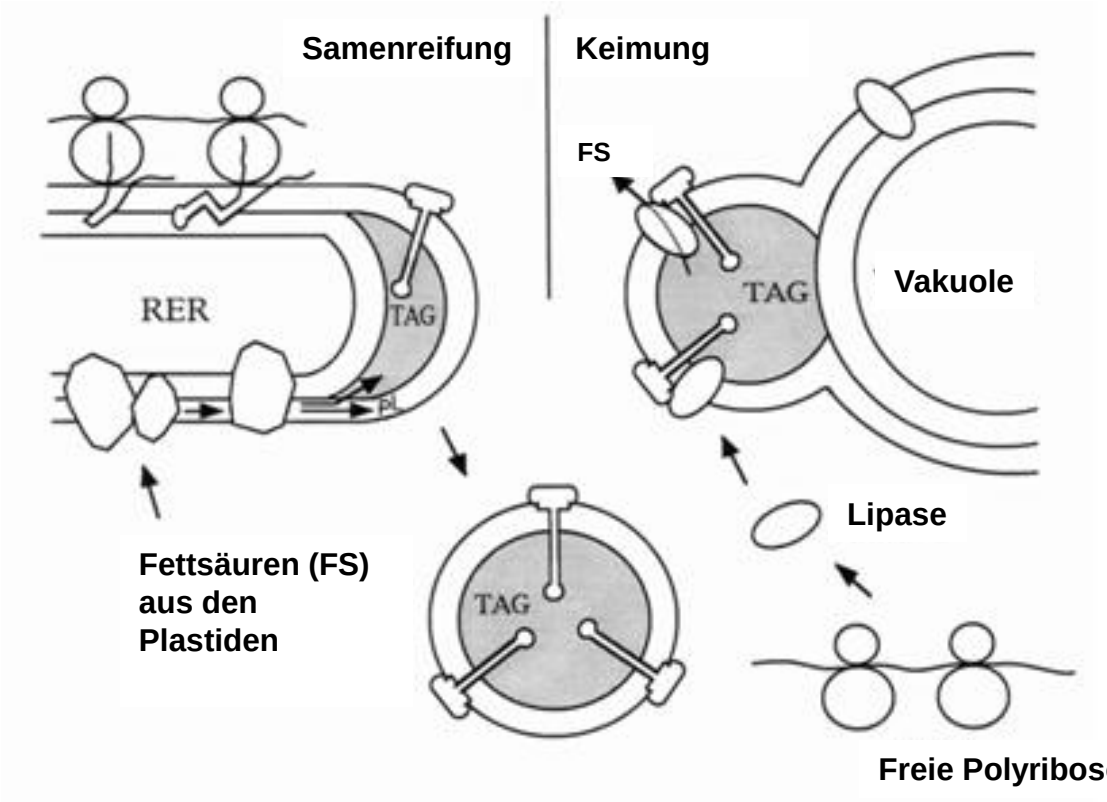

Abb. 3: Modell nach Huang (*15*) für die Synthese und den Abbau von Oleosomen wahrend der Samenreifung bzw. der Keimung. RER, raues Endoplasmatisches Retikulum; TAG, Triacylglyceride; FS, Fettsäuren

Das in Abb. 3 gezeigte biologische Synthesemodell der Oleosome hat Ähnlichkeiten zur technischen Membranemulgierung. Bei dieser wird die dispergierte Phase durch eine Membran mit definierter Porengröße in die fließende kontinuierliche Phase gepresst. Die Größe des entstehenden Tröpfchens ist dabei auch von dem verwendeten Emulgator abhängig. (*17*)

1.2.2. KEIMUNG

Nach der Quellung der Sojabohne werden Lipasen aktiviert, welche die TAG an der Öl-Wasser Grenzfläche der Oleosome verdauen um somit Energie für den wachsenden Keimling zu liefern (Abb. 3). In diesem Stadium ist die Pflanze heterotroph und nicht zur Photosynthese fähig.

Abb. 4 zeigt die bereits bekannten Lipasen aus *Arabidopsis thaliana*:
SDP1 (Sugar-Dependent1) und SDP1-LIKE präferieren die Hydrolyse von TAG in DAG und MAG (*18*). Die DGL (DAG-Lipase) hydrolysiert anschließend die DAG in MAG und Fettsäuren und die MGL (MAG-Lipase) schließlich die MAG in Fettsäuren und Glycerin. Nach der Hydrolyse durch die Lipasen müssen die Fettsäuren vom Oleosom zum Peroxisom transportiert werden. (*19*) Das Peroxisom ist das einzige Organell in der Pflanzenzelle in der die β-Oxidation der Fettsäuren stattfindet. (*20*) Die β-Oxidation ist der biochemische

Mechanismus zum Abbau von Fettsäuren (Katabolismus). Zur Aktivierung werden die Fettsäuren mit Coenzym-A verknüpft, dabei bildet sich der energiereiche Thioester Acyl-CoA. In welcher Form (Fettsäure oder Acyl-CoA) die Fettsäuregruppe in das Peroxisom importiert wird ist noch unklar. (*19*) Gesichert ist der physische Kontakt zwischen Oleosomen und Peroxisomen durch Mikroskopie Studien, welche jedoch auch Kontakt zur ER- und Tonoplastenmembran (Vakuole) zeigen. (*20*) Untersucht wird die Beteiligung von Fettsäuretransporten und ob eine direkte Assoziation der Organellmembranen notwendig ist. (*19*)

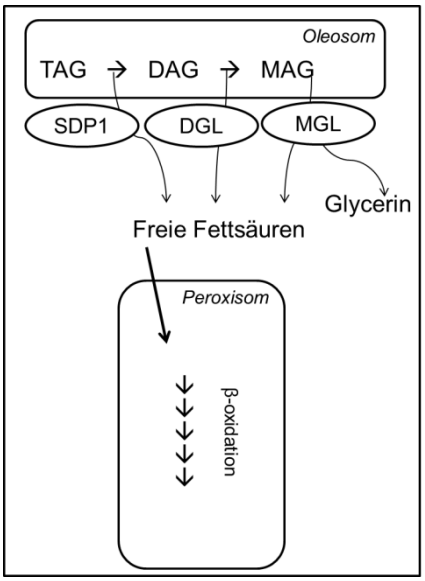

Abb. 4: Lipolyse, Metabolismus und Transport von TAG aus Oleosomen. TAG wird an der Öl-Wasser-Grenzfläche der Oleosome zu freien Fettsäuren und Glycerol hydrolysiert durch verschiedene Lipasen (SDP1=TAG-Lipase, DGL=DAG-Lipase, MGL= MAG-Lipase). Die Fettsäuren werden über Transporterproteine entweder als Fettsäuren oder Acyl-CoA in das Peroxisom transportiert (angelehnt an (*19*)).

1.3. GEMEINSAMKEITEN UND UNTERSCHIEDE ZU ANDEREN LIPIDSPEICHERSTRUKTUREN

Lipidtröpfchen wurden lange Zeit als metabolisch relativ inert angesehen. Neuere Untersuchungen zeigen jedoch die vielfältige Dynamik und Funktion dieser „Organellen“, mit einem Durchmesser von 1-100 µm, bestehend aus Neutralfetten, polaren Lipiden und speziellen Proteinen. Diese intrazellulären Lipidtröpfchen (Abb. 5) haben einen ähnlichen Aufbau wie die viel kleineren und bekannteren Lipoproteine (z.B. LDL, Tab. 2), welche sekretiert und mit dem Blutplasma transportiert werden. (*21*)

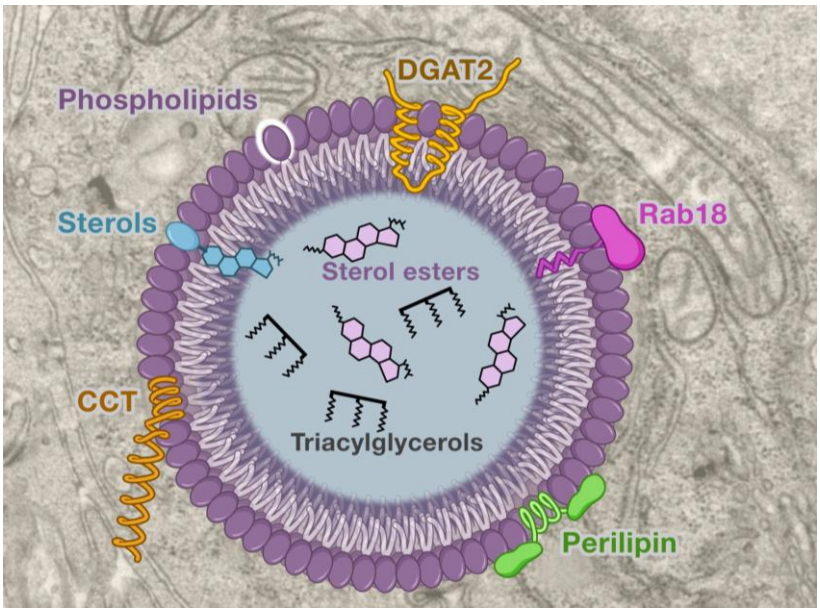

Abb. 5: Die strukturellen Eigenschaften eines intrazellulären Lipid Tröpfchens in tierischen Zellen, z.B. Adipozyten (*21*). Die unpolaren Lipide (TAG und Sterol Ester) bilden den Kern, die amphiphilen Phospholipide und Cholesterol bilden die äußere Monolage. An der Oberfläche des Lipid Tröpfchens interagieren lokal verschieden Proteine (z.B. Perilipin, Rab18) mit der äußeren Monolage aus Phospholipiden und Cholesterol.

Die Proteine auf der Oberfläche der Lipidspeicherstrukturen zeigen eine große Vielfalt in ihrer Faltung, Funktion und Wechselwirkungen mit den Lipiden. Sie verändern nicht nur die Mobilität der Lipide an der Grenzfläche und Verhindern die Koaleszenz, sondern sind auch Schnittstelle (Rezeptor, Anker für oder Schutz vor Lipasen) für die Interaktion mit anderen Organellen und Enzymen des intrazellulären Lipidmetabolismus. Eine wichtige Funktion der Lipidkörper-assoziierten Proteine ist die Determinierung der Größe (siehe 1.2) der Lipidtröpfchen. Entweder über ihre Struktur wie bei den Oleosinen und/ oder durch Eingriff in den Metabolismus, die hormonelle Regulation und den Transport der Lipide wie bei den Perilipinen (*22*). In den bereits bekannten Signaltransduktionskaskaden ändern Perilipine beispielsweise durch Phosphorylierung nach einer Hormonrezeptoraktivierung ihre Konformation. (*23*) Diese Konformationsänderung führt zu einem besseren Zugang von

Lipasen. Eine sinnvolle Verschaltung von Strukturgebung (Größe und Grenzfläche des Lipidtröpfchens) durch die Lipid-assoziierten Proteine und Interaktionen mit dem Stoffwechsels (Enzyme, Organellen) ist dabei auch bei den Oleosinen anzunehmen. (*21*)

Wie vorher erwähnt, haben Oleosine die längste bekannte hydrophobe Aminosäurensequenz, aufgrund derer sie in der TAG Matrix verankert sind. Diese stabile Verankerung im Öl fehlt anderen mit Lipidkörpern assoziierten Proteinen, wie den Apolipoproteinen (Tab. 2) oder den Perilipinen (Abb. 5). Für ihre Funktion, die Abschirmung der Phospholipide, bedecken die Oleosine die gesamte Oberfläche eines Oleosoms, dies ist wiederum ein Alleinstellungsmerkmal der Oleosome und Oleosine.

Bekannte Lipidspeicherstrukturen, die von Zellen sekretiert werden sind die Lipoproteine (HDL, LDL, Chylomikronen) und Milchfettkügelchen („Milk fat globule“). Sowohl LDLs als auch die Milchfettkügelchen haben eine Bedeutung für lebensmittelrelevante Grenzflächen und erfahren Umwandlungen an ihnen. Die Bestandteile der LDLs haben beispielsweise den größten Beitrag zur guten Emulgiereigenschaft von Eigelb (24). Tab. 2 vergleicht die Größe, den Aufbau der Außenhülle und die Lokalisation der enthaltenen Proteine von Oleosomen, Milchfettkügelchen und LDL:

Tab. 2: Vergleich des Aufbaus lebensmittelrelevanter Fetttröpfchen gefüllt mit Neutralfetten

System	Größe	Aufbau Außenhülle	Proteinlokalisation
Oleosom (*11, 13*)	0,2 – 2 µm (in Kakaobohnen bis zu 7 µm)	Monolage aus PL	in der TAG-Matrix verankert und die gesamte Oberfläche bedeckend
Milchfettkügelchen (*25*)	4 – 5 µm	von innen nach außen: 1.) Monolage aus Phospholipiden 2.) eine mit Cytoplasma gefüllte Zwischenenphase 3.) Doppelschicht aus polaren Lipiden (PL mit Sphingomyelinen + Cholesterol)	 1.) vereinzelte in der PL-Monolage 2.) lösliche im Cytoplasmazwischenraum 3.) alle drei Schichten durchziehende
LDL (Low Density Lipoprotein) (*26*)	17 – 60 nm	Monolage aus Phospholipiden und Cholesterol	wenige lange Proteinketten durchziehen die äußere Monolage

Milchfettkügelchen sind 4 bis 5 µm groß und bestehen aus einem Kern aus Milchfett, umgeben von einer Monolage und einer Doppellage aus Phospholipiden und Cholesterol, welche vereinzelt von Proteinen durchzogen wird (*25*).

LDL-Partikel sind viel kleiner als Milchfettkügelchen und Oleosome und haben deswegen auch eine größere Grenzfläche und höheren Proteinanteil. Im Eigelb sind sie 17-60 nm groß, bestehen zu 11-17% aus Protein und zu 83-89% aus Lipiden (im einzelnen 69% TAG, 27% Phospholipide und 4% Cholesterol und Cholesterolester). (*26*) Ihre Proteine sind die sogenannten Apolipoproteine (z.B. das Apolipoprotein B (UniProtKB: Q197x2) in Eigelb, mit 4631 Aminosäuren), welche als einzelne lange Proteinkette die Oberfläche des LDL-Partikels durchziehen. Dies schränkt die Bewegungsfreiheit der Phospholipide an der Oberfläche ein und stabilisiert somit die gesamte Struktur. (*27*) In mehreren Arbeiten (*26*, *28*) wurde das Verhalten von LDL-Partikeln an der Luft-Wasser-Grenzfläche einer Filmwaage untersucht und Phasenübergänge in Isothermen des Gesamtsystem systematisch den Einzelkomponenten zugeordnet. Diese Herangehensweise und die Interpretationen dieser Daten konnten in vielen Fällen auf das Verhalten der Oleosome übertragen werden und rechtfertigen die LDL-Partikel trotz ihrer unterschiedlichen Größe und ihrer teilweise unterschiedlichen Komponenten (Cholesterol, Cholesterolester, andere Proteine) als Vergleichssystem zu den Oleosomen.

1.4. INDUSTRIELLE BEDEUTUNG VON OLEOSOMEN

Oleosome und ihre chemischen Komponenten sind schon immer Bestandteil der menschlichen Nahrung, anfänglich als Rohkost (Nüsse, Saaten, Samen) und später als Bestandteil von prozessierten Lebensmitteln. Sie sind einerseits die Quelle für pflanzliche Öle und den Emulgator Lecithin und deswegen für die Ölextraktion von Bedeutung. Andererseits bilden sie den Fettanteil von vielen prozessierten Lebensmitteln wie pflanzlichen Drinks, Mousse oder Jogurts oder im asiatischen Raum Tofuprodukten und Yuba.

Parallel zu dieser Entwicklung hat sich die Forschung an Oleosomen verändert: von systembiologischen und botanischen Fragestellungen (*2*) hin zu industrieller und anwendungsbezogener Forschung (*11*). Dabei ist insbesondere ihre naturgegebene Langzeitstabilität und die Schutzfunktion für ihre natürlichen Inhaltstoffe (α-Tocopherol und ungesättigte Fettsäuren (*29*)) und zugeführte Aroma- und Duftstoffe (*30*) von großem Interesse für die Kosmetik (*31*) und Lebensmittelindustrie (*11*).

1.4.1. LEBENSMITTEL, ERNÄHRUNG UND MEDIZIN

Oleosomen kommen in Saaten, Bohnen, Nüssen, Mais, Reis, Sesam und vielen weiteren natürlichen Rohprodukten vor und sind für die Agrarwirtschaft von großer Bedeutung.

Da eine Diät aus diesen pflanzlichen Produkten bei bestimmten Krankheitsbildern, wie Herz-Kreislauf-Erkrankungen (*32*), empfohlen wird und bei Laktoseintoleranz oder Milchallergien pflanzlicher Ersatz von Milchprodukten vertrieben wird, betonen viele der neueren Arbeiten über Oleosome ihren ernährungsphysiologischen und gesundheitlichen Aspekt. Hierbei sind besonders das Verhalten der Oleosome im menschlichen Verdauungstrakt (*33, 34*) und die daraus resultierende Verfügbarkeit essentieller Fettsäuren und Mikronährstoffe wie α-Tocopherol (*29*) interessant. Ein Einsatz von Oleosomen zum gezielten Transport und Freisetzung lipophiler Duft- und Aromastoffe, wie z.B. den Terpenen Carvon, Limonen oder Menthol scheint möglich. (*30*) Genauso wie die Nutzung der Oleosome zur pflanzlichen Expression großer Mengen rekombinanter Proteine mit therapeutischem Nutzen (Impfstoffe oder Antikörper) als Oleosin-Fusionsproteine Bestandteil der Forschung ist. (*35*) Hierbei ist die zu anderen Proteinreinigungen, wie Chromatographie oder Elektrophorese, vergleichsweise einfache und theoretisch in größerem Maßstab (*36*) durchführbare Extraktion der Oleosome durch Zentrifugation von großem Vorteil. Auch für diese Technologie ist eine vollständige Abtrennung der Speicherproteine und anderer Allergene während dem Extraktionsverfahren (Kap. 1.5.1) essentiell.

1.4.2. WÄSSRIGE ÖLGEWINNUNG

Einen großen Beitrag zur Optimierung der Oleosomenextraktion aus Soja haben Arbeiten erbracht, welche sich mit der „wässrigen Ölgewinnung“ beschäftigen. Diese sind dadurch motiviert, dass insbesondere Sojaöl größtenteils mit Hexan extrahiert wird. Diese Methode liefert Ausbeuten von über 95%, jedoch mit einem erheblichen Sicherheitsrisiko für das Personal aufgrund der leichten Entflammbarkeit und Toxizität des Hexans. Auch aus Gründen des Umweltschutzes (Hexan führt bei Reaktion mit Stickoxiden zur Bildung von Ozon) und der Nachhaltigkeit (Hexan ist ein Erdöl Destillat) wird nach alternativen Ölextraktionsmethoden gesucht. (*37*)

Die Verfahren zur wässrigen Ölgewinnung enthalten auch immer Zentrifugationsschritte zur Oleosomenextraktion. Auch Enzyme werden hierbei eingesetzt um die Ölausbeute durch eine bessere Freisetzung der Oleosome (*38*) und schließlich des Öls zu erreichen. Die Ausbeute beträgt dabei bis zu 90 % (*39*). Das bei den Zentrifugationsschritten eingesetzte zuckerhaltige Medium erhöht die Dichtedifferenz zwischen Oleosomen und wässriger Phase und führt somit zu einer besseren Ausbildung der „Rahmschicht“ (Abb. 6). (*40*) Außerdem kann die Saccharose in Prozessen mit größerem Maßstab (*36*) recycelt werden (*41*).

1.4.3. SOJAPRODUKTE

Beim Herstellungsprozess von Sojaprodukten wie Sojamilch und Tofu werden die Prozessparameter festgelegt, welche auf die Oleosome bei der Herstellung wirken. Diese sind Einflüsse durch Scherung, Temperatur, pH-Wert, Ionenstärke und Wechselwirkungen mit anderen Inhaltsstoffen wie z.B. andere Proteine (Speicherproteine), Zucker oder Calciumionen. Salze wie Natriumchlorid können Ladungen an der Oberfläche der Oleosome abschirmen (*11*).

In Soja Drinks wird oft Zucker und Calcium als Tricalciumphosphat oder in Form der calciumhaltigen Meeresalge *Lithothamnium calcareum* zugeben. Außerdem wird bei dessen Herstellung mit hohen Scherkräften („Zerkleinern und Mixen“) und Temperaturen („Pasteurisieren“) gearbeitet. Letzteres dient der Inaktivierung von Trypsininhibitoren und Lipoxygenasen.(*42*) Trypsininhibitoren hemmen die Proteolyse im Verdauungstrakt. (*42*) Lipoxygenasen katalysieren die Hydroperoxidbildung durch Sauerstoff mit den ungesättigten Fettsäuren wie Linol- und Linolensäure, welche in der Folge zu geschmacklich teilweise unterwünschten Aldehyden und Ketonen (z.B. n-Hexanal oder 2,4-Decadienal) zerfallen. (*43*)

Tofu wird aus Sojamilch mittels Fällung mit Calciumsulfat oder Magnesiumsulfat („Nigari“) bei 65 °C hergestellt. (*42*) Das Endprodukt kann als Gelnetzwerk aus Speicherproteinen angesehen werden, in welches die Oleosome eingebaut sind. (*44*) Ein anderes sojabasiertes Lebensmittel bei dem Oleosome in ein Proteinnetzwerk eingebaut werden ist die Yuba. (*45*)

Sie ist die Haut, welche sich beim Erhitzen der Sojamilch an der der Luft-Wasser-Grenzfläche bildet.

Welche Rolle Oleosome bei der Stabilisierung von Grenzflächen, in Schäumen („Soja-Sahne“) oder Emulsionen („Mayonnaise“) spielen ist noch weitestgehend unbekannt. Diese Arbeit soll auch in Hinblick auf die beschriebenen Produkte zu einem besseren Verständnis des Verhaltens und der Funktion von Oleosomen in Lebensmitteln führen.

1.5. ZUSAMMENFASSUNG DER CHEMISCHEN UND PHYSIKALISCHEN PARAMETER

1.5.1. EXTRAKTIONSVERFAHREN UND DURCHMESSER

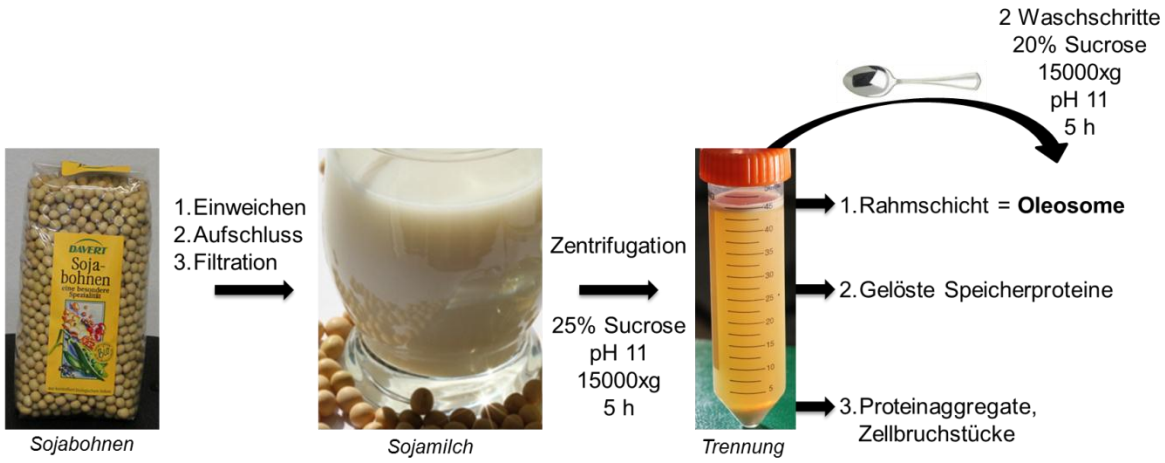

Abb. 6: Bildliche Darstellung des Extraktionsverfahrens der Oleosome aus Sojabohnen.

Die Oleosome werden in mehreren Zentrifugationsschritten aus der rohen und gefilterten Sojamilch isoliert. (*27*) Dabei wird die Aufrahmung der Oleosome beschleunigt und diese dabei von den restlichen Bestandteilen der rohen Sojamilch getrennt. Insbesondere der pH-Wert der rohen Sojamilch und des in den Waschschritten benutzten Mediums hat einen großen Einfluss auf den Erfolg der Abtrennung der Speicherproteine. (*46*) Bei pH 11 und zwei Waschschritten wird eine gute Trennung der Oleosome von den Speicherproteinen Glycinin und β-conglycinin und anderen Allergenen wie der Thiolprotease „Gly m Bd 30K“ (*47*) erreicht. (*46*) Im letzten Schritt werden die Oleosome dann dialysiert um die Sucrose zu entfernen. Die Saccharose wurde vorher in den Waschlösungen und der Sojamilch zugesetzt zur Stabilisierung der Oleosomen während der langen Zentrifugationsschritte. Durch die Erhöhung der Dichtedifferenz zwischen wässriger Phase und Oleosome, führt die Sucrose zu einer beschleunigten Aufrahmung und einer besseren Ausbildung der Rahmschicht. (*40*)

Andere Forschergruppen (*11, 48*) benutzen gepufferte Medien ohne Saccharose bei der Extraktion von Oleosomen, diese ist jedoch dann nur noch unter Benutzung von Ultrazentrifugen (30 000 rpm) möglich.

Extraktionen bei neutralerem pH-Wert (pH 7,5) benötigen zusätzliche Reinigungsschritte (*49*) mit Detergenzien (z.B. Tween-20), chaotropen Verbindungen (Harnstoff) und Lösemitteln (Hexan, „Ausschütteln“ des freien Öls) um eine ähnliche gute Abtrennung von den Speicherproteinen zu erreichen wie die gezeigte Extraktion in drei Schritten bei pH 11 (Abb. 6).

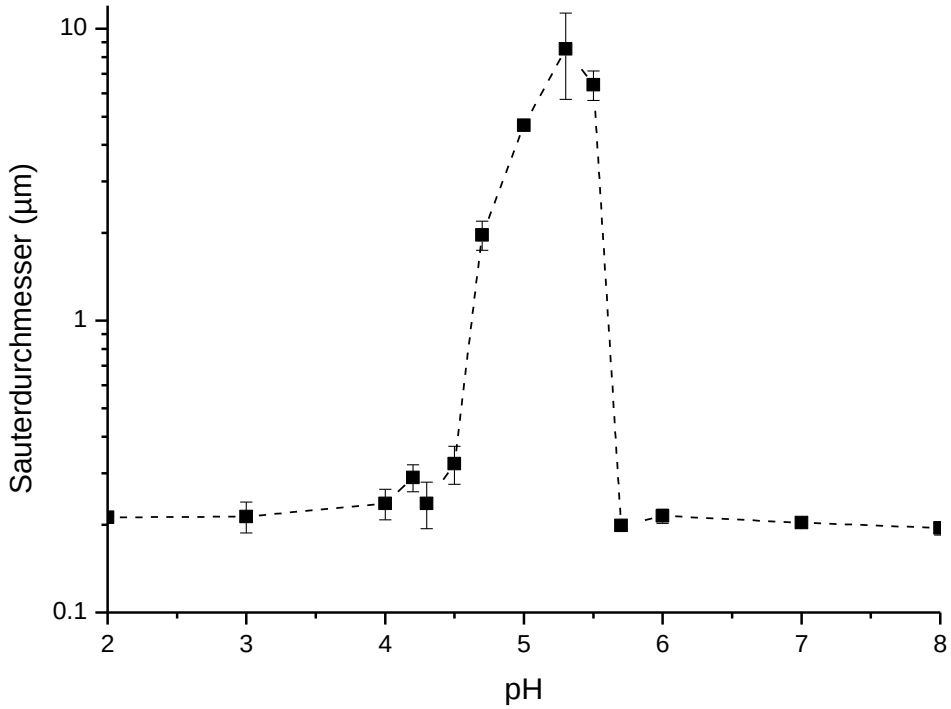

Abb. 7: Sauterdurchmessers der Oleosome in Abhängigkeit vom pH-Wert. Gemessen von Sania Maurer im AK Schuchmann am KIT mittels Laserbeugung (Horiba LA-950, Retsch Technology, Deutschland).

Die Größe der Oleosome ist abhängig vom pH-Wert und beträgt wie
Abb. 7 zeigt außerhalb des isoelektrischen Punktes (pH 4,7 bis 5,5) 0,19-0,32 µm. Zum isoelektrischen Punkt hin nimmt die Polydispersität der Oleosome durch Aggregation zu. Die Aggregation ist reversibel. Eine gleichzeitige Koaleszenz wurde nicht beobachtet. Andere Partikelgrößenbestimmungen von Soja-Oleosomen (*11*) zeigen einen Aggregationsbereich von pH 3 bis 6, was auf eine Verbreiterung des isoelektrischen Punktes aufgrund unvollständiger Abtrennung der Speicherproteine hindeutet. Die genaue Größenbestimmung der Oleosome über einen großen Bereich (Nanometer bis Millimeter) ist technisch schwierig und bedarf unterschiedlicher Methoden (Laserbeugung, Mikroskopie), welche genauer in der Doktorarbeit von Sania Maurer (MPI für Polymerforschung, Mainz) beleuchtet werden.

1.5.2. PROTEINANALYTIK

Der Erfolg der Reinigung (siehe Publikation 1 (*27*)) und des Verdaus (siehe Publikation 2 (*50*), 2 und Kap. 1.9) wurde über Commassie gefärbte SDS-PAGE Gele überprüft (Abb. 8). Die Untereinheiten der Speicherproteine, die saure (AS) und basische (BS) Untereinheit des Glycinins und die α-, α'-, β-Untereinheiten des β-Conglycinins konnten durch die Zentrifugationsschritte bei pH 11 erfolgreich abgetrennt werden. Auch die unerwünschte Lipoxygenase, welche ungesättigte Fettsäuren oxidiert und das Allergen „Gly m Bd 30K"

(*47*) wurden entfernt. Nach der Reinigung (Kap. 1.5.1) sind bei der verwendeten Oleosomenkonzentration (40 µg) deutliche Banden von drei Proteinen zu sehen, die im Größenvergleich den Soja-Oleosinen (P29530, P29531, C2VHQ8, C6SZ13) zugeordnet werden konnten.

Das für den Verdau der Oleosome verwendete Trypsin führt zu Oleosinfragmenten kleiner als 8 kDa. Trypsin hat theoretische Schnittstellen nach den basischen Aminosäuren Arginin und Lysin. (*51*)

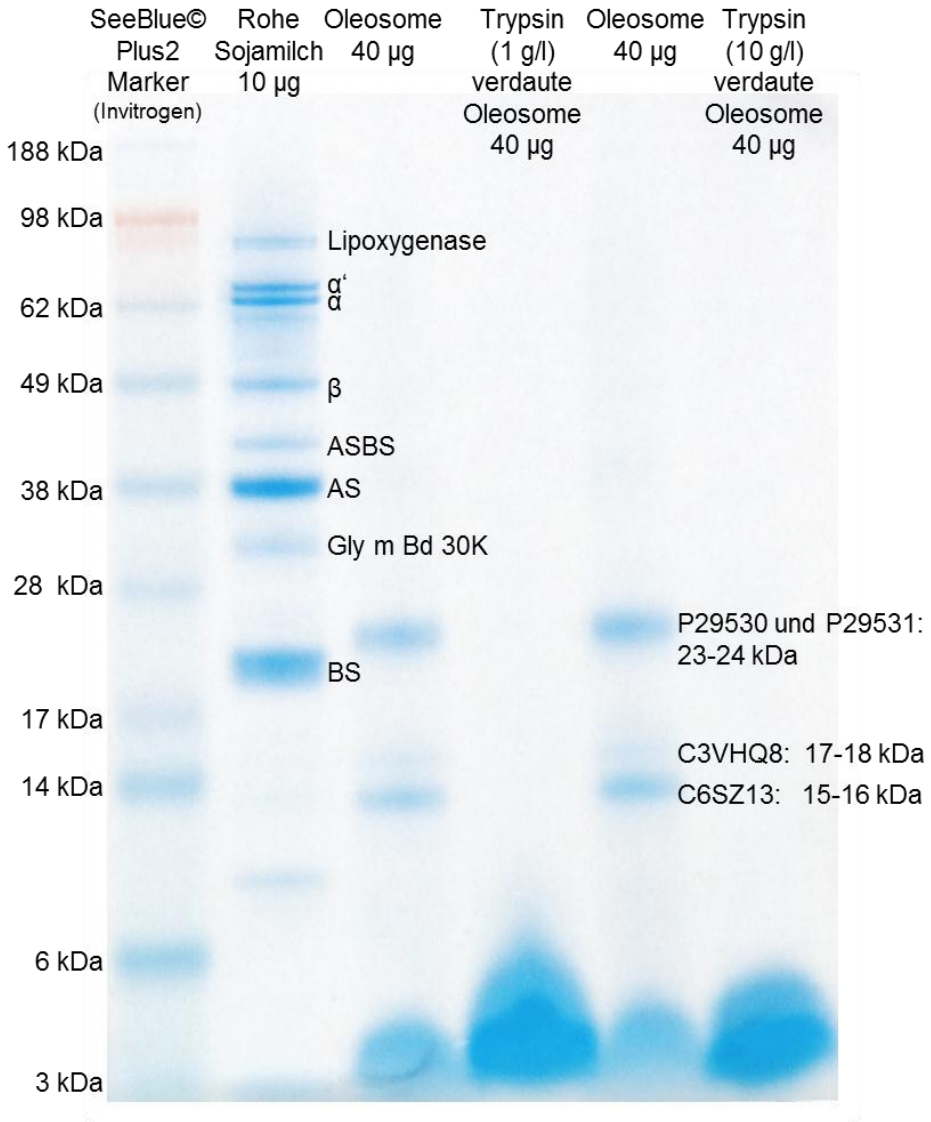

Abb. 8: Mit Comassie gefärbtes SDS-PAGE Gel zur Verdeutlichung des Extraktionsprozesses aus roher Sojamilch und dem Verdau mit Trypsin. In der rohen Sojamilch sind die Untereinheiten der Speicherproteine Glycinin (AS: Saure Untereinheit, BS: Basische Untereinheit) und β-Conglycinin (α, α', β), sowie die Lipoxygenase und das Allergen Gly m Bd 30K enthalten. Die Olesosome wurden mit 1 mg/ml und 10 mg/ml Trypsin bei 25 °C für 1 h verdaut. Die tryptischen Fragmente waren unter 8 kDa. (*50*)

Über den Stickstoffgehalt der getrockneten Oleosome wurde mittels der Dumas Methode (*52*) der Proteingehalt bestimmt (Stickstoffgehalt aus der Elementaranalyse x 5,89). Zur Bestimmung des Faktors 5,89 wurde das Molekulargewicht eines Oleosins durch das Molekulargewicht seiner enthaltenen Stickstoffatome geteilt und dann der Mittelwert von allen zu diesem Zeitpunkt bekannten Soja-Oleosinen(*51*) bestimmt (Tab. 3). Die Proteinkonzentration der Sojaoleosome lag bei 4.4 bis 5.8% ähnlich der photometrisch nach Bradford (*53*) bestimmten Proteingehalte von Oleosomen anderer Pflanzenspezies (0.6-4% (*54*) (*55*)). Die Proteinbestimmungen verschiedener Forschergruppen zeigen zum Teil höhere Werte (*11, 56-58*), dies geht möglicherweise mit einem höheren Gehalt an Speicherproteinen in den Präparationen einher.

Tab. 3: Berechnung des Faktors für die Proteinbestimmung nach Dumas für Soja-Oleosine

Protein	Molekulargewicht in g/mol	Anzahl der Stickstoffatome	Molekulargewicht Stickstoff in g/mol	Faktor
P29530	23501.6	295	4131.98	5.69
P29531	23392.6	294	4117.97	5.68
C3VHQ8	17416.8	197	2759.32	6.31
C6SZ13	15777.3	191	2675.28	5.90
			Mittelwert	**5.89**

Zu Soja-Oleosinen gibt es in der Literatur keine Identifizierung durch Sequenzierung, Massenspektrometrie, Röntgen oder NMR Strukturdaten. Die Primärsequenz der Oleosine ist jedoch in Protein-Datenbanken wie Uniprot (*51*) zu finden und hat den Status „Evidence at transcript level“. Ihr Transkript, die mRNA wurde also in der Pflanze nachgewiesen. Viele der folgenden Argumentationen gehen auf Vergleiche mit anderen Oleosinen (z.B. Mais (*15*), Sonnenblume (59)) und die für die zwei Hauptoleosine in Tab. 4 gezeigte Verteilung von hydrophilen und hydrophoben Aminosäuren innerhalb der Aminosäurensequenz zurück. Auch die Auswertung der FTIR Daten im folgenden Kapitel ist nur durch Vergleiche mit Arbeiten zu anderen Oleosinen möglich.

Tab. 4: Darstellung aus Uniprot der hydrophoben (violett) Aminosäuren und der negativ (rot) und positiv (grün) geladenen Aminosäuren der zwei Hauptoleosinen (P29530 und P 29531). (*51*). Auffällig ist die ca. 70 Aminosäuren lange hydrophobe mittlere Sequenz. Die theoretischen Schnittstellen von Trypsin liegen außerhalb des hydrophoben Bereiches nach den basischen Aminosäuren Arginin (R) und Lysin (K).

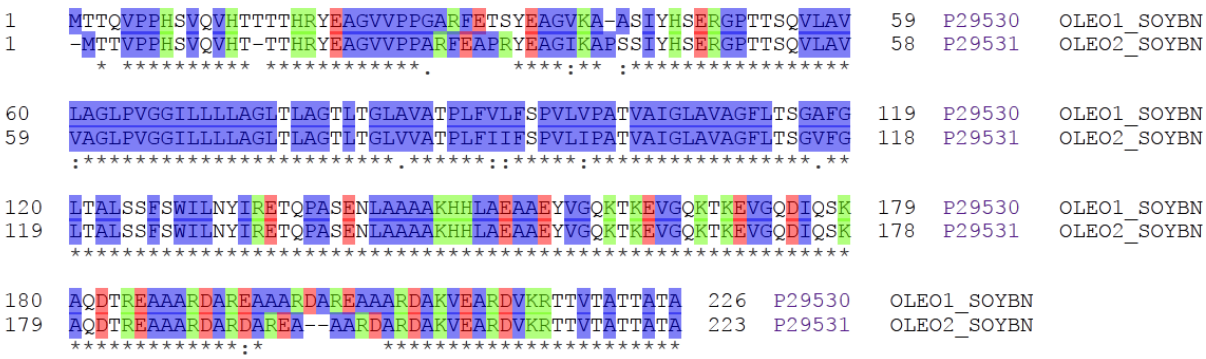

1.5.3. SEKUNDÄRSTRUKTURANALYSE DER OLEOSINE

Die Anteile der Sekundärstrukturen der Oleosine können über FTIR Spektroskopie bestimmt werden. In dieser Arbeit wurde die Methode zum ersten Mal auf Soja-Oleosine angewendet. Die gezeigten Spektren (Abb. 9) wurden von nativen Oleosinen, d.h. im Oleosom, und von Trypsin-verdauten Oleosomen aufgenommen. Der Verdau (Kap. 1.9) führte zu einem nachweisbaren Verlust von Sekundärstrukturen (vor allem β-Faltblätter und „random coils“) der Oleosine. Das Absorbtionsspektrum der Oleosine zeigt Abb. 9, vergrößert auf die für die Sekundärstrukturanalyse entscheidende Amid I Region. Die daraus abgeleitete Zuordnung der Banden zu bestimmten Sekundärstrukturen in Tab. 5 hat Ähnlichkeiten zu Oleosinen anderer Pflanzenspezies wie Distel und Sonnenblume. Diese Daten von Lacey et al. (60) zeigen auch eine Zunahme des α-helicalen Anteils nach der Verdauung mit Trypsin, was auf einen hohen Anteil an α-Helices im mittleren hydrophoben und für das Enzym unzugänglichen Proteinteil hindeutet. Dies ist in Einklang mit der Modellvorstellung (*61*) über die Faltung des mittleren Oleosinteils als eine Haarnadel, bestehend aus zwei α-Helices, welche über den Prolin-Knopf verbunden sind (Abb. 15). Besonders über diesen stark konservierten Abschnitt der Oleosine besteht Uneinigkeit unter den Forschern, denn deren spektroskopische Daten (zusätzlich von CD-Spektroskopie) belegen sowohl α-helicale (*59*) als auch β-Faltblatt artige (*62*) Sekundärstrukturen. Dieser Gegensatz zeigt deutlich die Schwierigkeit der Strukturaufklärung von extrem hydrophoben Peptiden im Lösemittel Öl. (*1*)

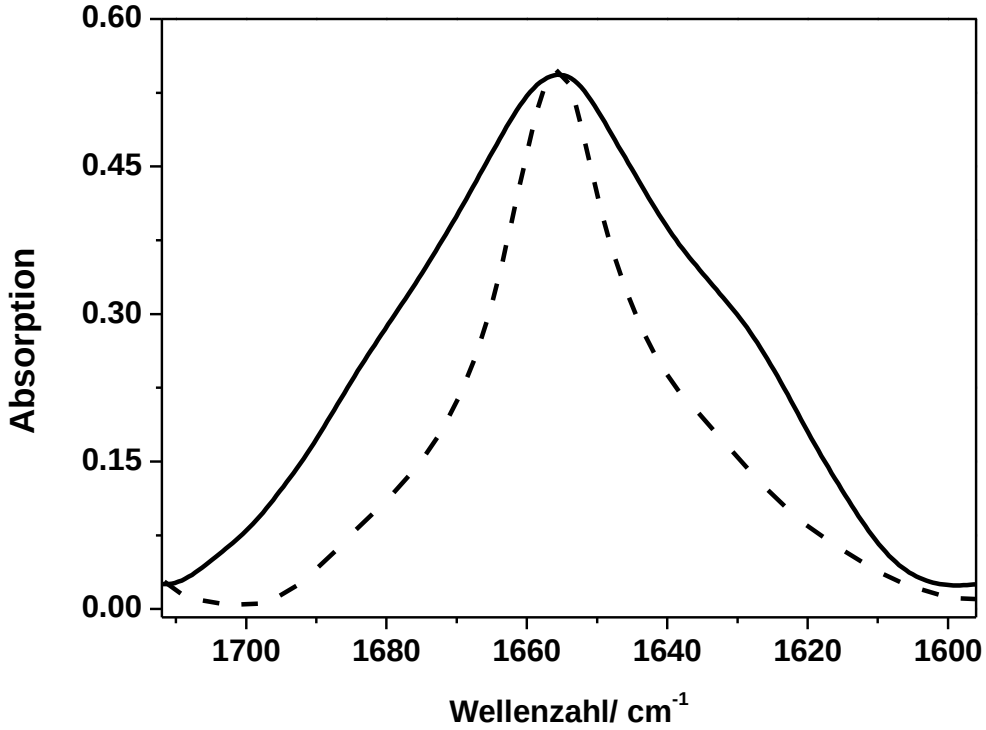

Abb. 9: Absorptionsspektrum in der Amid I Region von nativen (durchgehende Linie) und Trypsin-verdauten (gestrichelte Linie) Soja-Oleosomen.

Die N- und C-terminalen hydrophilen Domänen der Soja-Oleosine sind laut der FTIR-Spektroskopie eher dominiert von „random coils“ und β-Faltblättern, aber auch kleinere α-helicale Anteile sind möglich. Diese äußeren Bereiche sind für Enzyme wie Trypsin zugänglich und deren Fragmente sind nach dem Verdau größtenteils wasserlöslich.

Insbesondere in der C-terminalen Domäne, welche in ihrer Länge stark variiert, können amphipathische α-Helices gebildet werden, welche horizontale Wechselwirkungen mit den geladenen Köpfen der Phospholipidmonolage und der Oberfläche der Oleosome eingehen können. (*1*)

Die Funktion der mittleren Haarnadelstruktur ist die stabile Verankerung der Oleosine im Oleosom. Für die N- und C-terminalen Bereiche ist eine Funktion als Rezeptor für Lipasen während der Keimung möglich. (*1*)

Tab. 5: Bandenzuordnung der FTIR-Spektren der Amid I Region für native und mit Trypsin verdaute Soja Oleosome im Vergleich zu Distel und Sonnenblumen Oleosomen (*60*). Besonders hervorgehoben ist der α-helicale Anteil der Oleosine, welcher nach dem Verdau ansteigt, was auf einen großen Anteil an α-Helices im mittleren hydrophoben und für Enzyme unzugänglichen Bereich hindeutet.

A.) Soja				B.) Distel (*60*)		C.) Sonnenblume (*60*)	
Bande/ cm^{-1}	FWHM/ cm^{-1}	Fläche/ %	Zuordnung	Bande/ cm^{-1}	Fläche/ %	Bande/ cm^{-1}	Fläche/ %
Nativ				Nativ		Nativ	
1624	18	6	intermolekulares β-Faltblatt	1618	9	1621	6
1634	24	13	Antip.β-Faltblatt/ β-Faltblatt	1628/ 1641	5/ 26	1628/ 1639	4/ 22
1653	30	17	random coil				
1657	**34**	**47**	**α-Helix**	**1657**	**50**	**1654**	**33**
1673	31	5	β-turns	1671	6	1668	23
1682	26	12	β-Faltblatt	1682	3	1678	2
-	-	-	β-Faltblatt/ β-Schleife	1690	1	1687	10
Verdaut				Verdaut		Verdaut	
-	-	-	-	1618	6	1617	7
1633	25	21	Antip.β-Faltblatt / β-Faltblatt	1629/ 1641	5/ 20	1632/ 1640	13 / 8
1656	**22**	**73**	**α-Helix**	**1656**	**60**	**1655**	**59**
			β-Schleife	1670	5	1667	11
1680	14	6	β-Faltblatt	1680	4	1681	2

1.5.4. LIPIDANALYTIK

Eine qualitative Phospholipidanalyse der Soja-Oleosome wurde mittels Dünnschichtchromatographie durchgeführt und bestätigte deren Gehalt an Phosphatidylcholin, Phosphatidylethanolamin und Phosphatidylinositol im Vergleich mit Soja-Lecithin (Tab. 6) als Referenz (R_f = 0.2-0.5) (*63*).

TAG (R_f = 0.9) und deren Hydrolyseprodukte nach Lipaseverdau wurden mit einem anderen Laufmittel (*64*) wiederum mittels Dünnschichtchromatographie bestätigt (R_f = 0 für MAG, R_f = 0.3 für DAG und R_f = 0.5 für Fettsäuren).

Die Phospholipidkomposition von Soja Oleosomen ist qualitativ von Analysen des Sojalecithins ableitbar (*65*), welche jedoch erheblichen Schwankungen unterliegen. Eine quantitative Aussage über die Zusammensetzung der Oleosomenmonolage ist darüber nicht möglich, da während des Extraktionsprozesses („degumming“) von Lecithin Phospholipide aus anderen Organellen erfasst werden und die Extrahierbarkeit der verschiedenen Phospholipide generell unterschiedlich ist. Auffällig ist, dass bei kommerziellen Lecithinen meistens eine Angabe für Phosphatidylserin fehlt, welches jedoch mit hoher Sicherheit in Sojaoleosomen zu finden sein müsste. Oleosome anderer Spezies enthalten bis zu 25%

Phosphatidylserin (*5*) und dieses Phospholipid wurde auch in Sojalecithin nachgewiesen (*66*). Die beiden dominierenden Fettsäuren in Soja-Lecithin sind Linolsäure (18:2) und Palmitinsäure (16:0). Daraus ergeben sich die in Abb. 10 gezeigten Strukturformeln der häufigsten in Soja-Oleosomen enthaltenen Phospholipide.

Phosphatidylcholin (PC)

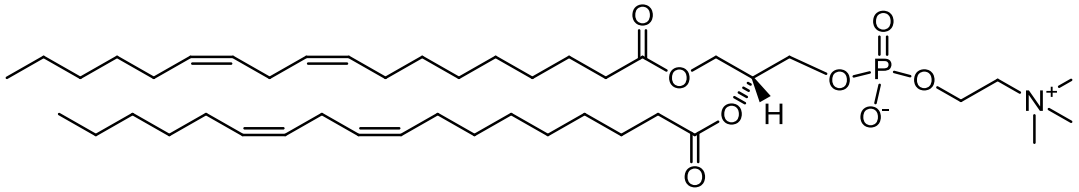

Phosphatidylethanolamin (PE)

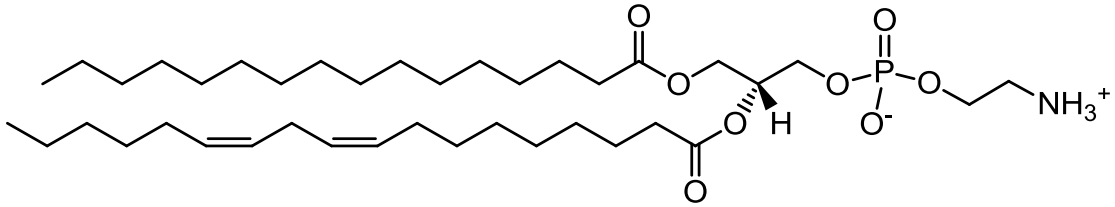

Phosphatidylglycerol (PG)

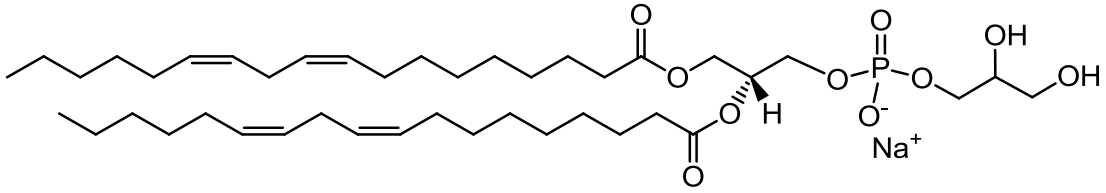

Phosphatidylserin (PS)

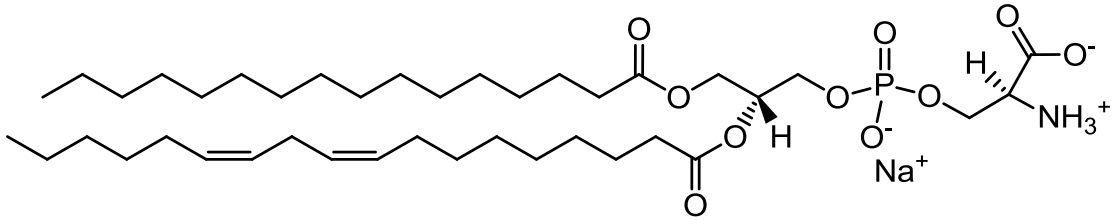

Phosphatidylinositol (PI)

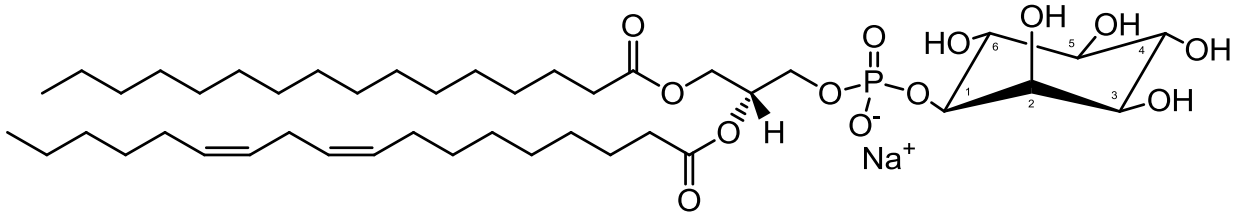

Phosphatidsäure (PA)

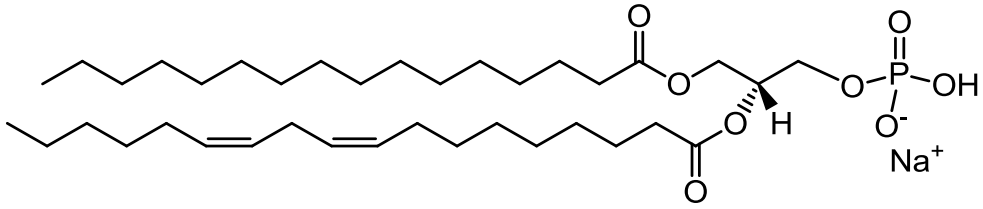

Abb. 10: Strukturformeln der häufigsten aus Sojabohnen extrahierbaren Phospholipide (*67*).

Tab. 6: Zusammensetzung des als Referenz benutzen Lecithins aus Sojabohne (Kat.Nr. 57556, SERVA)

Phosphatidylcholin	18 – 25 %
Phosphatidyethanolamin	10 – 16 %
Phosphatidylinositol	14 – 19 %
Phosphatidsäure	4 – 7 %

1.5.5. LADUNGSZUSTÄNDE DER OLEOSOMENHÜLLE

Für die Argumentationen und Erklärungen in allen drei Veröffentlichungen wurden die pH-abhängigen Ladungszustände der grenzflächenaktiven Komponenten der Soja-Oleosome herangezogen. Für die Phospholipide sind im Vergleich zu den Oleosinen einfacher Aussagen über den genauen Anteil der Ionisierung der sauren und basischen Gruppen zu treffen. Eine genaue Faltung der Oleosine und somit die Exposition polarer Gruppen in die wässrige Umgebung ist ohne vollständige Strukturaufklärung nur schwierig zu prognostizieren.

Die Ionisation bzw. Protonierung und Deprotonierung und die dadurch erzeugte relative Ladung für Phospholipide kann als Funktion des pH-Wertes dargestellt werden (*67*) oder ist über die Gleichgewichtskonstanten (pK_A) qualitativ abschätzbar.

Abb. 11 zeigt beispielhaft diesen Verlauf für Phosphatidylcholin mit nur einer protonierbaren Gruppe und Phosphatidylethanolamin mit zwei protonierbaren Gruppen.

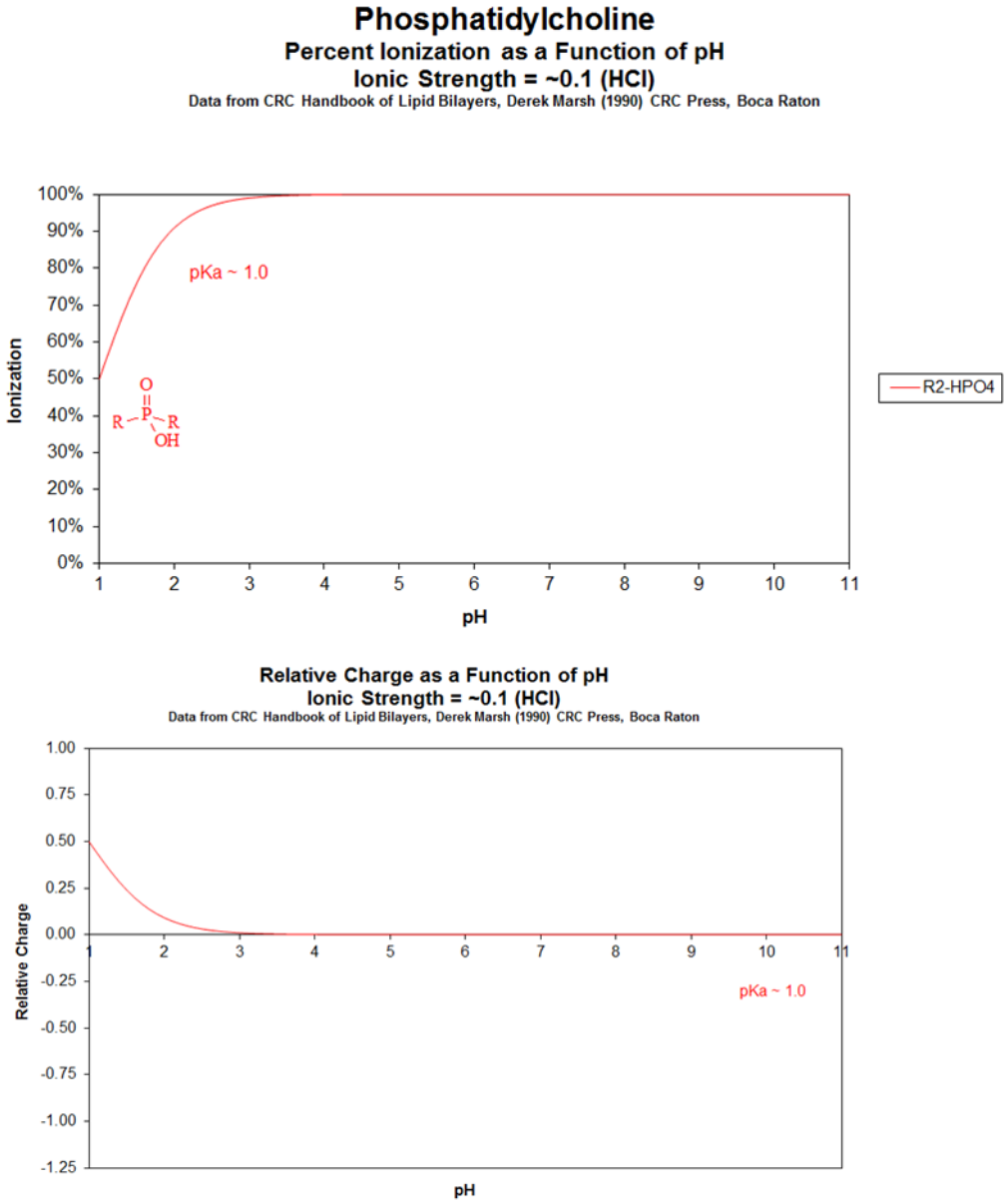
Phosphatidylcholine
Percent Ionization as a Function of pH
Ionic Strength = ~0.1 (HCl)
Data from CRC Handbook of Lipid Bilayers, Derek Marsh (1990) CRC Press, Boca Raton
Ionization
100%
90%
80%
70%
60%
50%
40%
30%
20%
10%
0%
pKa ~ 1.0
O
P
R
R
OH
1
2
3
4
5
6
7
8
9
10
11
pH
R2-HPO4
Relative Charge as a Function of pH
Ionic Strength = ~0.1 (HCl)
Data from CRC Handbook of Lipid Bilayers, Derek Marsh (1990) CRC Press, Boca Raton
Relative Charge
1.00
0.75
0.50
0.25
0.00
-0.25
-0.50
-0.75
-1.00
-1.25
pKa ~ 1.0
pH

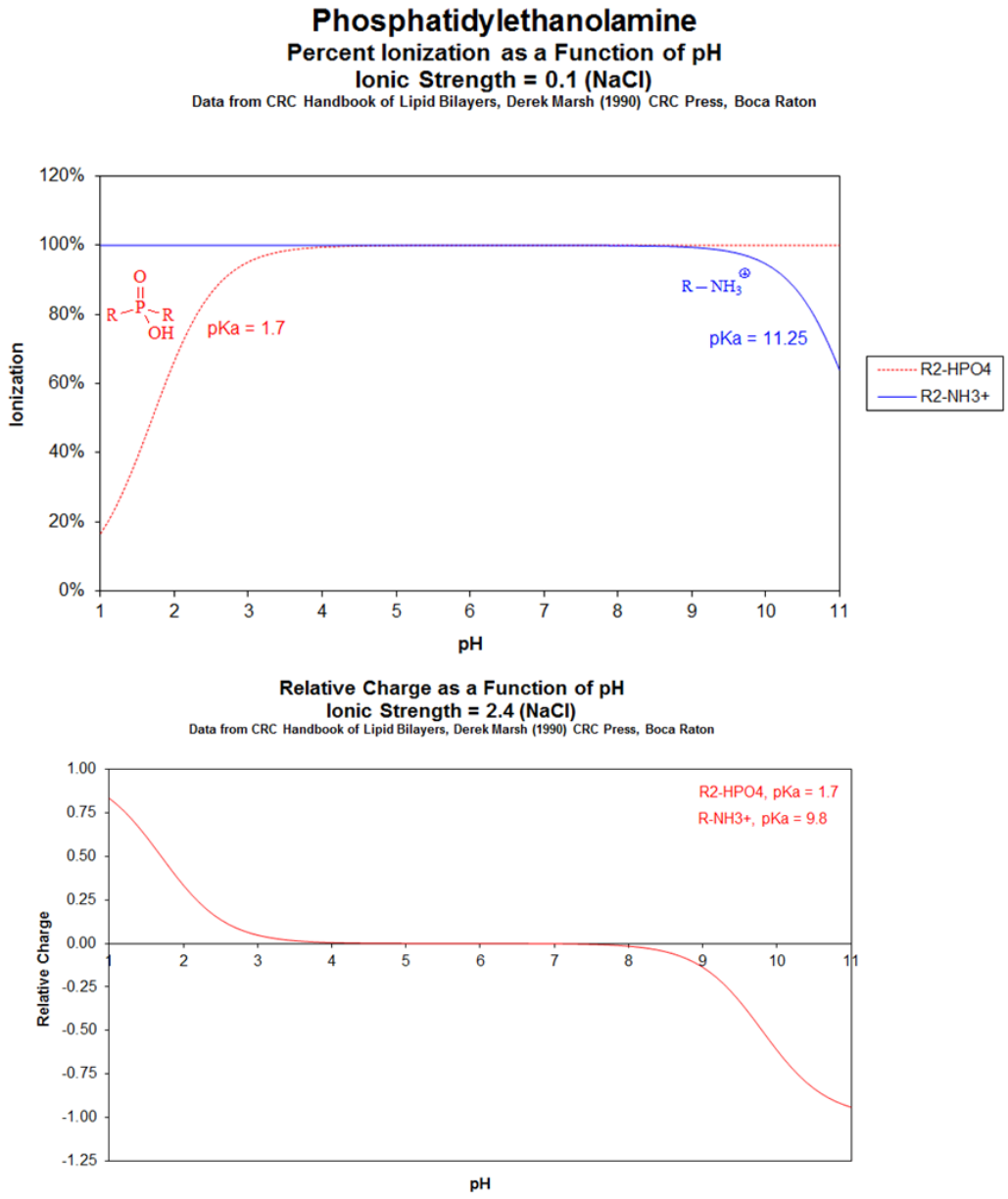

Abb. 11: Ionisation und relative Ladung als Funktion des pH-Wertes von Phosphatidylcholin und Phosphatidylethanolamin aus (*67*).

Hiermit können den in den Sojaoleosomen vorhandenen Phospholipiden Ladungszustände an den drei bei den Experimenten an der Luft-Wasser-Grenzfläche (Kap. 1.8) vorhandenen pH-Werten zugeordnet werden (Tab. 7). Zusätzlich kann über das Zeta-Potential der verdauten Oleosome (Publikation 2 und Abb. 12) ein Gesamtladungszustand der Außenhülle bestimmt werden, welcher größtenteils auf die Phospholipide zurück zu führen ist. Die in Tab. 7 aufgeführten Ladungen der Oleosine bei den pH-Werten 2, 5 und 8 sind auch von den Zeta-Potentialen der nativen Oleosome aus Abb. 12 abgeleitet.

Tab. 7: Zusammenfassung der Ladung der Moleküle an der Öl-Wasser-Grenzfläche von Oleosomen. Die Ladung der Phospholipide sind Literaturwerte (*68*) und die der Oleosine sind über das Zeta-Potential nativer Oleosome abgeleitet.

Komponenten	pH = 2	pH = 5	pH = 8
Oleosine	+	±	-
Phosphatidylcholin	+	±	±
Phosphatidylethanolamin	+	±	±
Phosphatidylinositol	0	-	-
Phosphatidsäure	0	-	2-

Der theoretische isoelektrische Punkt (pI) der Sojaoleosine kann mathematisch bestimmt werden (*51*) und ist zusammen mit der Anzahl der sauren und basischen Aminosäuren in Tab. 8 aufgeführt. Alle Soja-Oleosine enthalten ein bis drei mehr basische Aminosäuren als saure.

Tab. 8: Theoretischer pI und Anzahl der sauren (Asparaginsäure und Glutaminsäure) und basischen (Arginin und Lysin) Aminosäuren aus uniprot (*51*) der vier Sojaoleosine.

	P29530 (226 AS)	P29531 (223 AS)	C3VHQ8 (165 AS)	C6SZ13 (147 AS)
Theoretischer pI	8,02	8,89	7,75	9,35
Asparaginsäure (-) $pK_{s,\beta\text{-}COOH}$ = 3,90 (*69*)	6	7	6	5
Glutaminsäure (-) $pK_{s,\gamma\text{-}COOH}$ = 4,25 (*69*)	14	13	3	2
Arginin (+) $pK_{B,Guanidin}$ = 12,48 (*69*)	12	13	5	5
Lysin (+) $pK_{\varepsilon\text{-}NH3}^{+}$ = 10,28 (*69*)	9	9	5	5

Der über das Zeta-Potential (Abb. 12) ermittelte isoelektrische Punkt der Oleosome ist vom theoretischen pI weit entfernt und liegt bei einem pH-Wert von 5. Dies zeigt, dass für die Bestimmung des isoelektrischen Punktes eines Proteins die genaue dreidimensionale Struktur bekannt sein muss, denn nicht alle Aminosäuren, die theoretisch einen Beitrag zur

Gesamtladung der Oleosomenaußenhülle erbringen könnten, sind auch wirklich nach außen exponiert.

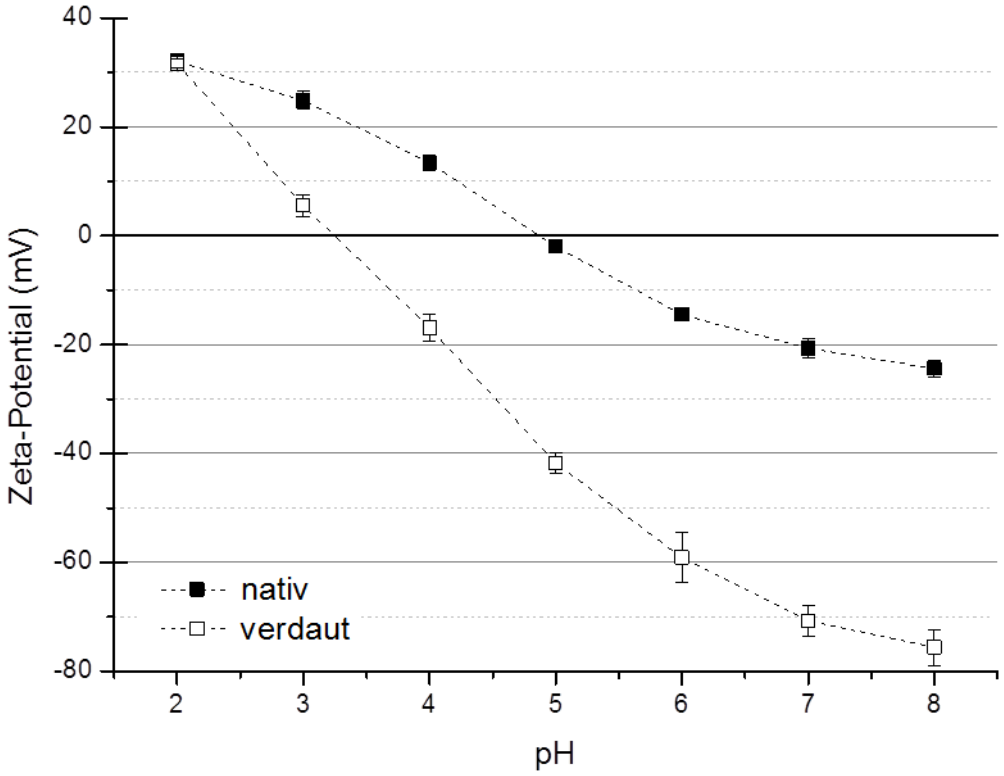

Abb. 12: Zeta-Potential nativer und verdauter (siehe Kap. 1.9) Oleosome in Abhängigkeit des pH-Wertes

Wie der Verlauf des pH-abhängigen Zeta-Potentials zeigt, ist die Ladung der Oleosomenaußenhülle vom pH Wert des umgebenden Mediums bestimmt. Im Sauren von pH 2 bis 5 ist die Außenhülle der Oleosome positiv geladen, bei pH 5 nach außen hin neutral und von pH 5 bis 8 negativ geladen. Die Ladung der äußeren Hülle der Oleosome verändert auch ihr Verhalten an Grenzflächen, was im folgenden Abschnitt erläutert wird.

Die Ladung der verdauten Oleosome (Kap. 1.9) wird dominiert von den negativen Ladungen der Fettsäuren und Phospholipide, wie Phosphatidylinositol und Phosphatidsäure.

1.6. GRENZFLÄCHEN IN LEBENSMITTELN (SCHÄUME UND EMULSIONEN)

Alle Lebensmittel enthalten Grenzflächen und ihre Zubereitung führt oft zur Bildung neuer Grenzflächen zwischen Wasser und Luft oder Wasser und Öl. Einfache Beispiele sind Schäume oder Emulsionen mit niedermolekularen Emulgatoren wie Lecithin. Emulgatoren mit mehreren und höhermolekularen Komponenten (Proteine), wie die LDL-Partikel zeigen an Grenzflächen ein komplizierteres Verhalten in Form von mehrstufiger Kinetik. Anton et al. (*24*) beschreiben die Adsorption von Eigelb LDL- Partikeln an die Luft-Wasser-Grenzfläche (Abb. 13) als dreistufigen Prozess:

1.) Die Diffusion der LDL an die Grenzfläche
2.) Die Verankerung der amphiphilen Apolipoproteine an der Wasseroberfläche und ein dadurch verursachtes Aufreißen der LDL-Struktur
3.) Ausbreitung der LDL Komponenten (TAG, Phospholipide, Cholesterol, Cholesterolester und denaturierte Apolipoproteine) auf der Wasseroberfläche

Dies zeigt die besondere Rolle der Proteine beim Verhalten von Lipidspeicherstrukturen an Grenzflächen.

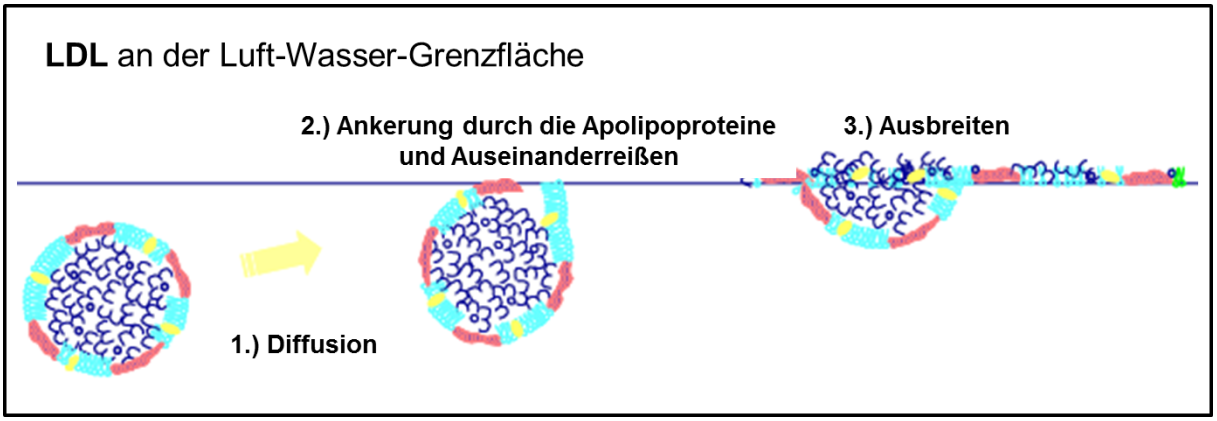

Abb. 13: Von Anton et al. (*24*) vorgeschlagenes Modell der Adsorbtion von LDL-Partikeln an der Luft-Wasser-Grenzfläche mit den Komponenten: Apolipoproteine (rot), Phospholipide (türkis), Cholesterol (gelb) und TAG und Cholesterolester (blau).

Das Modell der Anton-Gruppe stützt sich auf die Daten zweier Publikationen (*26*, *28*) in denen die Druck-Flächen-Isothermen ganzer LDL und ihrer Einzelkomponenten verglichen wurden. Somit konnte der Kurvenverlauf den Komponenten oder Molekülgrüppen zugeordnet werden (Abb. 14). Die Phasenübergänge der Lipide (TAG und Cholesterolester) der LDL und der Phospholipidkollaps wurde zur Interpretation der Oleosomenisotherme herangezogen. Insbesondere die Betrachtung der Kinetik (Verhalten der Oleosomen als Funktion der Zeit) wurde sehr viel detaillierter untersucht und zeigt ein vielfältigeres Verhalten als die LDL

(Abb. 14, klein). Darüber hinaus berücksichtig Publikation 1 noch den Einfluss von pH-Wert und Ionenestärke auf das Verhalten der Oleosome an der Luft-Wasser-Grenzfläche. (*27*)

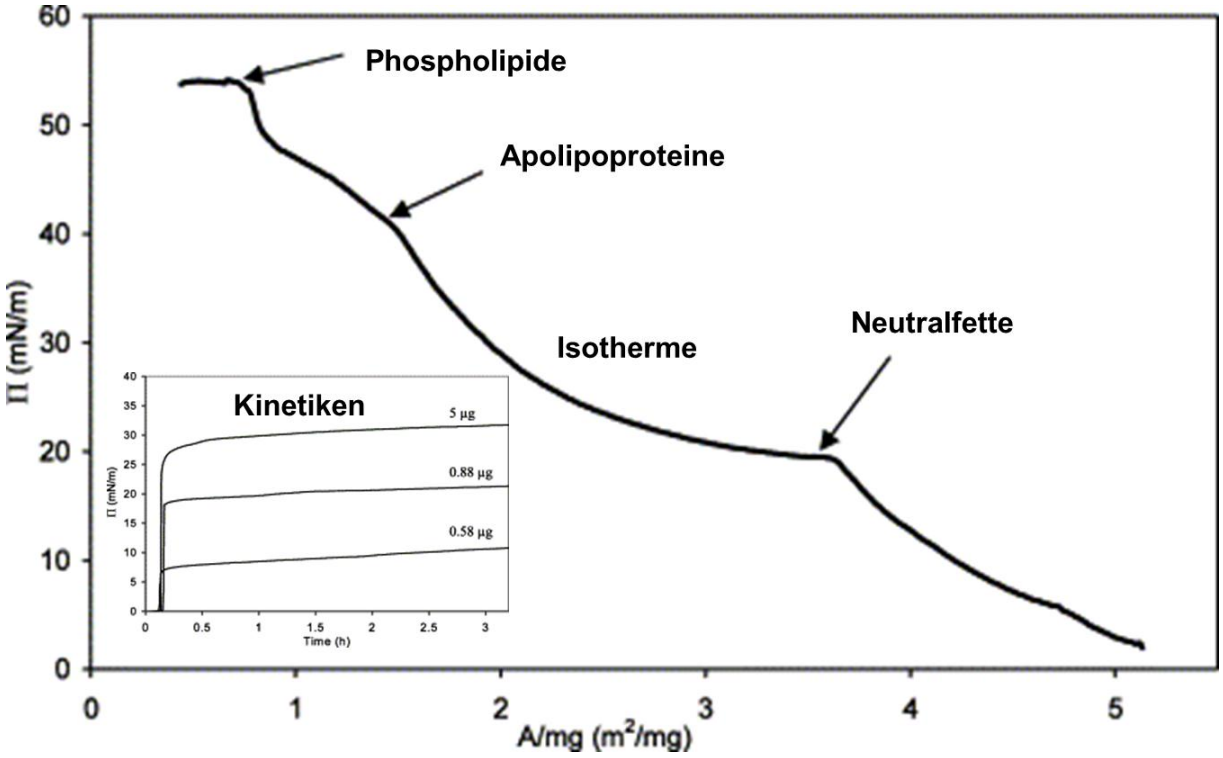

Abb. 14: Druck-Flächen-Isotherm von LDL aus Eigelb an der Luft-Wassergrenzfläche eines Langmuir Trogs (16 µg LDL; Komprimierungsgeschwindigkeit = 100 cm^2/min) aus (*26*). Dem Kurvenverlauf der Isotherme sind die verursachenden Komponenten der LDL zugeordnet. Zusätzlich sind verkleinert Kinetiken (Oberflächendruck als Funktion der Zeit) von drei verschiedenen LDL-Mengen dargestellt.

Aufgrund des stärkeren Auftriebs der Oleosome im Vergleich zu den LDL-Partikeln konnte auch eine andere Art der Aufbringung der grenzflächenaktiven Substanzen gewählt werden. Die LDL Partikel wurden in wässriger Lösung auf die Wasseroberfläche „getropft“ (*28*), während die Oleosome in die Subphase injiziert wurden. Die Injektionsmethode führt zu schnelleren Effekten (Anstieg des Oberflächendrucks) und Beobachtungen (Mikroskopie) (siehe Kap. 1.8) und benötigt eine größere Konzentration an grenzflächenaktiven Substanzen (LDL µg/ l; Oleosome mg/l). (Publikation 1 (*27*))

1.7. PROTEINE UND PHOSPHOLIPIDE AN GRENZFLÄCHEN

Proteine verändern sich an Grenzflächen. Globuläre Proteine falten sich auf. Proteine, welche schon nativ in einer Grenzfläche gefaltet waren (Oleosine, Hydrophobine (*70*)), erfahren möglicherweise weniger Veränderung und eignen sich besser eine Grenzfläche zu stabilisieren.

Abb. 15 zeigt eine mögliche Faltung der Oleosine an ihrer natürlichen Öl-Wasser-Grenzfläche innerhalb eines Oleosoms. Beschrieben wird eine Haarnadel aus zwei α-Helices, welche über das Prolin-Knopf-Motiv (-**P**LFVLF**SP**VLV**P**- für P29530) verbunden sind. Die äußeren terminalen Bereiche können amphipathische α-Helices enthalten. Elektrostatische Anziehung zu den negativ geladenen Phospholipiden ist über einzelne und richtig platzierte positiv geladene Aminosäuren wie Arginin (R) möglich. (*61*)

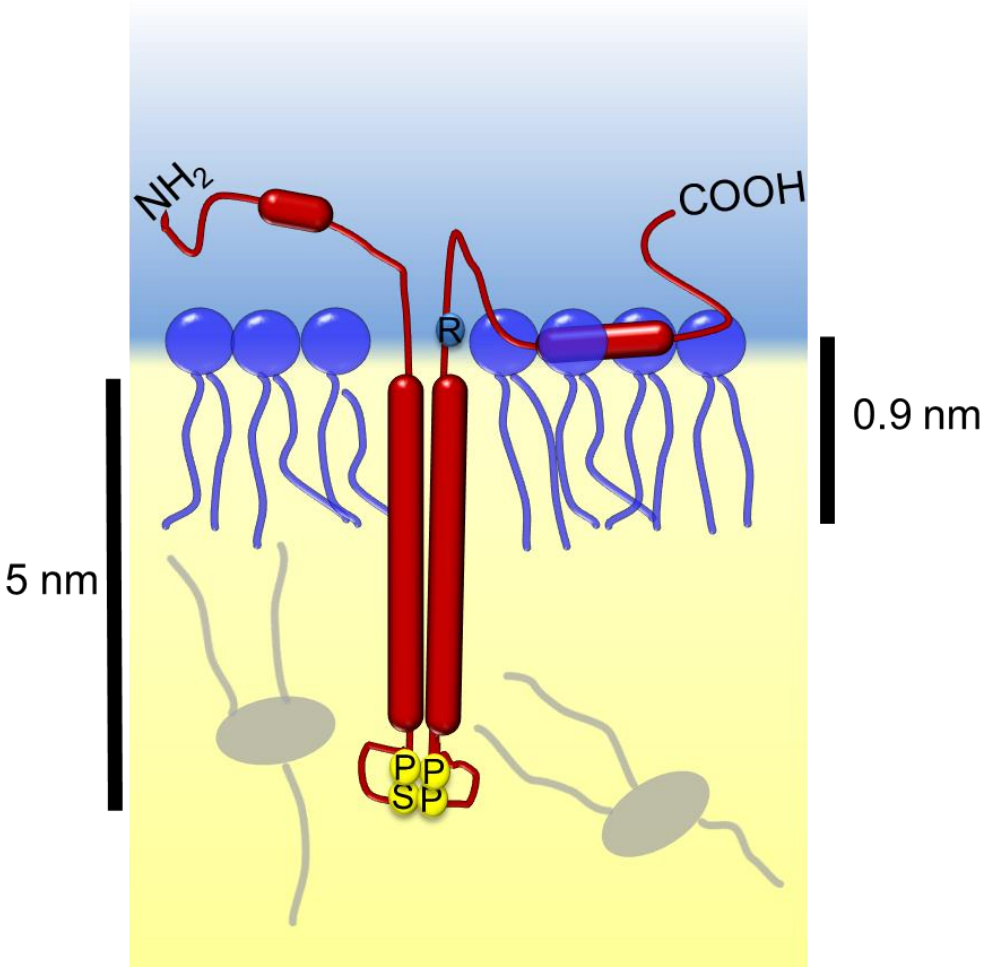

Abb. 15: Vorschlag zur Oleosinfaltung mit dem konservierten Prolin-Knopf-Motif (gelb), α-helicalen Anteilen (rote Säulen) und möglichen Wechselwirkungen von positiv geladenen Aminosäurenresten (z.B. Arginin, R) mit den negativ geladenen Phosphat-Kopfgruppen der Phospholipide. Zur Verbesserung der Darstellung sind Phospholipide und Oleosin in unterschiedlichem Maßstab dargestellt. Die hydrophobe Haarnadelstruktur der Oleosine ist 5 nm lang und eine Phospholipidmonolage ca. 0,9 nm tief. Angelehnt an (*61*)

An der Luft-Wasser-Grenzfläche kann sowohl eine Auffaltung von Proteinen, als auch eine Oxidation durch den Luftsauerstoff stattfinden.

Das Verhalten von Phospholipiden an der Luft-Wasser Grenzfläche ist von großem Interesse und wurde in vielen Arbeiten (*71*, *72*) untersucht. Auch ist bekannt, das bestimmte Proteine das Phasenverhalten von Phospholipiden beeinflussen (*73*).

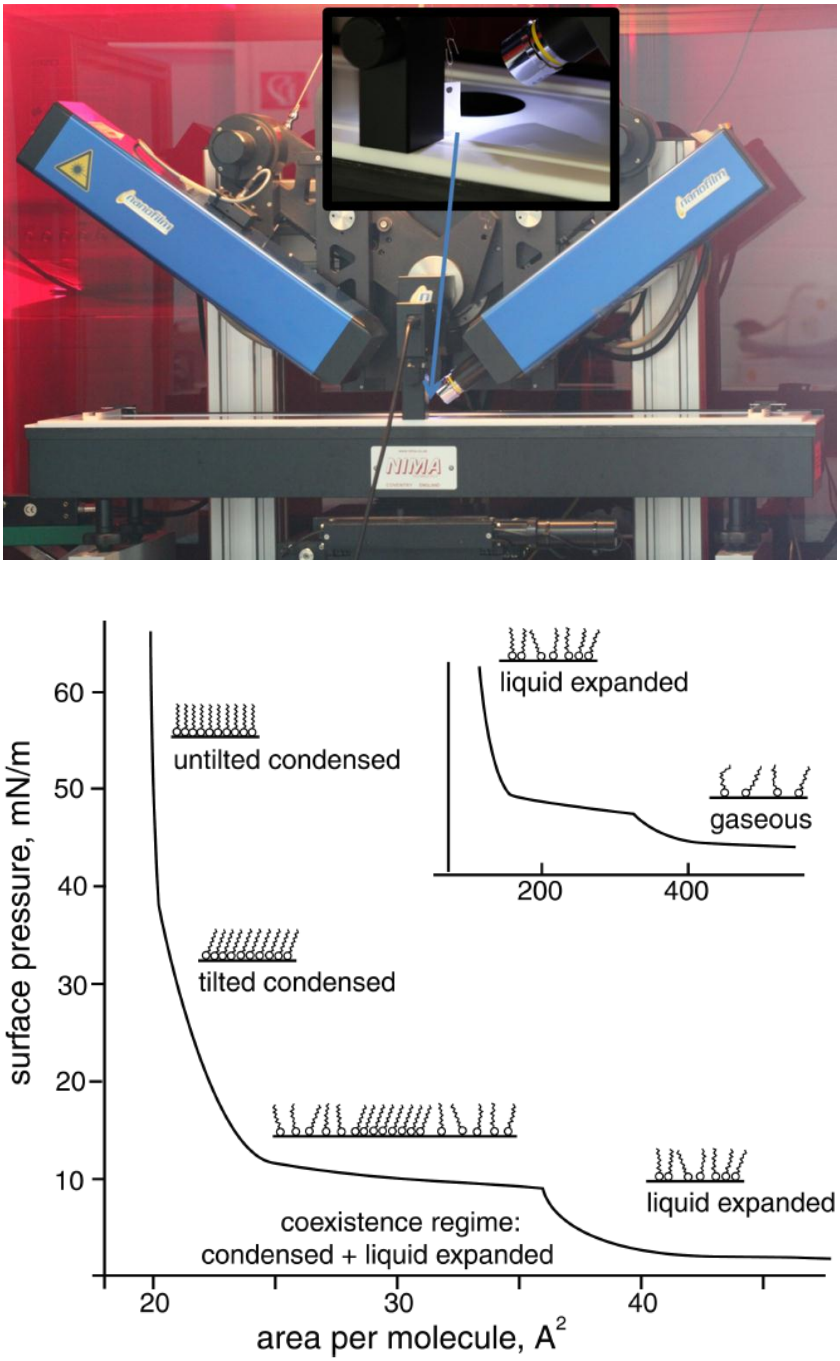

Abb. 16: Fotographie des benutztens Langmuir Trogs mit BAM-Aufbau (oben) und eine idealisierte Isotherme einer Langmuir Monolage (unten). Horizontale Bereiche sind Phasenkoexistenzen bei Übergängen erster Ordnung, Knicke bedeuten kontinuirliche Übergänge von einer Phase in die nächste. Aus (*71*)

Abb. 16 zeigt eine ideale Isotherme einer Langmuir Monolage (aus beispielsweise Phospholipiden) mit den vier Phasen: gasförmig, flüssig-expandiert, geneigt kondensiert und aufrecht kondensiert. Mit dem gezeigten Aufbau (Filmwaage und BAM Abb. 16) können sowohl ganze Oleosomen an der Luft-Wasser-Grenzfläche als auch ihr weiteres Verhalten und das ihrer Bestandteile erfasst werden. Dies beinhaltet Phasenübergänge von Phospholipiden, deren Domänbildung- und Aggregat und Netzwerkbildung von Proteinen.

1.8. VERHALTEN DER OLEOSOME AN DER LUFT-WASSER-GRENZFLÄCHE (PUBLIKATION 1)

Messungen des Oberflächendrucks als Funktion der Zeit oder der Fläche wurden kombiniert mit Aufnahmen eines Brewsterwinkel-Mikroskops (BAM, Abb. 18) um das Verhalten der Oleosome an der Luft-Wasser-Grenzfläche eines Langmuir Trogs zu untersuchen. Abb. 17 zeigt den typischen Verlauf einer Kinetik bei „geringen“ (27) Oleosomenkonzentrationen und die dazugehörigen Szenarien. Nach der Injektion der Oleosome in die Subphase diffundiert die Emulsion aufgrund ihrer geringeren Dichte und dem daraus resultierenden Auftrieb an die Grenzfläche. Die Injektionsstelle liegt dabei in ca. 20 cm Entfernung von der Messstelle mit dem Wilhelmy-Plättchen aus Papier. Darauf folgt ein steiler Anstieg des Oberflächendrucks auf 12 mN/m, welcher durch das schnelle Ausbreiten der Oleosome auf der gesamten Grenzfläche verursacht und im BAM von hellen, schnellen, Mikrometer großen Partikeln begleitet wird. Zu diesem Zeitpunkt und Oberflächenbelegung sind die Oleosome noch intakt und nach Verlangsamung der Bewegung als dreidimensional wirkende Objekte im BAM sichtbar. Nach dem steilen folgt ein langsamer Druckanstieg bis ca. 16 mN/m während dessen sich die Anzahl der Oleosome auf der sichtbaren Grenzfläche verringert. Bei Verwendung von hochreinem Wasser („MilliQ“) als Subphase und „hohen“ (*27*) Oleosomenkonzentrationen sind in diesem Abschnitt Platzvorgänge zu sehen. Die Zeitspanne zwischen Injektion der Oleosome und dem Platzen ist abhängig von den Parametern der Subphase (pH-Wert und Ionenstärke) und der Oleosomenkonzentration. Je dichter die Packung der intakten Oleosome an der Grenzfläche, desto schneller kommt es zu Platz- und/ oder Koaleszenzvorgängen. Nach dem Erreichen des Druckmaximums sind alle Oleosome geplatzt und ihre Bestandteile verteilen sich auf der Grenzfläche. Die entstehende Monolage aus Phospholipiden, Triacylglyceriden und Oleosinen beginnt sich nach dem Platzen neu zu ordnen. Diese Phasenseparation, Aggregat- und Domänenbildung ist sowohl durch den darauf folgenden Druckabfall, als auch aus den sich verändernden BAM-Bildern (z.B. Abb. 18) ablesbar und wird bestimmt von der Ladung der Oleosine (Kap.1.5.5). Dabei sind am isoelektrischen Punkt (pH 5) die größten Aggregate auf der Wasseroberfläche zu sehen.

Bei einer Kompression der Fläche vor dem Maximum gibt es keine Phasenübergänge in der Isotherme, bei Kompresseion nach dem Peak sind Phasenübergänge der Lipide als Knicke in der Isotherme und durch Veränderung des Brechungsindex im BAM zu sehen. Es muss also eine genügend große Anzahl an Oleosomen geplatzt sein, um einen Phasenübergang der vorher unzugänglichen Lipide in der Lipidmonolage, zu beobachten. Der Verlauf durch ein Maximum ist nur bei Konzentrationen unter 0,4 mg/l zu beobachten. Bei Konzentrationen höher 0,8 mg/l ist in derselben Zeit ein konstanter langsamer Anstieg des Oberflächendrucks messbar, da fortlaufend neue Oleosome die Grenzfläche erreichen und platzen.

Für die freien Oleosine gibt es 4 mögliche Arrangements an der Luft-Wasser-Grenzfläche, welche von ihrer Ladung bedingt durch die Subphase (pH, Ionenstärke), der Zeit und der Oleosomenkonzontration abhängig sind (Abb. 17):

a. Die Denaturierung der Oleosine, insbesondere eine Auffaltung des hydrophoben Haarnadelmotivs
b. Die Aggregatbildung durch die Zusammenlagerung der hydrophoben Domänen, möglicherweise gefolgt von einer Diffusion in die Subphase nach dem Erreichen einer kritischen Größe und Gewicht
c. Die Faltung eines Oleosins in die Monolage aus Phospholipiden
d. Die Faltung eines Oleosins in einen Öltropfen auf der Wasseroberfläche

Darüber hinaus kommt es bei Oleosomenkonzentrationen größer 0,8 mg/l, pH 5-8 und einer Zeit von über 5 h zur Ausbildung eines netzwerkartigen Films aus Protein-Lipid-Komplexen, welcher eine Diffusion in die Subphase verhindert und die Mobilität des Films stark einschränkt. Dieser Film wird beim Komprimieren zusammengeschoben und kann als Fäden aus der komprimierten Oberfläche gezogen werden. Sowohl Proteine (Amid I) als auch Lipide (Carbonyl Streckschwingung) wurden durch SFG-Spektroskopie an der Grenzfläche nachgewiesen. (Publikation 3)

Zusätzlichen Einfluss auf die Filmbildung kann die Oxidation durch den Luftsauerstoff haben, da Sojaöl zu einer radikalischen Netzwerkbildung, ausgelöst durch Autoxidation von ungesättigten Fettsäuren fähig ist. (*74*)

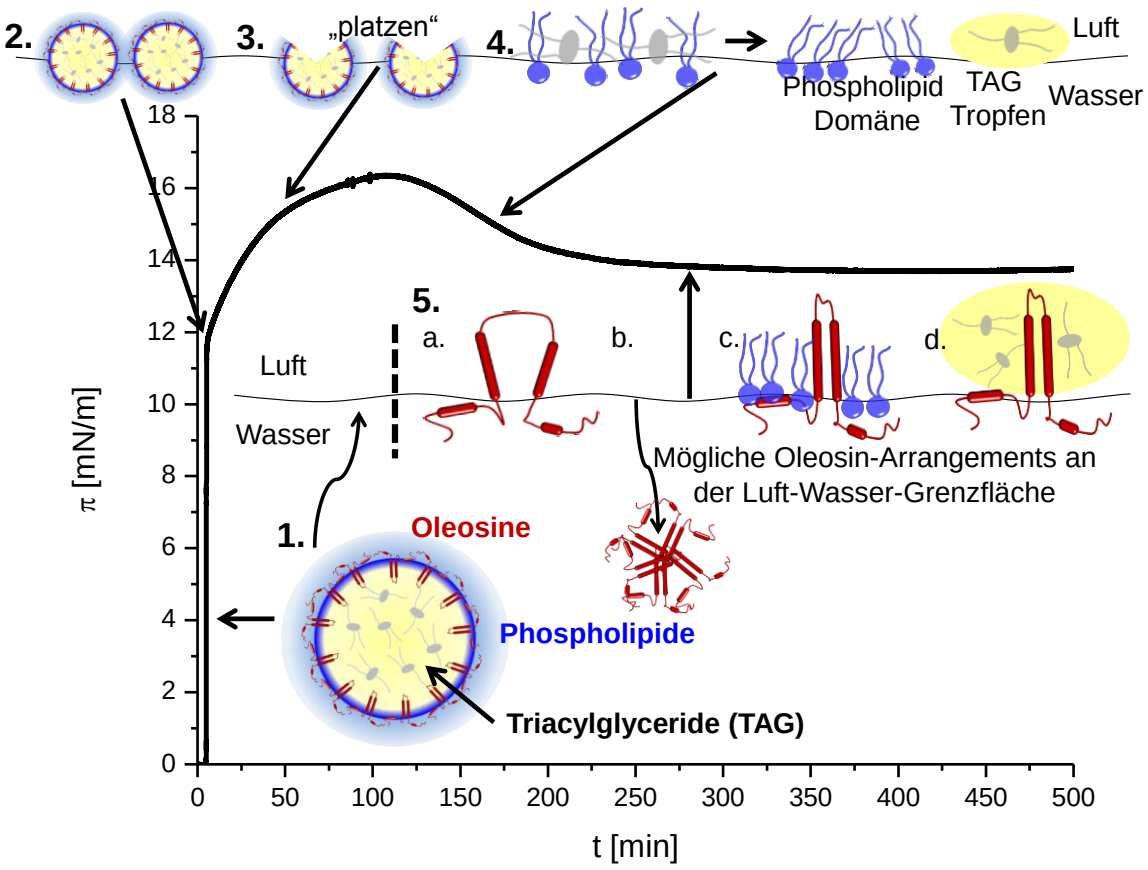

Abb. 17: Typischer zeitlicher Verlauf des Oberflächendrucks und die dazugehörigen Szenarien an der Luft-Wasser-Grenzfläche bei offenen Barrieren und „geringen“ Oleosomenkonzentrationen als schematische Darstellung mit unterschiedlichem Maßstab. (*27*)

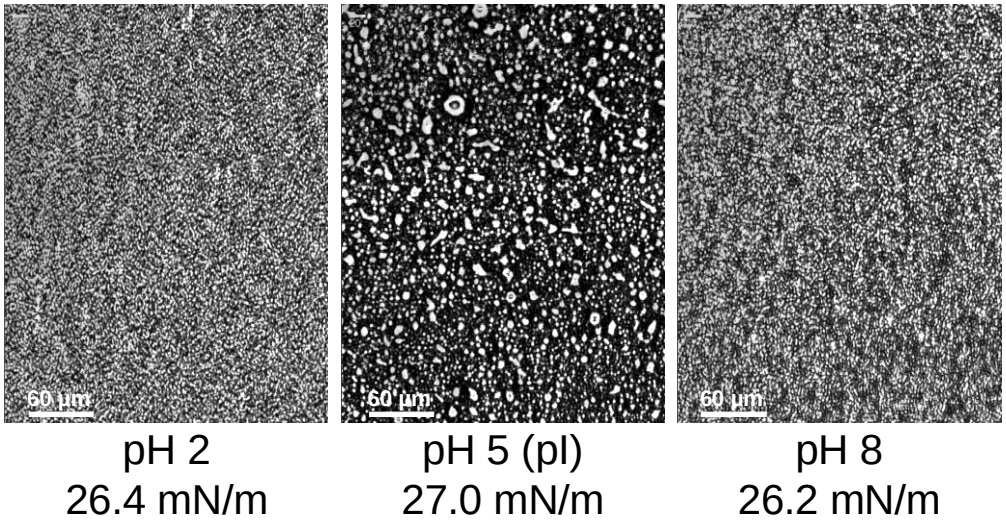

Abb. 18: Exemplarische BAM-Aufnahmen der Luft-Wasser-Grenzfläche nach dem Platzen der Oleosome bei verschiedenen pH-Werten. Am isoelektrischen Punkt der Oleosine (pH 5) sind größere Aggreagate zu sehen als bei niedrigen oder höheren pH-Werten.

1.9. VERDAU VON OLEOSOMEN (PUBLIKATION 2 UND 3)

Der enzymatische Verdau von Oleosomen wird zum einen zur Strukturaufklärung der Oleosine (siehe 1.5.3 und (*60*)) genutzt und zum anderen zur Simulation der Vorgänge im menschlichen Magen-Darm-Trakt nach dem Konsum oleosomenhaltiger Lebensmittel (*33*) und dem Katabolismus der Oleosome während der Keimung (siehe 1.2.2).

Bei der Strukturaufklärung der Oleosine wurden Proteasen wie Proteinase K angewendet um die innen und außen liegenden Proteindomänen zu bestimmen. (*60*) Proteinase K hat auch im mittleren öllöslichen Anteil der Oleosine theoretische Schnittstellen. (*51*) Diese sind jedoch für die Protease unzugänglich und das Enzym schneidet nur innerhalb der hydrophilen Domänen, dabei bleiben nach einem Proteinase K Verdau 6 und 8 kDa große Fragmente übrig, deren Sekundärstruktur dann über FTIR Spektroskopie analysiert werden kann. (*60*) Auch das Pankreas-Enzym Trypsin ist nach heutigen Erkenntnissen über Proteasen an Öl-Wasser-Grenzflächen für die Strukturaufklärung geeignet, da es auch viele theoretische Schnittstellen in den hydrophilen Bereiche der Oleosine besitzt, aber keine in den lipophilen. (*51*)

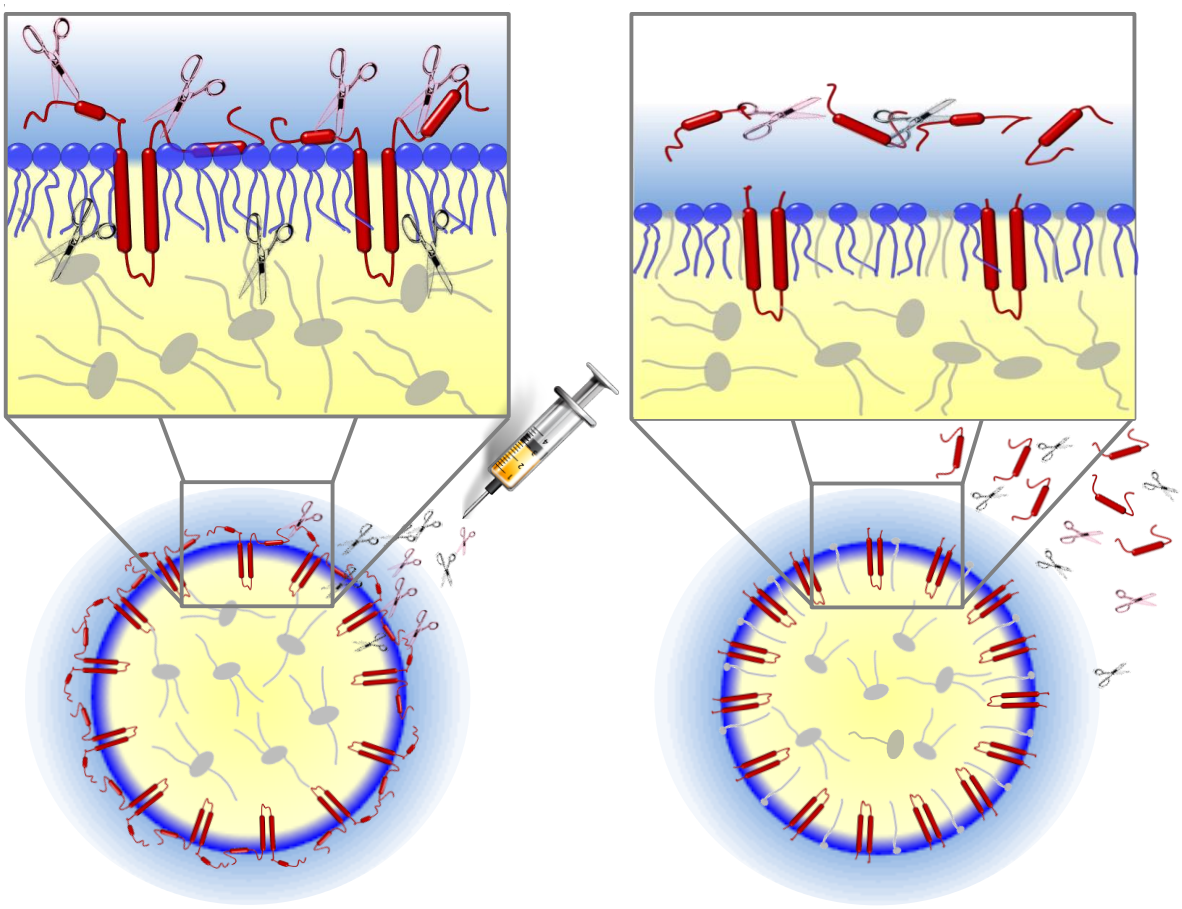

Abb. 19: Enzymatischer Verdau von Oleosomen. Proteasen schneiden die Oleosin-Proteine an der Oberfläche des Oleosoms und Pankreaslipasen hydrolysieren TAG an ihrer Öl-Wasser-Grenzfläche.

Das gewählte Verdauungsenzym Trypsin spaltet Peptide im menschlichen Dünndarm selektiv nach den basischen (und geladenen) Aminosäuren Lysin (K) und Arginin (R) und gehört somit zu den Endopeptidasen. Diese theoretischen Schnittstellen für Trypsin sind in den Oleosinen nur in den äußeren hydrophilen Bereichen zu finden. Die aus dem Verdau resultierenden Peptidfragmente lassen sich mit UniProt (*51*) bestimmen und sind beispielhaft für das Soja-Oleosin P24 Isoform A (P29530) in Tab. 9 aufgeführt.

Tab. 9: Masse, Position und Peptidsequenz der Fragmente nach einem tryptischen Verdau des Soja-Oleosins P24 Isoform A (P29530), Mw (mittlere Masse) = 23501.67 (uniprot (*51*)).

Masse	Position	Peptidsequenz
8390.8207	50-134	GPTTSQVLAVLAGLPVGGILLLLAGLTLAGTLTGLAVATPLFVLFSPVLV PATVAIGLAV AGFLTSGAFGLTALSSFSWI LNYIR
2158.0822	1-19	MTTQVPPHSVQVHTTTTHR
1452.723	149-161	HHLAEAAEYVGQK
1400.7016	135-148	ETQPASENLAAAAK
1130.5364	31-40	FETSYEAGVK
1115.5843	20-30	YEAGVVPPGAR
1033.5061	41-49	AASIYHSER
1003.5054	171-179	EVGQDIQSK
937.4836	217-226	TTVTATTATA
590.2892	180-184	AQDTR
560.3038	164-168	EVGQK
517.2729	185-189	EAAAR
517.2729	193-197	EAAAR
517.2729	201-205	EAAAR
474.267	209-212	VEAR
361.2081	213-215	DVK
361.183	190-192	DAR
361.183	198-200	DAR
333.1768	206-208	DAK
248.1605	162-163	TK
248.1605	169-170	TK
175.1189	216-216	R

Nach dem Verdau ist die Ladung der Außenhülle der Oleosome verändert und somit der Verlauf ihres pH-abhängige Zeta-Potentials (Abb. 12) zu negativeren Werten verschoben. Dies deutet auf eine von den Ladungen der Phospholipide und Fettsäuren dominierte Außenladung hin. Der Verlauf des Zeta-Potentials als Funktion des pH-Wertes zeigt außerdem Ähnlichkeiten zu den Messungen ähnlicher Systeme, also Lecithin-stabilisierten Emulsionen wie z.B. den parenteralen Emulsionen (*75*).

Durch den Verdau mit Trypsin zeigt sich auch der Einfluss der Oleosine auf das Verhalten der Oleosome an der Grenzfläche. Durch das Abschneiden von Bindungstellen zwischen Protein und Lipiden wird nach dem Platzen der Oleosome eine größere Freisetzung insbesondere von Phospholipiden erreicht. Dies führt zu einem viel höheren Druckanstieg als bei nativen Oleosomen. Auch kommt es nicht zur Ausbildung des starren Films an der Grenzfläche, was zusätzlich die Phasenseparation und Domänbildung der Lipide verstärkt. Der erste Effekt führt zu einem höheren Druckanstieg bei Injektion der gleichen Menge an Oleosomen und der zweite Effekt zu einem schnelleren Druckabfall im Vergleich zu den nativen Oleosomen (Abb. 20).

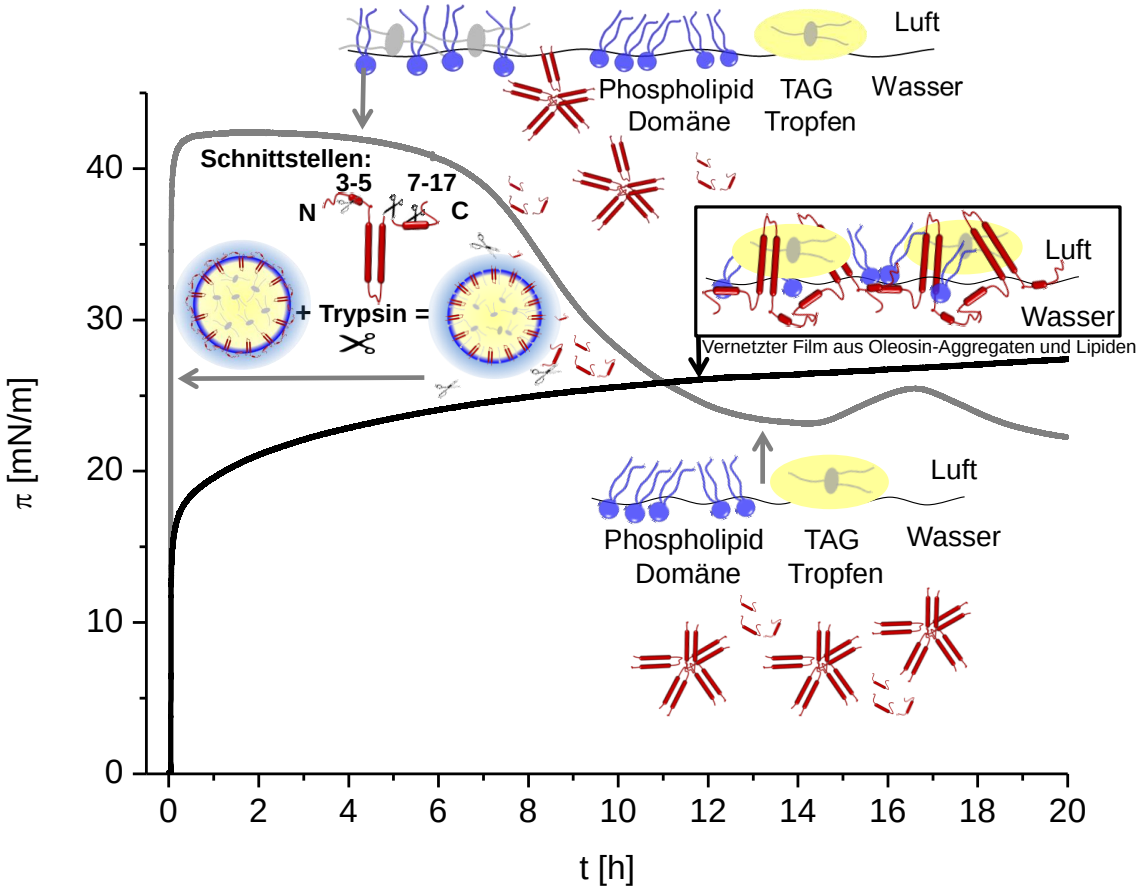

Abb. 20: Zeitlicher Verlauf des Oberflächendrucks und die dazugehörigen Szenarien an der Luft-Wasser-Grenzfläche für native und mit Trypsin verdaute Oleosomen bei pH 8 als schematische Darstellung mit unterschiedlichem Maßstab.

Als Lipidspeicherstruktur sind die Oleosome im physiologischen Sinne eher Substrat für Lipasen, sowohl in der Pflanze als auch bei der menschlichen Verdauung.

Betreffend der Größe der Fetttröpfchen findet man bei den pankreatischen Lipasen andere Argumente als bei der Lipolyse in Pflanzen. In Pflanzen soll die Kinetik der Lipolyse direkt proportional zur Größe der Grenzfläche (*76*) sein bei Pankreaslipasen scheint es keine Korrelation zu geben (*77*). Hier ist die Situation aber auch komplexer da zusätzliche Emulgatoren in Form von Gallensäuren (z.B. Cholsäure) die dynamische Zusammensetzung der Öl-Wasser-Grenzfläche beeinflussen. Auch ist noch ungeklärt in welcher Form Proteolyse und Lipolyse der Oleosome zusammenspielen. In Pflanzen wird vermutet, dass die äußeren Bereiche der Oleosine als Rezeptor oder Bindungsstelle für Lipasen fungieren könnten. (*35*) Es gibt jedoch auch Hinweise, dass die Oleosine oder allgemein der Aufbau der Oleosomenhülle die Lipolyse im Darm verlangsamen. Dies geschieht durch die Akkumulation von Fettsäuren an der Grenzfläche, wodurch die Lipaseaktivität herabgesetzt wird. (*33*)

In dem benutzten Trypsin war auch lipolytische Aktivität feststellbar. Sowohl in FTIR-Spektren als auch in der Dünnschichtchromatographie wurden Lipaseprodukte (Fettsäuren und MG und DG) nachgewiesen. Die Lipolyse war jedoch nie vollständig und große Mengen TAGs konnten auch nach 1 h Verdauzeit gefunden werden (siehe Publikation 2). Erste Versuche zur Kinetik der Lipolyse von Oleosomen unter Magen- und Darmbedingungen wurden vom AK Denkov der Universität Sofia durchgeführt und zeigte auch nach 1 h unter Magenbedingungen und 4 h unter Darmbedingungen (mit Gallensalzen) keine vollständige Hydrolyse der TAGs. (*64, 78*) Somit ist anzunehmen, dass die hydrolysierte Menge an TAG durch den einstündigen Verdau mit dem oben genannten Trypsin sehr viel geringer ist, als unter den in Vinarov et al. (*64, 78*) beschriebenen künstlichen Verdau.

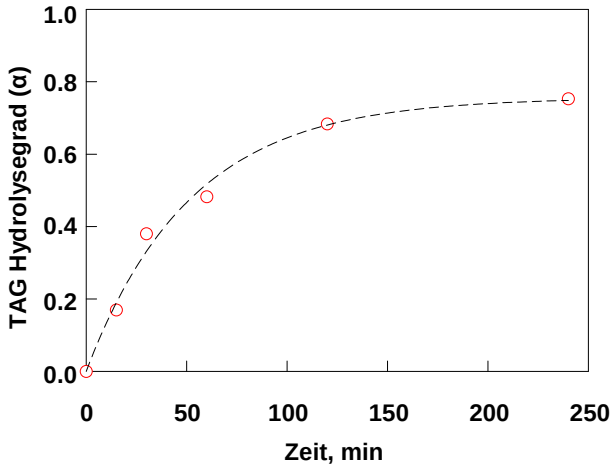

Abb. 21: Verlauf der TAG Hydrolyse für Soja-Oleosome unter Darmbedingungen nach 1 stündigem Verdau unter Magenbedingungen (Einfachbestimmungen). Gemessen von Zahari Vinarov, AK Denkov unter Benutzung ihrer in-vitro-Verdauung und anschließender Analytik im Gas Chromatographen. (Beschrieben in: (*64, 78*))

1.10. STABILISIERUNG DER ÖL-WASSER-GRENZFLÄCHE (MAYONNAISE) DURCH OLEOSOME

Überträgt man das Verhalten der Oleosome an der Luft-Wasser-Grenzfläche auf die Öl-Wasser-Grenzfläche, beispielsweise einer Mayonnaise, ist folgendes Szenario beim Emulgieren denkbar:

1.) Die Oleosomen geraten durch den Homogenisator (z.B. UltraTurrax) in Bewegung.
2.) Durch Zugabe des zusätzlichen Öls und die Homogenisierung entstehen neue nicht stabilisierte Öltropfen, welche bei Berührung mit den Oleosomen zu einer Fusion/ Koaleszenz von Öltropfen und Oleosom führen.
3.) Die Phospholipide und Oleosine verteilen sich nach der Fusion gleichmäßig auf dem entstanden Öltropfen.

Während der Herstellung der Mayonnaise laufen diese drei Schritte in einer großen Vielzahl und sich wiederholend ab.

Wie auch bei Eigelb-basierenden Mayonnaisen (*79*) ist die Rolle der Proteine, also der Oleosine bei der Stabilisierung der Emulsion entscheidend. Molekulare Änderungen auf Proteinebene führen zu makroskopischen Effekten, wie der Herabsetzung der Viskosität der Mayonnaise.

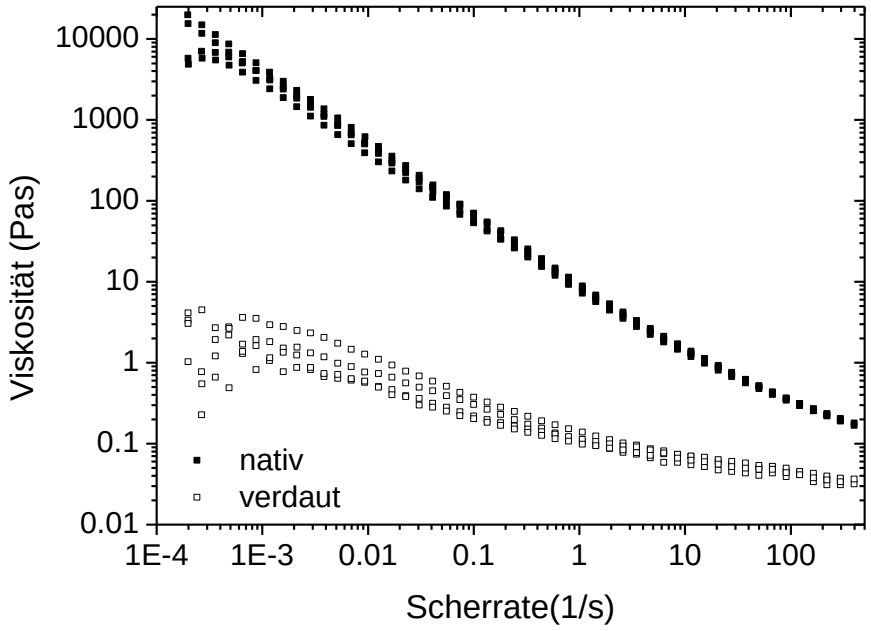

Abb. 22: Viskosität von Emulsionen hergestellt aus nativen und verdauten Oleosomen. 50 g Sojaöl wurde in kleinen Portionen zu 25 ml einer 23,3%igen Oleosomen-Lösung in 5 mM Tris/NaCl Puffer (I = 5 mM) pH 8 zugegeben und mit einem UltraTurrax homogenisiert (15.600 rpm, 4 min).

Die Emulsionen aus nativen und verdauten (Kap. 1.9) Oleosomen zeigen eine um den Faktor 1000 unterschiedliche Viskosität (Abb. 22) und einen Unterschied in der mittleren Tröpfchengröße von ca. 20 µm. Emulsionen mit intakten Oleosinen haben also ein größere Viskosität und stabilisieren kleinere Tröpfchen als ihre tryptischen Verdauungsfragmente. Beide Emulsionen enthalten Phospholipide und Fettsäuren als Emulgatoren. Bei der Stabilisierung der Grenzflächen zwischen den Tropfen scheinen jedoch native Oleosine zu einer besseren sterischen Abschirmung der Tröpfchen zu führen. Außerdem setzen sie die Fluidität der „Trennwände“ herab und bilden möglicherweise ein stabilisierendes Netzwerk in der kontinuierlichen Phase der Emulsion. Diese Funktion der Oleosine ist durch ihre amphiphile Struktur gegeben. Diese führt sowohl zu einer stabilen Verankerung im Öl als auch zu Wasserstoffbrücken und ionischen Wechselwirkungen mit anderen Oleosinen in den äußeren Domänen. Die äußeren Domänen haben wie auch an der Luft-Wasser-Grenzfläche eine Fähigkeit zur Gel- und Netzwerkbildung.

2. ZUSAMMENFASSUNG UND AUSBLICK

Die Untersuchung der Oleosome an der Luft-Wasser-Grenzfläche einer Filmwaage und die Beobachtung mit einem Brewster-Winkel-Mikroskop hat viele Fragen über das Verhalten dieser Strukturen beantwortet. Sinnvolle Vergleiche mit ähnlichen Systemen und Modifikationen an den Oleosomen können das in dieser Arbeit erlangte Verständnis von Protein-Lipid-Wechselwirkungen noch erweitern.

Das Aufbrechen der Oleosome an der Luft-Wasser-Grenzfläche konnte gezeigt werden und wird bestimmt von dem Ladungszustand ihrer Außenhülle insbesondere von den Oleosinen. Die Kinetik des Aufbrechens wird somit beeinflusst durch die Ionenstärke und den pH-Wert des umgebenden Mediums und der lokalen Konzentration an Oleosomen. Die Morphologie der Luft-Wasser-Grenzfläche wird im BAM durch die unterschiedlichen Schichtdicken und Brechungsindizes beschrieben. Eine genauere Auflösung und molekulare Differenzierung kann durch die Wiederholung der Versuche mit fluoreszenzmarkierten Oleosinen und Phospholipiden unter Benutzung eines Fluoreszenzmikroskops erreicht werden. Erste Versuche mit 2% NBD-DPPE (*80*), einem mit dem Fluorophor Nitrobenzoxadiazol markierten Phosphoplipid, welches sich nur in die LE-Phase der Phospholipide einlagert, sind vielversprechend und sollten durch fluoreszenzmarkierte Oleosine (z.B. mit Fluoresceinisothiocyanat/ FITC) erweitert werden. Die BAM Aufnahmen der Luft-Wasser-Grenzfläche, nach Aufgabe von Trypsin verdauten Oleosomen, zeigen bei pH 2 und pH 8 sternförmige Domänen, welche bei pH 5 nicht auftreten, dies sollte weiter verfolgt werden, beispielsweise durch Untersuchung der Reversibilität der Domänbildung bei Änderung des pH-Wertes der Subphase.

Der Einfluss des Sauerstoffs auf die Denaturierung der Oleosine und die Aggregat- und Domänbildung kann durch Wiederholung der Versuche unter Schutzatmosphäre (Stickstoff oder Argon) untersucht werden. Insbesondere die Vernetzung des Films könnte sauerstoffabhängig sein. Hier wäre es von Vorteil, zwischen einem proteingesteuerten Prozess und der radikalischen Netzwerkbildung, ausgelöst durch Autoxidation der ungesättigten Fettsäuren in den Soja-Lipiden zu unterscheiden (*74*).

Erste Versuche weisen darauf hin, dass die gleiche Menge an Phospholipiden und Sojaöl wie sie in den Oleosomen vorkommen zu einem viel geringeren Druckanstieg auf der Filmwaage führen. Dieses Vergleichssystem wurde mittels Hochdruckhomogenisierung hergestellt und weist eine ähnliche Größe wie die Oleosome auf. Dies deutet auf den Einfluss der Oleosine und deren Fragmente auf das Verhalten der Oleosome an der Luft-Wasser Grenzfläche („Platzen“) hin. Des Weiteren ist es möglich, dass die Proteinfragmente das Phasenverhalten der Phospholipide dahingehend beeinflussen, dass es zu einer höheren Packungsdichte durch die Reduzierung des Neigungswinkels der Aliphatischen Ketten kommt. Ein Effekt, der z.B.

für die Phospholipase A2 (PLA2) Adsorption an d-Dipalmitoylphosphatidylcholin (d-DPPC) Monolagen beschrieben wurde. (*73*) Für das allgemeine Verständnis von Protein-Phospholipid-Wechselwirkungen wäre es wichtig, die genaue Proteinsequenz innerhalb der Oleosine zu finden, welche mit den Phospholipiden interagiert. Mit hoher Wahrscheinlichkeit liegen diese Proteindomänen in den amphiphilen Abschnitten der Oleosine und beinhalten beispielsweise positiv geladen Aminosäuren wie Arginin (R). Durch geschickte Wahl von Enzymen mit bestimmten Schnittstellen könnte dieser Effekt zugeordnet werden und beispielsweise die betreffende Sequenz in einem Peptidsynthesizer synthetisiert werden. Eine über die SDS-PAGE hinausgehende Proteinanalytik der Proteinfragmente ist dabei unbedingt heran zu ziehen. Vielversprechend ist hierbei die Massenspektrometrie nach dem Verdau der Oleosine am intakten Oleosom.

Da die genaue Faltung der Oleosine im nativen Oleosom, genauso wie die generelle „Öllöslichkeit“ von Proteindomänen, immer noch debattiert wird, sehe ich zwei Möglichkeiten die Struktur der Außenhülle weiter zu untersuchen. Eine Möglichkeit ist die Bestimmung der Stärke der Außenhülle mittels Neutronenstreuung unter Benutzung der Kontrastvariation. Die zweite Möglichkeit ist Spektro-Mikroskopie (CARS) an großen Oleosomen wie sie z.B. in der Kakaobohne zu finden sind. Dabei sollte die Bande für die aromatischen Aminosäuren von außen nach innen geringer werden und somit ein experimenteller Nachweis der Verankerung der Oleosine in der TAG-Matrix möglich sein.

Die Untersuchung der Oleosome auf ihre Stabilität bei typischen Prozessen der Lebensmittelindustrie sollte noch ausgeweitet werden. Die Veränderungen auf Proteinebene beim Erhitzen, Einfrieren oder unter Scherung mit Infrarotspektroskopie und Zeta-Potential Messungen zu untersuchen ist dabei ein sinnvoller Ansatz. Interessante Fragestellungen und Anwendungen ergeben sich außerdem aus den Wechselwirkungen der Oleosome mit anderen Nährstoffen in Formulierungen. Auf molekularer Ebene scheinen besonders die Wechselwirkungen mit anderen Proteinen, Zucker und Calcium interessante Effekte hervor zu rufen. Zucker wie Saccharose werden bei der Extraktion der Oleosome eingesetzt und scheinen über Vergrößerung der Hydrathülle die Oleosome zu stabilisieren und gegen Koaleszenz und Aufbrechen zu schützen. Calcium ist dafür bekannt Proteine zu Vernetzen und wird bei der Herstellung von Sojaprodukten eingesetzt. Von verfahrenstechnischer Seite ist der sogenannte „Scale-up“ der Oleosomenextraktion für eine großtechnische Produktion interessant, befindet sich jedoch noch in den Anfängen. Im Rahmen dieser Arbeit konnte die Extraktion aus Sojabohnen im größeren Labormaßstab ausgehend von 1,5 l roher Sojamilch etabliert werden. Die Überprüfung der Anwendbarkeit der Extraktion auf andere Oleosomenquellen (z.B. Mais, Mandeln oder Amaranth) wäre von Vorteil und ist vom Erfolg des Aufschlusses der Saaten abhängig.

3. ABBILDUNGSVERZEICHNIS

4. TABELLENVERZEICHNIS

5. QUELLENANGABEN

1. Huang, A. C., Oleosins and Endoplasmic Reticulum in Seeds and Anthers. In *The Plant Endoplasmic Reticulum*, Robinson, D., Ed. Springer Berlin Heidelberg: 2006; Vol. 4, pp 187-204.

2. Hsieh, K.; Huang, A. H. C., Endoplasmic Reticulum, Oleosins, and Oils in Seeds and Tapetum Cells. *Plant Physiol.* **2004,** *136,* 3427-3434.

3. Yoshida, H.; Hirakawa, Y.; Murakami, C.; Mizushina, Y.; Yamade, T., Variation in the content of tocopherols and distribution of fatty acids within soya bean seeds (Glycine max L.). *Journal of Food Composition and Analysis* **2003,** *16,* 429-440.

4. Huang, A. H. C., Oil Bodies and Oleosins in Seeds. In *Annu. Rev. Plant Physiol. Plant Mol. Biol.*, 1992; Vol. 43, pp 177-200.

5. Tzen, J.; Cao, Y.; Laurent, P.; Ratnayake, C.; Huang, A., Lipids, Proteins, and Structure of Seed Oil Bodies from Diverse Species. *Plant Physiol.* **1993,** *101,* 267-276.

6. Hsieh, K.; Huang, A. H. C., Lipid-rich tapetosomes in Brassica tapetum are composed of oleosin-coated oil droplets and vesicles, both assembled in and then detached from the endoplasmic reticulum. *The Plant Journal* **2005,** *43,* 889-899.

7. Frandsen, G. I.; Mundy, J.; Tzen, J. T. C., Oil bodies and their associated proteins, oleosin and caleosin. *Physiol. Plant.* **2001,** *112,* 301-307.

8. Ting, J. L.; Lee, K.; Ratnayake, C.; Platt, K.; Balsamo, R.; Huang, A. C., Oleosin genes in maize kernels having diverse oil contents are constitutively expressed independent of oil contents. *Planta* **1996,** *199,* 158-165.

9. Siloto, R. M.; Findlay, K.; Lopez-Villalobos, A.; Yeung, E. C.; Nykiforuk, C. L.; Moloney, M. M., The accumulation of oleosins determines the size of seed oilbodies in Arabidopsis. *Plant Cell* **2006,** *18,* 1961-74.

10. Shimada, T. L.; Shimada, T.; Takahashi, H.; Fukao, Y.; Hara-Nishimura, I., A novel role for oleosins in freezing tolerance of oilseeds in Arabidopsis thaliana. *Plant J.* **2008,** *55,* 798-809.

11. Iwanaga, D.; Gray, D. A.; Fisk, I. D.; Decker, E. A.; Weiss, J.; McClements, D. J., Extraction and Characterization of Oil Bodies from Soy Beans: A Natural Source of Pre-Emulsified Soybean Oil. *J. Agric. Food. Chem.* **2007,** *55,* 8711-8716.

12. Beisson, F.; Ferté, N.; Bruley, S.; Voultoury, R.; Verger, R.; Arondel, V., Oil-bodies as substrates for lipolytic enzymes. *Biochimica et Biophysica Acta (BBA) - Molecular and Cell Biology of Lipids* **2001,** *1531,* 47-58.

13. Jolivet, P.; Roux, E.; d'Andrea, S.; Davanture, M.; Negroni, L.; Zivy, M.; Chardot, T., Protein composition of oil bodies in Arabidopsis thaliana ecotype WS. *Plant Physiol. Biochem.* **2004,** *42,* 501-509.

14. Bair, C. W.; Snyder, H. E., Electron microscopy of soybean lipid bodies. *J. Am. Oil Chem. Soc.* **1980,** *57,* 279-282.

15. Huang, A. H. C., Oleosins and Oil Bodies in Seeds and Other Organs. *Plant Physiol.* **1996,** *110,* 1055-1061.

16. Abell, B. M.; Holbrook, L. A.; Abenes, M.; Murphy, D. J.; Hills, M. J.; Moloney, M. M., Role of the proline knot motif in oleosin endoplasmic reticulum topology and oil body targeting. *Plant Cell* **1997,** *9*, 1481-93.

17. Joscelyne, S. M.; Trägårdh, G., Membrane emulsification — a literature review. *J. Membr. Sci.* **2000,** *169*, 107-117.

18. Kelly, A. A.; Quettier, A. L.; Shaw, E.; Eastmond, P. J., Seed storage oil mobilization is important but not essential for germination or seedling establishment in Arabidopsis. *Plant Physiol.* **2011,** *157*, 866-75.

19. Theodoulou, F. L.; Eastmond, P. J., Seed storage oil catabolism: a story of give and take. *Curr. Opin. Plant Biol.* **2012,** *15*, 322-328.

20. Graham, I. A., Seed storage oil mobilization. In *Annu. Rev. Plant Biol.*, Annual Reviews: Palo Alto, 2008; Vol. 59, pp 115-142.

21. Farese Jr, R. V.; Walther, T. C., Lipid Droplets Finally Get a Little R-E-S-P-E-C-T. *Cell* **2009,** *139*, 855-860.

22. Greenberg, A. S.; Egan, J. J.; Wek, S. A.; Garty, N. B.; Blanchette-Mackie, E. J.; Londos, C., Perilipin, a major hormonally regulated adipocyte-specific phosphoprotein associated with the periphery of lipid storage droplets. *J. Biol. Chem.* **1991,** *266*, 11341-11346.

23. Tansey, J.; Sztalryd, C.; Hlavin, E.; Kimmel, A.; Londos, C., The Central Role of Perilipin A in Lipid Metabolism and Adipocyte Lipolysis. *IUBMB Life* **2004,** *56*, 379-385.

24. Anton, M., Recent advances concerning the functional properties of egg yolk low-density lipoproteins. **2006**, paper 352.

25. Lopez, C., Milk fat globules enveloped by their biological membrane: Unique colloidal assemblies with a specific composition and structure. *Current Opinion in Colloid & Interface Science* **2011,** *16*, 391-404.

26. Martinet, V.; Saulnier, P.; Beaumal, V.; Courthaudon, J.-L.; Anton, M., Surface properties of hen egg yolk low-density lipoproteins spread at the air-water interface. *Colloids Surf. B. Biointerfaces* **2003,** *31*, 185-194.

27. Waschatko, G.; Schiedt, B.; Vilgis, T. A.; Junghans, A., Soybean Oleosomes Behavior at the Air–Water Interface. *The Journal of Physical Chemistry B* **2012,** *116*, 10832-10841.

28. Dauphas, S.; Beaumal, V.; Riaublanc, A.; Anton, M., Hen Egg Yolk Low-Density Lipoproteins Film Spreading at the Air−Water and Oil−Water Interfaces. *J. Agric. Food. Chem.* **2006,** *54*, 3733-3737.

29. White, D. A.; Fisk, I. D.; Makkhun, S.; Gray, D. A., In Vitro Assessment of the Bioaccessibility of Tocopherol and Fatty Acids from Sunflower Seed Oil Bodies. *J. Agric. Food. Chem.* **2009,** *57*, 5720-5726.

30. Fisk, I.; Linforth, R.; Taylor, A.; Gray, D., Aroma encapsulation and aroma delivery by oil body suspensions derived from sunflower seeds (Helianthus annus). *Eur. Food Res. Technol.* **2011,** *232*, 905-910.

31. Botaneco, C. Hydresia®. http://www.advitech.com/index-10.html

32. Maguire, L. S.; O'Sullivan, S. M.; Galvin, K.; O'Connor, T. P.; O'Brien, N. M., Fatty acid profile, tocopherol, squalene and phytosterol content of walnuts, almonds, peanuts, hazelnuts and the macadamia nut. *Int. J. Food Sci. Nutr.* **2004,** *55*, 171-8.

33. Gallier, S.; Singh, H., Behavior of almond oil bodies during in vitro gastric and intestinal digestion. *Food & Function* **2012,** *3*, 547-555.

34. Gallier, S.; Tate, H.; Singh, H., In Vitro Gastric and Intestinal Digestion of a Walnut Oil Body Dispersion. *J. Agric. Food. Chem.* **2012,** *61*, 410-417.

35. Capuano, F.; Beaudoin, F.; Napier, J. A.; Shewry, P. R., Properties and exploitation of oleosins. *Biotechnol. Adv.* **2007,** *25*, 203-206.

36. Kapchie, V. N.; Hauck, C. C.; Wang, H.; Murphy, P. A., Process Improvement for Semipurified Oleosomes on a Pilot-Plant Scale. *J. Food Sci.* **2011,** *76*, C853-C860.

37. Campbell, K. A.; Glatz, C. E.; Johnson, L. A.; Jung, S.; Moura, J. M. N.; Kapchie, V.; Murphy, P., Advances in Aqueous Extraction Processing of Soybeans. *J. Am. Oil Chem. Soc.* **2011,** *88*, 449-465.

38. Kapchie, V. N.; Wei, D.; Hauck, C.; Murphy, P. A., Enzyme-Assisted Aqueous Extraction of Oleosomes from Soybeans (Glycine max). *J. Agric. Food. Chem.* **2008,** *56*, 1766-1771.

39. Towa, L.; Kapchie, V.; Wang, G.; Hauck, C.; Wang, T.; Murphy, P., Quantity and Quality of Free Oil Recovered from Enzymatically Disrupted Soybean Oleosomes. *J. Am. Oil Chem. Soc.* **2011,** *88*, 1581-1591.

40. Kapchie, V. N.; Towa, L. T.; Hauck, C.; Murphy, P. A., Evaluation of enzyme efficiency for soy oleosome isolation and ultrastructural aspects. *Food Res. Int.* **2010,** *43*, 241-247.

41. Kapchie, V.; Towa, L.; Hauck, C.; Murphy, P., Recycling of Aqueous Supernatants in Soybean Oleosome Isolation. *J. Am. Oil Chem. Soc.* **2010,** *87*, 223-231.

42. Ternes, W., *Naturwissenschaftliche Grundlagen der Lebensmittelzubereitung*. Behr: Hamburg, 1994.

43. Rackis, J. J.; Sessa, D. J.; Honig, D. H., Flavor problems of vegetable food proteins. *Journal of the American Oil Chemists' Society* **1979,** *56*, 262-271.

44. Guo, S.-T.; Ono, T., The Role of Composition and Content of Protein Particles in Soymilk on Tofu Curding by Glucono-δ-lactone or Calcium Sulfate. *J. Food Sci.* **2005,** *70*, C258-C262.

45. Chen, Y.; Ono, T., The Mechanisms for Yuba Formation and Its Stable Lipid. *J. Agric. Food. Chem.* **2010,** *58*, 6485-6489.

46. Chen, Y.; Ono, T., Simple Extraction Method of Non-allergenic Intact Soybean Oil Bodies That Are Thermally Stable in an Aqueous Medium. *J. Agric. Food. Chem.* **2010,** *58*, 7402-7407.

47. Masilamani, M.; Commins, S.; Shreffler, W., Determinants of Food Allergy. *Immunology and Allergy Clinics of North America* **2012,** *32*, 11-33.

48. Iwanaga, D.; Gray, D.; Decker, E. A.; Weiss, J.; McClements, D. J., Stabilization of Soybean Oil Bodies Using Protective Pectin Coatings Formed by Electrostatic Deposition. *J. Agric. Food. Chem.* **2008,** *56*, 2240-2245.

49. Tzen, J. T. C.; Peng, C.-C.; Cheng, D.-J.; Chen, E. C. F.; Chiu, J. M. H., A New Method for Seed Oil Body Purification and Examination of Oil Body Integrity Following Germination. *J. Biochem.* **1997,** *121*, 762-768.

50. Waschatko, G.; Junghans, A.; Vilgis, T. A., Soy milk oleosome behaviour at the air-water interface. *Faraday Discuss.* **2012,** *158*, 157-169.

51. Consortium, T. U., Reorganizing the protein space at the Universal Protein Resource (UniProt). *Nucleic Acids Res.* **2012,** *40*, D71-D75.

52. Jung, S.; Rickert, D. A.; Deak, N. A.; Aldin, E. D.; Recknor, J.; Johnson, L. A.; Murphy, P. A., Comparison of kjeldahl and dumas methods for determining protein contents of soybean products. *J. Am. Oil Chem. Soc.* **2003,** *80*, 1169-1173.

53. Bradford, M. M., A rapid and sensitive method for the quantitation of microgram quantities of protein utilizing the principle of protein-dye binding. *Anal. Biochem.* **1976,** *72*, 248-254.

54. Tzen, J. T. C.; Cao, Y. Z.; Laurent, P.; Ratnayake, C.; Huang, A. H. C., *Plant Physiol.* **1993,** *101*, 267.

55. Beisson, F.; Ferté, N.; Voultoury, R.; Arondel, V., Large scale purification of an almond oleosin using an organic solvent procedure. *Plant Physiol. Biochem.* **2001,** *39*, 623-630.

56. Towa, L.; Kapchie, V.; Hauck, C.; Wang, H.; Murphy, P., Pilot Plant Recovery of Soybean Oleosome Fractions by an Enzyme-Assisted Aqueous Process. *J. Am. Oil Chem. Soc.* **2011,** *88*, 733-741.

57. Wu, N.-n.; Yang, X.-q.; Teng, Z.; Yin, S.-w.; Zhu, J.-h.; Qi, J.-r., Stabilization of soybean oil body emulsions using κ, ι, λ-carrageenan at different pH values. *Food Res. Int.* **2011,** *44*, 1059-1068.

58. Wu, N.-N.; Huang, X.; Yang, X.-Q.; Guo, J.; Yin, S.-W.; He, X.-T.; Wang, L.-J.; Zhu, J.-H.; Qi, J.-R.; Zheng, E.-L., In Vitro Assessment of the Bioaccessibility of Fatty Acids and Tocopherol from Soybean Oil Body Emulsions Stabilized with ι-Carrageenan. *J. Agric. Food. Chem.* **2012,** *60*, 1567-1575.

59. Alexander, L.; Sessions, R.; Clarke, A.; Tatham, A.; Shewry, P.; Napier, J., Characterization and modelling of the hydrophobic domain of a sunflower oleosin. *Planta* **2002,** *214*, 546-551.

60. Lacey, D. J.; Wellner, N.; Beaudoin, F.; Napier, J. A.; Shewry, P. R., Secondary structure of oleosins in oil bodies isolated from seeds of safflower (Carthamus tinctorius L.) and sunflower (Helianthus annuus L.). *Biochem. J* **1998,** *334*, 469-477.

61. Purkrtova, Z.; Jolivet, P.; Miquel, M.; Chardot, T., Structure and function of seed lipid body-associated proteins. *C. R. Biol.* **2008,** *331*, 746-754.

62. Li, M.; Murphy, D. J.; Lee, K.-H. K.; Wilson, R.; Smith, L. J.; Clark, D. C.; Sung, J.-Y., Purification and Structural Characterization of the Central Hydrophobic Domain of Oleosin. *J. Biol. Chem.* **2002,** *277*, 37888-37895.

63. Samoto, M.; Maebuchi, M.; Miyazaki, C.; Kugitani, H.; Kohno, M.; Hirotsuka, M.; Kito, M., Abundant proteins associated with lecithin in soy protein isolate. *Food Chem.* **2007,** *102*, 317-322.

64. Vinarov, Z.; Petkova, Y.; Tcholakova, S.; Denkov, N.; Stoyanov, S.; Pelan, E.; Lips, A., Effects of Emulsifier Charge and Concentration on Pancreatic Lipolysis. 1. In the Absence of Bile Salts. *Langmuir* **2012,** *28*, 8127-8139.

65. van Nieuwenhuyzen, W.; Tomás, M. C., Update on vegetable lecithin and phospholipid technologies. *Eur. J. Lipid Sci. Technol.* **2008,** *110*, 472-486.

66. Scholfield, C. R., Composition of soybean lecithin. *J. Am. Oil Chem. Soc.* **1981,** *58*, 889-892.

67. AvantiPolarLipids http://avantilipids.com/index.php?option=com_content&view=article&id=110&Itemid=118

68. Gunstone, F. D.; Harwood, J. L.; Dijkstra, A. J., *The Lipid Handbook:*

With CD-Rom. 3rd ed.; CRC Press: 2007

69. Römpp, T. http://www.roempp.com/prod/

70. Wosten, H.; De Vries, O.; Wessels, J., Interfacial Self-Assembly of a Fungal Hydrophobin into a Hydrophobic Rodlet Layer. *The Plant Cell Online* **1993,** *5*, 1567-1574.

71. Kaganer, V. M.; Möhwald, H.; Dutta, P., Structure and phase transitions in Langmuir monolayers. *Reviews of Modern Physics* **1999,** *71*, 779-819.

72. Möhwald, H., Phospholipid and Phospholipid-Protein Monolayers at the Air/Water Interface. *Annu. Rev. Phys. Chem.* **1990,** *41*, 441-476.

73. Dahmen-Levison, U.; Brezesinski, G.; Möhwald, H., Specific adsorption of PLA2 at monolayers. *Thin Solid Films* **1998,** *327–329*, 616-620.

74. Poth, U., Drying Oils and Related Products. In *Ullmann's Encyclopedia of Industrial Chemistry*, Wiley-VCH Verlag GmbH & Co. KGaA: 2000.

75. Wabel, C., Influence of lecithin on structure and stability of parenteral fat emulsions. *PhD Thesis. Friedrich-Alexander-University, Erlangen-Nürnberg, Germany.* **1998**.

76. Leprince, O.; van Aelst, A. C.; Pritchard, H. W.; Murphy, D. J., Oleosins prevent oil-body coalescence during seed imbibition as suggested by a low-temperature scanning electron microscope study of desiccation-tolerant and -sensitive oilseeds. *Planta* **1997,** *204*, 109-119.

77. Day, J. P. R.; Rago, G.; Domke, K. F.; Velikov, K. P.; Bonn, M., Label-Free Imaging of Lipophilic Bioactive Molecules during Lipid Digestion by Multiplex Coherent Anti-Stokes Raman Scattering Microspectroscopy. *J. Am. Chem. Soc.* **2010,** *132*, 8433-8439.

78. Vinarov, Z.; Tcholakova, S.; Damyanova, B.; Atanasov, Y.; Denkov, N. D.; Stoyanov, S. D.; Pelan, E.; Lips, A., Effects of Emulsifier Charge and Concentration on Pancreatic Lipolysis: 2. Interplay of Emulsifiers and Biles. *Langmuir* **2012,** *28*, 12140-12150.

79. Kiosseoglou, V., Egg yolk protein gels and emulsions. *Current Opinion in Colloid & Interface Science* **2003,** *8*, 365-370.

80. Moy, V. T.; Keller, D. J.; Gaub, H. E.; McConnell, H. H., Long-range molecular orientational order in monolayer solid domains of phospholipid. *The Journal of Physical Chemistry* **1986,** *90*, 3198-3202.

6. ERKLÄRUNG ZUM ANTEIL AN DEN FOLGENDEN WISSENSCHAFTLICHEN PUBLIKATIONEN

Die Extraktion der Oleosomen unter den in 1.5.1 aufgeführten Parametern wurde von mir etabliert und für die beschriebenen Messungen und Analytiken selbst durchgeführt. Die Kinetiken und Isothermen an der Filmwaage und die BAM-Aufnahmen wurden anfänglich unter Anleitung von Dr. Ann Junghans aufgenommen. Außer Abbildung 4, 5, und 6 in Publikation 1 (*27*) wurden alle weiteren Messungen selbstständig durchgeführt und ausgewertet. Die dritte Publikation war eine Zusammenarbeit mit den aufgeführten Autoren unter meiner allgemeinen Anleitung und Konzeptionierung. Im speziellen war die Zusammenarbeit und Durchführung der Versuche nach Methoden: Partikelgrößenbestimmung und Zeta-Potential (Sania Maurer), Rheologie (Dr. Birgitta Schiedt), Spektroskopie (Dr. Denise Schach, Dr. Tobias Weidner, AK Bonn) und Lipidanalytik (Jakob Dahl).

7. DANKSAGUNG

Ich danke Prof. Dr. Thomas A. Vilgis für die Möglichkeit diese Arbeit in seinem Arbeitskreis anzufertigen, außerdem für seine Unterstützung und die Vermittlung von wissenschaftlichen und kulinarischen Wissen und Inhalten.

Prof. Dr. Gerald Gimpl danke ich für die Begutachtung und Mitbetreuung dieser Arbeit und Hilfestellungen bei biochemischen Fragestellungen.

Dr. Birgitta Schiedt und Dr. Ann Junghans danke ich für die Einarbeitung in verschiedene Physikalische Methoden und die Beratung und Diskussionen bei der Interpretation der Ergebnisse.

Dr. Denise Schach, Dr. Nils Billecke, Martin Scherer und Sania Maurer danke ich für die gute Zusammenarbeit und die gemeinsam durchgeführten Versuche.

Unseren Praktikanten und „HiWis“ Natalie Russ, Lydia Krebs, Jakob Dahl, Henriette Jaurich und Marta Ghebremedhin danke ich vielmals für ihre Arbeit und Mithilfe.

Den Projektleitern Dr. Sapun Parekh, Dr. Christine Peter, Dr. Tobias Weidner danke ich für ihre Beratung und die gute Zusammenarbeit.

Besonders möchte ich Prof. Kremer und dem ganzen Arbeitskreis „Theorie der Polymere“, sowie allen Mitarbeitern des MPI für Polymerforschung für die schöne Zeit danken.

8. PUBLIKATIONEN

1 Waschatko, G.; Schiedt, B.; Vilgis, T. A.; Junghans, A., Soybean Oleosomes Behavior at the Air–Water Interface. *The Journal of Physical Chemistry B* 2012, 116 (35), 10832-10841

THE JOURNAL OF PHYSICAL CHEMISTRY B

Article

pubs.acs.org/JPCB

Soybean Oleosomes Behavior at the Air−Water Interface

Gustav Waschatko,[†,‡,*] Birgitta Schiedt,[†] Thomas A. Vilgis,[†] and Ann Junghans[†]

[†]Max Planck Institute for Polymer Research, Ackermannweg 10, 55128 Mainz, Germany

[‡]Institut für Pharmazie und Biochemie, Johannes Gutenberg Universität Mainz, Johann-Joachim-Becher-Weg 30, 55128 Mainz, Germany

Web-Enhanced Feature

ABSTRACT: Soy milk is a highly stable emulsion, the stability being mainly due to the presence of oleosomes or oil bodies, spherical structures filled with triacylglycerides (TAGs) and surrounded by a monolayer of phospholipids and proteins called oleosins. For oleosomes purified from raw soymilk, surface pressure investigations and Brewster angle microscopy have been performed to unveil their adsorption, rupture and structural changes over time at different subphase conditions (pH, ionic strength). Such investigations are important for (industrial) food applications of oleosomes, but are also useful for the understanding of the general behavior of proteins and phospholipids at interfaces. In addition a better comprehension of the highly stable oleosomes can lead to advancements in liposome manufacturing, e.g., for storage and transport applications. Although oleosomes have their origin in food systems, their unique stability and physical behavior show transferable characteristics which lead to a much better understanding of the description of any kind of emulsion. This study is one of the first steps toward the comparison of natural emulsification concepts based on different physical structures: e.g., the animals' low density lipoproteins, where apolipoproteins with phospholipids are located only at the interface and plant oleosomes with its oleosins, which are embedded in a phospholipid monolayer and reach deep inside the oil phase.

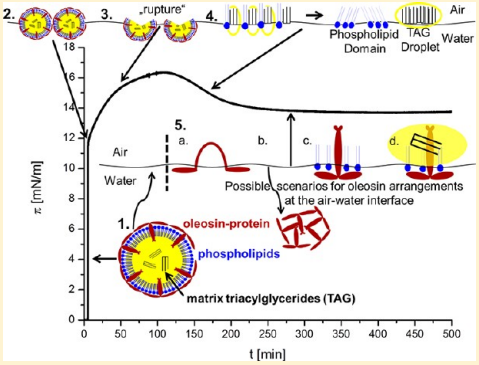

INTRODUCTION

Emulsions, e.g., mixtures of typically immiscible liquids such as water and triacylglycerides, contain stable droplets of oil immersed in water, which are stabilized by emulsifiers. "Classical" emulsifiers are based on the interface activity of their hydrophilic and hydrophobic (lipophilic) part. Obviously, this arrangement and their polarity define their emulsifying capacity usually expressed by the HLB (hydrophilic−lipophilic balance) value.[1] The charge of the hydrophilic part depends on the pH-value and the ionic strength of the solution, which thereby defines the stability of the emulsion. Of course, the nature of the emulsifying process is determined by the architecture of the surface active molecules. Whereas in phospholipid stabilized systems, a simple head−tail structure is sufficient, emulsifying proteins need a certain primary structure to produce a relevant surface activity (see, for example, refs 2−4). Although nature has a limited amount of natural emulsifiers, i.e., phospholipids and proteins, evolution has developed different native structures to solubilize oil in water via small droplets: in animals lipoproteins (HDL = high-density lipoprotein, LDL = low-density lipoprotein, chylomicrometers), in milk lipid or fat globules, in plants oleosomes or oil bodies (OB).[5−7] For example, on closer examination the lipid droplets produced in animals are completely different with regards to their surface proteins than plant oleosomes. One very high mass apolipoprotein, e.g., hen apolipoprotein B (UniProtKB: Q197x2) in egg yolk, with its 4631 amino acids wound around the whole particle, is located more or less close to the surface made of phospholipids.[8,9] Thus, it significantly constrains the dynamics of the phospholipids in the domains close to the proteins. The benefit of the apolipoproteins is therefore obvious; they yield more stable droplets than "classical" emulsions where only phospholipids are used.

Nevertheless, oleosomes appear even more stable than LDL-particles, for example from egg yolk. The reason is a different arrangement of stabilizing proteins. Basically, oleosomes can be viewed as micelle-like structures with an outer phospholipid monolayer, an interior filled with TAGs (triacylglycerides), and associated proteins, the so-called oleosins (Figure 7).[7] Oleosins are alkaline proteins of 15−30 kDa expressed during seed development and maturation and presumably play a major role in the stability of oil bodies.[10] In contrast to the apolipoproteins in LDL particles these oleosins are not just located on the surface but are most likely anchored with their central hydrophobic stretch deep in the oil-phase (Figure 7). This assumption regarding the location of the hydrophobic domain, as well as the existence of a prolin knot forming a 180° turn of a "hairpin"-like sequence, are commonly accepted.[11] However, the secondary structure of the longest hydrophobic sequence known to date (about 70 amino acids) is not yet fully determined and is debated to be either antiparallel β-strands[12] or α-helical[13]. The N- and C-terminal domains are more

Received: December 9, 2011
Revised: July 20, 2012
Published: July 23, 2012

hydrophilic (e.g., amphipathic α-helix[10]), most probably remain umbrella-like outside of the oleosome, and are less conserved among plant species. The physics of the oil bodies is relatively complicated. In soybeans there are four oleosins with evidence at transcript level (UniProtKB, Isoforms P29530 and P29531 23−24 kDa; C3VHQ8, 17−18 kDa; C6SZ13, 15−16 kDa). Hence, the isoelectric point (pI) of soybean oleosomes is not sharp due to slight variations of the amino acid composition and distribution of the hydrophilic part (umbrella) of the different oleosins on their surface.

As already mentioned regarding their impact on coalescence, oil bodies of seeds seem to be the most efficient compared to other natural lipid storage organelles, probably due to the required protection against environmental stress during dormancy and germination. In accordance, soy lecithin gives more stable emulsions than egg lecithin.[14] Nevertheless, the usage of intact oil bodies in food products, food processing, and even cooking (e.g., desserts, instant drinks, salad dressing) has not yet commenced, especially in the western world, whereas egg yolk, cream, and other dairy products are very common in food emulsions. For TAGs and phospholipids (soy lecithin), the two main components of the oil bodies, the situation is reversed: compared to animal fat sources, their usage and popularity is higher. More and more animal fat is replaced by vegetable oil, and soy lecithin is the main emulsifier in processed food, for example in chocolate, bakery products, desserts, margarine, or creams. A more practical approach would be to use entire and intact oleosomes in food systems. One possible explanation for this neglect could be that the interest in oil bodies only quite recently changed from a botanical point of view to possible food applications. In 2007, Iwanaga et al.[15] showed the extraordinary stability of oil bodies against heat (90 °C), pH and salt concentrations in the bulk. Chen et al.[16] recently described the role of oleosomes for the formation of yuba, the "skin" formed on soy liquids. This traditional Asian soybean food product is formed as a film-like structure on the surface of heated soymilk.

Moreover, oleosomes are also attractive for genetic engineering and biotechnology, where they are used as plant expression system for recombinant proteins or peptides, e.g., antibodies or vaccines. The protein−oleosin fusions are enriched in the seed oil bodies, which are easy to harvest via flotation-centrifugation and, after cleavage, eukaryotic proteins without potential contamination of animal pathogens are obtained.[11] In addition, as the oil content of soybeans is around 20%, there is a high amount of oleosomes and oleosins available from soybean crops. Improvements with regards to the yield and the upscaling of the oleosome extraction process are promoted by researchers involved in the aqueous extraction of soybean oil.[17]

In summary, the understanding and controllability of the stability of soybean oleosomes are of interest for various applications, such as in food industry, biotechnology or basic research. Presumably, their beneficial behavior originates from their protective function. Oleosomes are oil bodies and function as lipid storage organelles in plants, e.g., in seeds.[7]

To better understand the nature of the oleosomes, systematic experiments have been performed in this study. First, oleosomes are purified at pH 11 similar to a procedure introduced by Chen and Ono.[18] Subsequently, oleosomes are investigated at the air−water interface of a film balance. This procedure allows studying the stability and the behavior of their three different constituents, i.e., the oleosins, the phospholipids and the TAGs. This method offers two basic types of measurements. First, kinetics are recorded, which show the instability and the "destruction" of the oleosomes at the air−water interface and second, the behavior of the oleosomes and their constituents under two-dimensional pressure is studied. Consequently, we can expect several physical scenarios. Oil bodies immersed in the subphase will rise to the surface. First, some oleosomes may stay intact and agglomerate at the interface. Others break up into a phase of TAGs, phospholipids and oleosins. The oil spreads on the surface as a film or droplets. The phospholipids separate from the oil droplets and either move straight to the air−water interface or form micelles in the subphase. Depending on their concentration and charge state on the surface, oleosins can aggregate or assemble in different conformations and arrangements with the surrounding lipids on the surface (Figure 7). Of course, these processes are influenced by many parameters, such as the pH-value and ionic strength, especially as proteins are involved, since their behavior depends strongly on their charge defined by their amino acids exposed to the aqueous environment.

Thus, when the oleosomes are (partially) destroyed at the air−water interface, four different components with competing interactions determine the physical picture at compression of the barriers of the film balance: TAG's, phospholipids, partially denatured oleosins, and still intact oil bodies, which will have different contributions to the area vs surface pressure relation. Depending on their concentration phospholipids will form different phases at the surface (see for example[19−23]), TAGs will partially wet[24] the interface, and oleosins can arrange in different configurations as shown in Figure 7.

So far, many advances[25−27] have been made to study isolated oleosins but as the purification process is difficult due to the high stability of the oil bodies, detergents[28,29] or chaotropic agents have to be used which might influence the protein structure and conformation and hence, no certain facts could be elucidated. However, the knowledge gained during the research of LDL particles can be of help here. In 2003, Martinet et al.[5] published a study on the "Surface properties of hen egg yolk low-density lipoproteins spread at the air−water interface" to investigate the surface active behavior of low-density lipoproteins and their lipid components to clarify the role of each constituent in the lipoprotein film. This approach may also be used to study the adsorption mechanism and surface organization of oleosomes at the air−water interface which should provide useful information about the otherwise difficult to access oleosins.

The physical scenarios of the suggested oleosome behavior are on the one hand supported by observations on hen egg yolk LDL-particles, as it was studied previously. On the other hand, Bonsegna et al.[30] reported that oil bodies purified from hazelnut and almond seeds exhibited a strong surface-active layer at the air−water interface, increasing the surface pressure to around 15 mN/m (available surface area not given), which is supposedly due to a migration of OB to the interface and the subsequent formation of a surface film. These authors report of a floating 2D film surrounding 3D domains of large and brilliant aggregates, visualized with Brewster angle microscopy, which they attribute to the formation of a fluid phospholipid monolayer, where intact oil bodies or oil body aggregates can be dynamically embedded. Bonsegna et al. conclude that the 3D aggregates coalesce with time and that simultaneously new oil bodies from the bulk of the aqueous subphase are reaching the interface, since the surface pressure remains practically

constant over time at constant surface area. They also claim that the 3D aggregates become progressively larger and brighter.

Brewster angle microscopy (BAM) is therefore the method of choice to visualize areas of different brightness due to a different molecular density and/or refractive index in a thin interfacial layer and has long been used to study, for example, lipids, proteins and mixed systems at the air−water interface.[31−34] This technique is indeed a very useful tool in the characterization of the interfacial behavior of oleosomes as no marking is necessary to visualize them. Also, the surface pressure is recorded simultaneously to the BAM micrographs, so the changes in surface tension can be correlated directly with the surface active components seen by BAM.

In the present paper, oleosomes purified from soybeans have been studied at the air−water interface at different subphase conditions to determine the effects behind oleosome stability. Such investigations are prerequisites to better understand the principal function of oleosins and are additionally of interest for food technological applications or carriers. As oleosins tend to form insoluble protein aggregates after being dissolved from the oil bodies, it would be highly desirable for industrial applications to develop methods that prevent this aggregation after oleosin purification.

MATERIALS AND METHODS

For all preparation steps, ultrapure water, filtered with a Millipore device (Billerica, MA/USA) was used and all experiments were carried out at room temperature.

Oleosome Purification. Isolation of soybean oleosomes was performed by a modified aqueous flotation-centrifugation method proposed by Chen and Ono.[17] Dried soybeans (Davert GmbH) were soaked in deionized water at 4 °C for at least 20 h. Then water was added to obtain a 10% soybean-to-water ratio, which was grounded in a Vorwerk Thermomix TM31 at highest speed (10,200 rpm) for 90 s. The resulting slurry was filtered through two layers of Kimtech science precision wipes 21 × 11 cm (Kimberly Clark) to obtain raw soymilk. 25% Sucrose (w/w) was added to the raw soymilk and the pH was adjusted to 11.0 with 1 mol/L NaOH (AVS Titrinorm, Prolabo/VWR) solution. The solution was filled into six 50 mL centrifuge tubes (Roth), which were centrifuged in a Thermo Heraeus Multifuge X1R with 15000xg at 4 °C for at least 5 h. The resulting floating fractions (creamlayer, fat pat, oleosomes) were lifted with a small spoon and resuspended in 45 mL of 20% (w/w) sucrose in deionized water (pH 11) in a new centrifuge tube. After anew centrifugation (15000xg, 4 °C, 5 h), this washing step was repeated once more. The resulting oleosomes were collected and dispersed in 20 mL of deionized water and dialyzed overnight with Thermo Scientific Slide-A-Lyzer G2 Dialysis Cassettes (20K MWCO). The final oleosome emulsion had a water content of 86−88%.

Sodium Dodecyl Sulfate−Polyacrylamide Gel Electrophoresis (SDS-PAGE). The SDS-PAGE was performed with the invitrogen NuPAGE-System. NuPAGE MES-Running Buffer and a 10% NuPAGE Novex Bis-Tris Mini Gel were applied according to the manufacturer's instructions but without heating the samples (diluted dialyzed oleosomes). Instead, they were solubilized overnight at room temperature with the NuPageLDS Sample Buffer and the NuPageLDS Reducing Agent. Further defatting of the samples was not necessary.

For the visualization of the protein bands Coomassie G-250 SimplyBlue SafeStain (invitrogen) was used. After staining for 1 h, the polyacrylamide gel was destained twice with ultrapure water for 1 h and subsequently overnight.

Buffer. For buffered subphases, the following chemicals were used: Phosphoric acid, ACS reagent, (Sigma-Aldrich, Munich/Germany, ≥85 wt % in H_2O), acetic acid (Sigma-Aldrich, Munich/Germany, ≥99.8%), monosodium phosphate (Fluka, Munich/Germany, ≥99%), MES/2-(*N*-morpholino)-ethanesulfonic acid (Carl Roth, Karlsruhe/Germany ≥99%) and Tris/Tris(hydroxymethyl)-aminomethane (Sigma-Aldrich, Steinheim/Germany, 99+%). For varying the ionic strength, the molarity of the buffer was kept constant and the required amount of sodium chloride (Prolabo/VWR, Darmstadt/Germany min. 99.5%) was added.

Film Balance. The surface pressure was measured as a function of time (Kinetics) and surface area (Isotherms) on a Nima (Biolin Scientific, Västra Frölunda/Sweden) BAM Trough (available area at completely opened barriers = 715 cm^2), with symmetric Delrin twin barriers. The trough was equipped with a surface pressure sensor that uses the Wilhelmy plate technique to determine the change in surface tension of the air−water interface in the presence of surfactant molecules. In general, measurements were repeated at least 3 times for any given set of parameters with a very good agreement between the different measurements.

Kinetics. The surface pressure was recorded as a function of time at maximum surface area. Different oleosome concentrations were inserted into the subphase with a pipet (Eppendorf, Hamburg/Germany). Preliminary experiments have shown that no agitation was necessary to enable proper mixing of oleosomes in the subphase. The total volume of the trough was 500 mL.

Isotherms. Immediately after oleosome injection or subsequently to a kinetic measurement, the surface pressure was recorded as a function of area, hence monitoring the changes in surface tension upon compressing. The barrier compression speed was 30 cm^2/min.

Brewster Angle Microscopy. All BAM micrographs were taken on a EP^3−BAM (Nanofilm, Göttingen/Germany) with a lateral resolution of around 1 μm. The size of the micrographs was 600 × 500 μm^2 and images were not processed in any way except for background correction carried out with the provided software. Simultaneously, the surface pressure was recorded.

RESULTS AND DISCUSSION

Oleosome Purification and Characterization. The dialyzed oleosomes had a water content of 86−88%. Their mean diameter of 300−350 nm was measured by means of Dynamic Light Scattering (DLS), at room temperature and diluted in water, with a Nicomp particle sizer (model 380, PSS, Santa Barbara, CA) at a scattering angle of 90° (data not shown). The Coomassie stained SDS−PAGE (Figure 1) confirmed three proteins of 15−16, 17−18, and 23−24 kDa corresponding to approximately the size of the four soybean oleosins known in protein databases (UniProtKB, Isoforms P29530 and P29531 23−24 kDa; C3VHQ8, 17−18 kDa; C6SZ13, 15−16 kDa), when compared to the molecular weight marker (SeeBlue Plus2 Pre-Stained Standard, Invitrogen).

This confirms that pH 11 extraction removed the unspecific bounded soybean storage proteins (glycinin and β-conglycinin), and further potentially allergenic proteins (such as Gly m Bd 30K)[14] from the surface of the oleosomes as shown in the

dx.doi.org/10.1021/jp211871v | J. Phys. Chem. B 2012, 116, 10832−10841

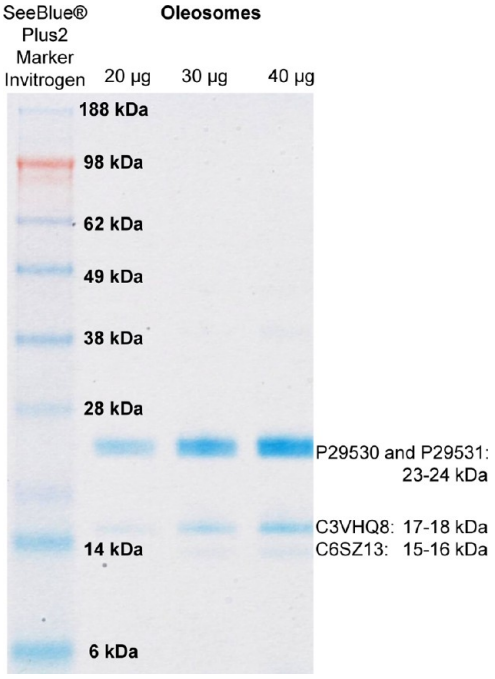

Figure 1. Coomassie-stained SDS–PAGE gel of purified and dialyzed soybean oleosomes in different quantities (20, 30, and 40 μg). Before loading the oleosome samples on the gel, they were solubilized with the NuPageLDS Sample Buffer and the NuPageLDS Reducing Agent overnight at room temperature.

SDS–PAGE. Compared to other oleosome purifications,[12] the oleosomes used here showed a very sharp aggregation behavior between pH 4.4 and 5.7 (data not shown).

Film Balance. Immediately after oleosome injection, the surface pressure increases from 0 mN/m to approximately 12 mN/m (Figure 2). Simultaneous BAM micrographs during these first seconds show a diffusion of round, very bright 3D particles in the size of the lateral resolution (approx. 1 μm) of the Brewster angle microscope to the air–water interface, presumably oleosomes (Figure 2C). This diffusion decelerates within the first minutes. This initial increase in surface pressure is independent of the subphase conditions but this is not the case for the following progression, which depends strongly on the oleosome concentration, pH and ionic strength of the subphase.

Oleosome Concentration. Surface pressure as a function of time with systematic variation of oleosome concentration is shown in Figure 2, revealing two different cases of surface pressure trends over time. At low concentrations ($\leq$0.4 mg/L), the surface pressure vs time shows a maximum, whereas at high concentrations ($\geq$0.8 mg/L), a slow but constant rise in surface pressure with time is observed. Apparently, between the concentration of 0.4 and 0.8 mg/L the behavior of the surface film changes drastically. Hence, 0.4 and 0.8 mg/L oleosome concentrations are discussed exemplarily for the two different scenarios of soybean oleosome behavior at the air–water interface:

When oleosomes of 0.4 mg/L concentration are added to the subphase, an initial steep rise of surface pressure up to 12 mN/m can be monitored and simultaneous BAM micrographs show round objects with a few micrometers in diameter at the air–water interface, presumably oleosomes. After this initial increase, the surface pressure increase flattens and the number of observed interfacial oleosomes decreases until a maximum pressure of approximately 16 mN/m is reached. This is the first indication of a rupture of the oleosomes during the rise of the surface pressure as this would lead to more components at the interface and subsequently higher surface pressures. When the pressure decreases beyond the maximum of the peak, no more oleosomes are observed by BAM, which further strengthens the rupture hypothesis. This decrease in surface pressure can be explained by the aggregation and descent of free oleosins and the subsequent formation of domains of free lipids.[35]

The onset of the surface pressure peak may occur at later times, but the described behavior is the same. We suppose this can be correlated with a different lifetime of intact oleosomes at the interface, which is dependent on air humidity, but future investigations are needed to verify this assumption.

For a better understanding of the composition of the interfacial film formed by a 0.4 mg/L oleosome concentration, isotherms were recorded before, on, and after the peak and BAM micrographs were taken (Figure 2C). When the area is decreased by compression before the surface pressure reached its maximum, hence prior to presumptive oleosome rupture, no phase transitions are visible in the isotherm. However, if the film is compressed at the peak of the surface pressure, a transition in the isotherm is observable at 20–25 mN/m, which becomes more pronounced for longer times (175 min compared to 75 min). Additionally, the longer the time between reaching the peak in the kinetic and compression of the film, the more precise the shape of this phase transition will be. This transition is supposedly due to free lipids (which are only available in significant quantities after most of the oleosomes are ruptured) and can get more distinct when lipids start to form domains. The latter is supported by the fact that structures resembling lipid domains are visible in the BAM pictures during the compression of 0.4 mN/m.

For higher concentrations, the same initial steep rise of surface pressure after oleosome injection as for low concentrations can be monitored. However, afterward, the surface pressure continues to rise slowly and BAM micrographs and isotherms are comparable to the ones described in more detail later (Phase Transitions after Different Times).

Figure 2B compares isotherms for these two different cases recorded at a "pseudo-equilibrium" stage after 5 h. For 0.4 mg/L, two phase transition are visible, one at 20–25 mN/m and one around 35 mN/m, while the isotherms of higher concentrations show only the latter around 35 mN/m. Because of the limited pressure range accessible for different concentrations, it is hard to determine whether the lower transition is just outside the accessible surface pressure range or is really not existent for higher concentrations due to a different film composition. However, isotherms at 0.8 mM/m after shorter kinetics as well as the different BAM micrographs recorded at intermediate surface pressures suggest a different film composition and strengthen the hypothesis that the lower transition only occurs for cases where the kinetic shows a maximum in the surface pressure. For the higher concentrations, distinctively different BAM micrographs are recorded during compression, showing structures indicating oleosin aggregates. Also a highly viscous film is formed. Before the isotherm reaches the plateau of 35–40 mN/m this protein film builds up layers which can be pulled out as thin viscoelastic strands at the end of the compression (Figure 2B). The previous phase behavior shows characteristics of a liquid

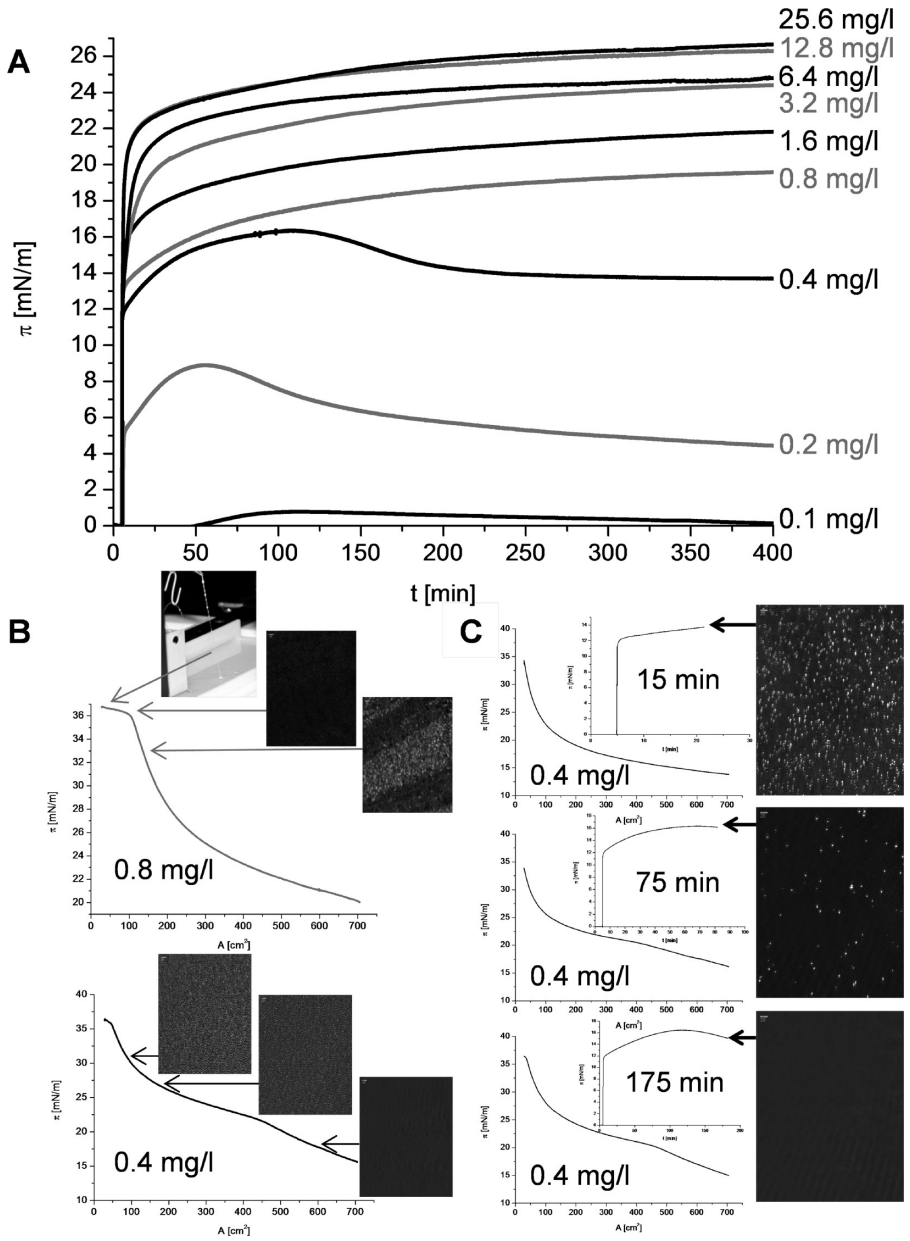

Figure 2. (A) Measurement of surface pressure as a function of time and for increasing oleosome concentrations ranging from 0.1 mg/L to 25.6 mg/L. Surface pressure of 0.1−0.4 mg/L oleosome concentration peaks at different times. Surface pressures of concentrations ≥0.8 mg/L are rising constantly during observation time with a maximum surface pressure of approximately 26 mN/m. (B) Isotherms (v_B = 30 cm²/min) and BAM micrographs of oleosome concentrations 0.4 and 0.8 mg/L after 5 h exhibit phase transitions at 20−25 mN/m and/or 35−40 mN/m. During compression lipid domains are visible in the BAM micrographs. For ≥0.8 mg/L oleosome concentration, aggregates occur and at the end of the compression thin viscoelastic strands can be pulled from the interface. (C) Kinetics and isotherms (v_B = 30 cm²/min) with BAM micrographs before, on, and after the surface pressure maxima indicating the rupture of oleosomes during the ascent and the formation of lipid domains during the descent. Conditions: 5 mM monosodium phosphate, pH 7.0; 3.36 μL (0.1 mg/L) to 859 μL (25.6 mg/L) of a 14902 mg/L dilution was introduced into the subphase of 500 mL.

expanded/liquid condensed coexistence[36] (LE/LC) of phospholipids.

Those observations let us assume that after oleosome injection, a two-step process takes place:

First, oleosomes diffuse to the air−water interface due to buoyant force, visible in the fast motion of very small objects and the increase in surface pressure. Bursting of oleosomes, which is faster for higher concentrations, results in further increase of surface pressure and a film of free lipids. After the peak, the formation of domains decreases the surface pressure, and if compressed, a clear phase transition and domains, very alike to phospholipid phase behavior during compression, can be observed. At low concentrations, no oleosin aggregates are visible in the BAM micrographs; presumably oleosins are soluble at the interface and/or in remaining lipid domains.

If, at the beginning, a bigger amount of oil bodies (≥0.8 mg/L) was added to the subphase than can be accommodated at the interface, oleosomes will follow when space gets available by domain formation or removal of oleosins to the subphase. This explains that the surface pressure is not decreasing with time for systems with higher concentrations of OB injected and aggregates are visible even after 1000 min of

dx.doi.org/10.1021/jp211871v | J. Phys. Chem. B 2012, 116, 10832−10841

waiting time. Additionally, oleosins are forced to aggregate and/or denature and form an interconnected film with the lipids that stays intact for a long time. This film hinders further diffusion of components (leading to larger domains) as well as a further diffusion of oleosin aggregates into the subphase, both resulting in a decrease in surface pressure. After the compression of this film, thin viscoelastic strands can be pulled out of the surface, but only if the oleosome concentration is ≥0.8 mg/L, a sufficient amount of time elapsed before compression (approximately 5 h) and at pH ≥ 5.

The reason for this is easily explainable as for concentrations ≥0.8 mg/L, the behavior of the surface film is strongly influenced by the charge of the oleosins, which is linked to the pH and the ionic strength of the subphase. Also the time before compression plays an important role.

Variation of pH. When the pH of the subphase differs from 5 (the pI of the oleosins) - in basic as well as acidic direction—the behavior after oleosome injection is similar to the one observed at the isoelectric point but the surface pressure, when the plateau stage is reached, is lower (Figure 3A). BAM micrographs after equal waiting time (60 min) after oleosome injection show much smaller particle sizes away from the isoelectric point compared to images made at pH 5 (Figure 3B). In accordance, the compression isotherms show higher area values for the higher surface pressure transition presumably related to a transition from LE to LE/LC region (Figure 3C). This is in very good accordance to the visibly smaller aggregate size as bigger, bulkier particles will lead to higher transition areas.

At subphase pHs away from the isoelectric point, the oleosins repel each other—the further away from pH 5, the stronger the repulsion—and are not able to pack as densely as uncharged oleosomes at pH 5. Thus, less free bindings can be saturated and the resulting surface pressure is lower.

In longtime kinetics for high oleosome concentrations, a second effect can be observed: for pH 8 as well as for pH 5 the surface pressure is slightly rising during the whole observation time, whereas for pH 2 the surface pressure peaks and drops afterward. This is correlated to the formation of the network-like film shown in Figure 2B, which occurs for pH 5 and 8, but not for pH 2. In the acidic regime, oleosins seem to be unable to form entanglements, because of a higher net charge. This might be related to the fact that oleosins continue to denature with time and thereby their pI is changed from around 5 to the alkaline regime. This is strengthened by the fact that they are alkaline proteins[10] with a theoretical pI for the soybean oleosins at: 8.02 (P29530), 8.89 (P29531), 7.75 (C3VHQ8) and 9.35 (C6SZ13). Hence, at pH 2 surface active substances might diffuse into the subphase and there is no barrier against phase separation and domain formation of the lipids, leading to a decrease in surface pressure. Digestion of the N- and C-termini of intact oleosomes also inhibits the integration of oleosins into a network-like interfacial film.[35]

Ionic Strength. As mentioned above, the ionic strength I of the subphase also has an effect on the surface active behavior if the oleosomes possess a charge.

At subphase pHs away from the isoelectric point, lower surface pressures are reached at smaller ionic strength at the same waiting times than for higher I. (Figure 4A)

This can be easily explained by the screening length of the salt ions. The higher the ionic strength I the smaller the Debye length ($\kappa \sim (1/I)^{1/2}$) and the better the charge of the oleosomes is screened. If the ionic strength is high enough that all charges are screened, no repulsion occurs and the oleosomes behave similar to uncharged oil bodies at pH 5, resulting in the same surface pressure after 60 min (compare Figure 3A and 4A), bigger aggregates (Figure 4B) and higher transition areas (Figure 4C).

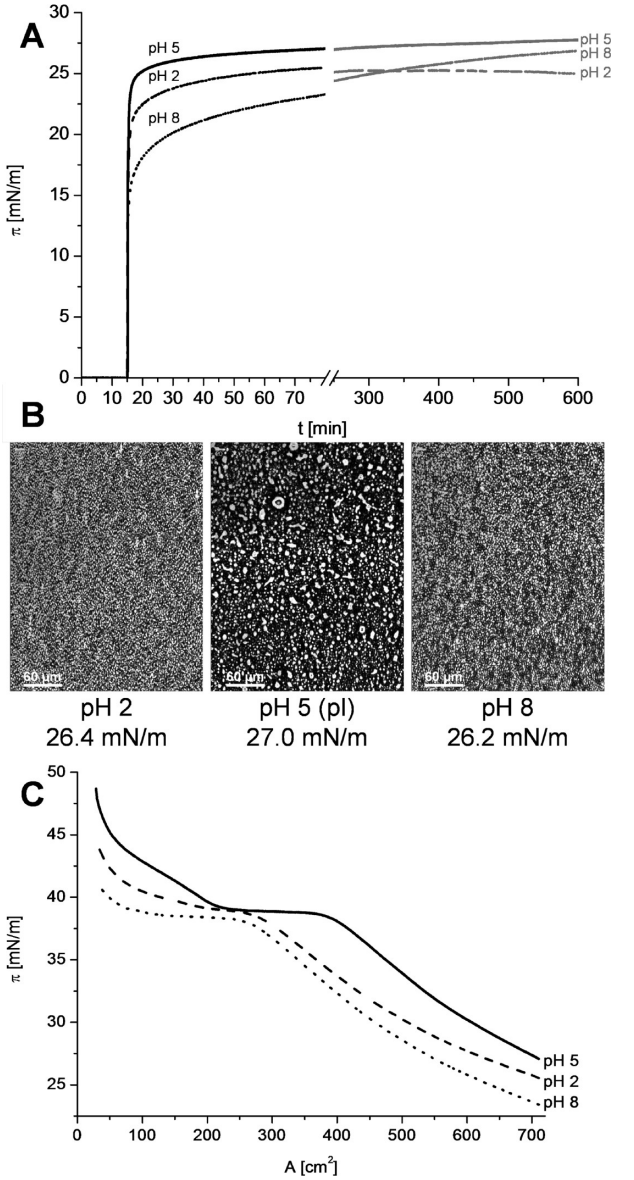

Figure 3. (A) Representative measurement of surface pressure as a function of time at different pH (I = 5 mM). At pH values away from the isoelectric point of oleosomes (pH 5) lower surface pressure values are recorded due to higher repulsion. In longtime kinetics, pH 2 and pH 8 surface pressure curves cross, since at pH 8 (and pH 5), but not at pH 2 a network like film is formed. (B) BAM micrographs at different pH after 60 min, taken at the beginning of the compression. At pH-values away from the isoelectric point, repulsion between the charged oil bodies occurs, leading to smaller aggregates. (C) Compression isotherm at different subphase pH (ν_B = 30 cm²/min, compression after 60 min). For pH values close to the isoelectric point the transition from LE to LE/LC occurs at higher areas. Conditions: 22 μL (6.6 mg/L) OB; pH 2, phosphoric acid; pH 5, acidic acid; pH 8, Tris; all with 5 mM buffer concentration.

Phase Transitions after Different Times. As already mentioned, additionally to pH and ionic strength, the time

dx.doi.org/10.1021/jp211871v | J. Phys. Chem. B 2012, 116, 10832–10841

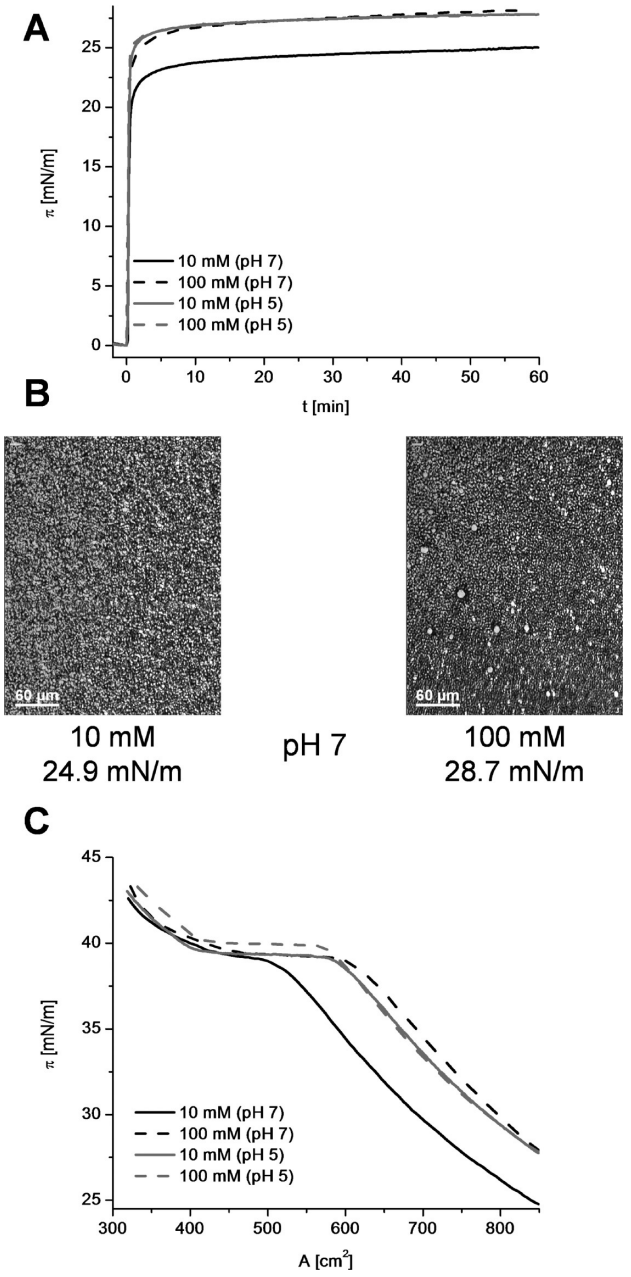

Figure 4. (A) Measurement of surface pressure as a function of time at different ionic strength and pH. Kinetics at pH 5 show no difference in surface pressure if the ionic strength is varied. At pH values away from the isoelectric point, higher ionic strength leads to less repulsion and thus higher surface pressure. (B) BAM micrographs at different ionic strength at pH 7 after 60 min. At pH-values away from the isoelectric point and higher ionic strength, the oleosomes' charge is screened, which induces bigger aggregates. (C) Compression isotherm at different ionic strength and pH (v_B = 30 cm^2/min, compression after 60 min). For higher ionic strength the transition from LE to LE/LC occurs at higher areas. Conditions: 22 μL (5.7 mg/L) OB; pH 5, MES; pH 7, monosodium phosphate; all with 5 mM buffer concentration and ionic strength was adjusted by adding the required amount of NaCl.

elapsing between oleosome injection and compression of the film is crucial for the resulting isotherm.

As shown before, for higher concentrations (≥0.8 mg/L) the surface pressure reaches a plateau stage for long times, where it is not or only slightly increasing (Figure 5A). The particles at the air−water interface are partly aggregating (Figure 5B), leading to bigger structures.

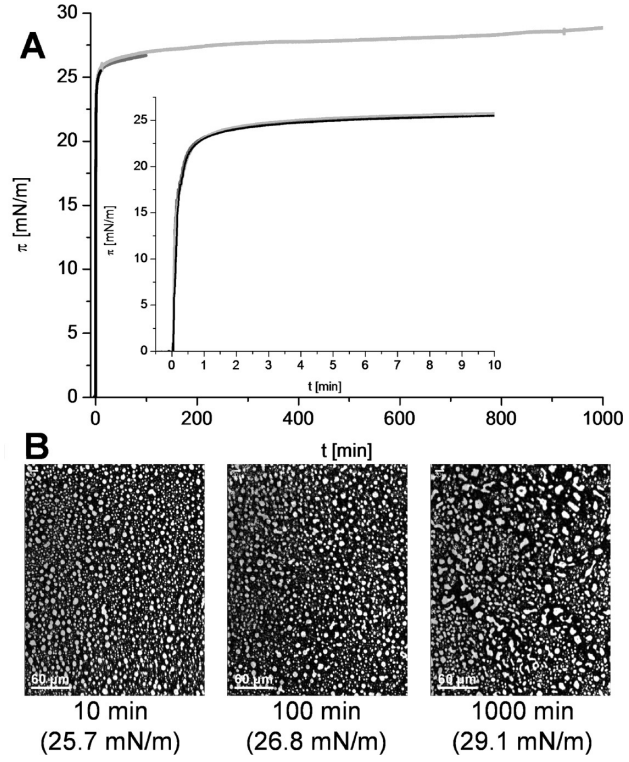

Figure 5. (A) Measurement of surface pressure as a function of time for different durations. The inset shows the first 600 s. (B) BAM micrographs after different waiting times. The longer the waiting time, the bigger are the aggregates. Conditions: 22 μL (5.7 mg/L) OB, 5 mM MES, pH 5.3.

This increase in aggregate size is also reflected in the isotherms. The longer the waiting time between oleosome addition and compression, the higher is the surface area at the LE-to-LE/LC transition and the bigger the plateau of the LE/LC coexistence (Figure 6A).

This can be explained by the bigger and bulkier aggregates which occur at longer waiting times and are forced to interact much earlier during compression than the small round particles that are visible just after injection. Additionally, the surface pressure during the LE/LC coexistence is the lower and elongated the longer the time before compression (Figure 6A). This effect cannot be explained by the growing aggregate size as they also increase in size with increasing ionic strength and at pH close to the isoelectric point were no significant decrease in surface pressure is visible. After approximately 5 h, oleosins seem to form entanglements that result in the network-like film shown in Figure 2B, which might give a preorientation to the phospholipids on the surface and therefore lowers the surface pressure of the LE/LC coexistence. This is observed for pH 5 to pH 8, but more pronounced for pH 5, which is the isoelectric point of soybean oleosomes.

Milli-Q. The events that occur immediately after addition of oleosomes into the subphase proceed very fast and thus focused BAM micrographs are not obtainable (see movie I.avi-LINK).

In the case of not or under-buffered systems those first steps seem to be decelerated and hence can be observed (see movie II.avi-LINK).

This deceleration can probably be attributed to two factors:

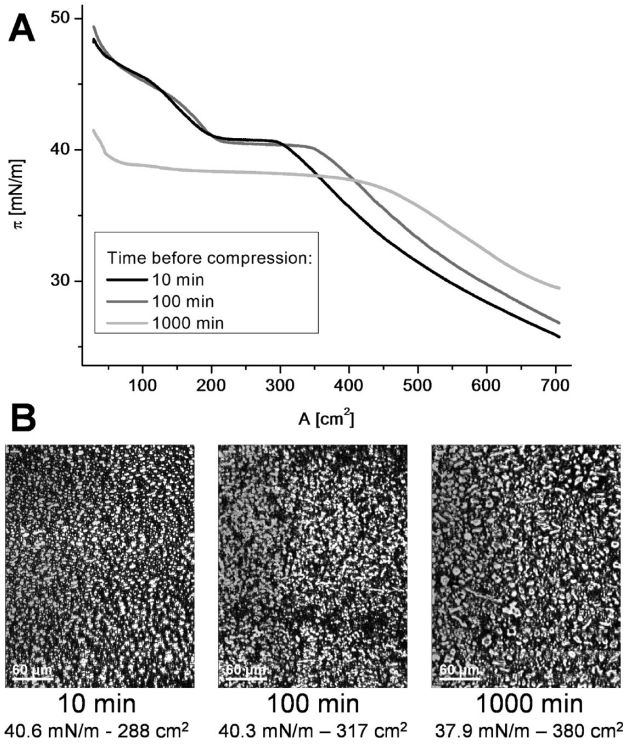

Figure 6. (A) Compression (v_B = 30 cm²/min) isotherm of soybean oleosomes after different waiting times. The longer the waiting time, the higher the area of the LE/LE–LC transition, the longer the LE/LC transition and the lower the surface pressure of this plateau. (B) BAM micrographs after different waiting times during compression. Images are taken at the onset of the plateau stage. Conditions: 22 μL (5.7 mg/L) OB, 5 mM MES, pH 5.3.

- competition for space at the interface
- van der Waals attraction of uncharged oleosomes in buffered systems

The characteristics of the kinetics in unbuffered-water are comparable to the measurements at small oleosome concentrations of around 0.4 mg/L (Figure 2), but in pure water, a higher amount of oleosomes can be used, which raises the chance to observe the "bursting events".

At small ionic strength (approximately below 0.1 mM), after the initial jump to approximately 12 mN/m, the surface pressure is only slowly and linear increasing with time. In this plateau stage, small particles (just above the limit of resolution) start to appear. After a certain amount of time (times scale of minutes), an increase in surface pressure is visible. Brewster angle micrographs during the second increase show an increased fluctuation of the micrometer sized particles, equal to the events after oleosome injection into the buffered subphase but additionally "bursting events" are visible in this stage (see movie III.avi-LINK). Those burstings decrease and disappear as the surface pressure reaches its maximum, according to the hypothesis that at this stage all oleosomes are burst.

CONCLUSIONS

The combination of surface pressure measurements and simultaneous Brewster angle microscopy revealed the oleosome behavior at the air–water interface which is a crucial factor in determining the driving forces in their surface active behavior and the key to using this in practical applications, e.g., food processing. The presumed actions are depicted in Figure 7.

In principle, oleosomes are micelle-like structures with an outer phospholipid monolayer and an interior filled with triglycerides, but with oleosins sticking hairpin-like in the structure with the hydrophilic parts remaining outside the oleosomes.

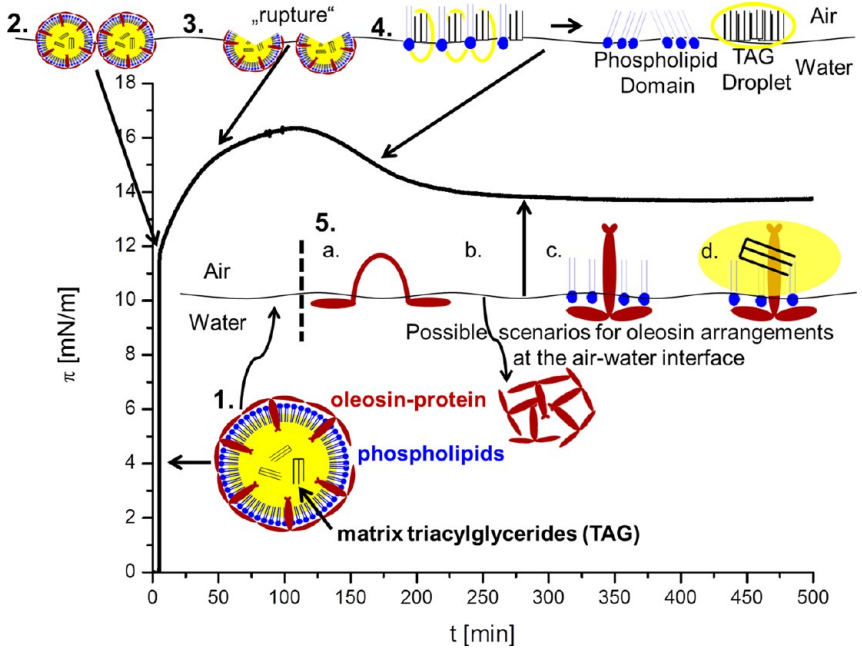

Figure 7. Simplified measurement of surface pressure as a function of time and corresponding scenarios at the air–water interface. The figure shows a typical measurement of the time evolution of the pressure at open barriers for small oleosome concentration (0.4 mg/L). A possible scenario of the oil bodies when exposed to an air–water interface is sketched for illustration (oleosome depiction adapted from Huang[7]).

After injection into the aqueous subphase the oleosomes diffuse immediately to the air−water interface due to their amphiphilic nature and buoyancy, visible in the steep increase in surface pressure and the bright, micrometer sized particles at the air−water interface during this diffusion. At this stage, oleosomes are presumably still intact. Depending on the amount of oleosomes at the surface, bursting of the round structures occurs within different time scales. This rupture can be seen in an additional increase in surface pressure and a decreasing amount of oleosomes visible by BAM. That the rupture is associated with the oil bodies packing at the interface is illustrated in kinetics executed at equal buffer conditions but different amount of oleosomes injected. At low concentrations (≤0.4 mg/L) the surface pressure peaks, whereas at high concentrations (≥0.8 mg/L) a constant rise in surface pressure with time is observed. When the film is compressed soon after an introduction of a small oleosome concentration (≤0.4 mg/L) and before the peak, no kinks are visible in the isotherm as no transitions due to free triglycerides and phospholipids occur. When the film is compressed after rupture of the oleosomes, one to two sharp kinks can be seen. The first, only observable if the initial surface pressure before compression is below 16 mN/m, can probably be attributed to the triglycerides and/or the gaseous/liquid expanded-transition of the phospholipids, which are both able to lower the surface tension after the breakage of the oil bodies. We assume that the second kink is the onset of the liquid expanded/liquid condensed-transition of the phospholipids released from the oleosomes after rupture. Another possible explanation for this kink would be desorption of the oleosin proteins, comparable to the desorption transition of lipopolymers.[37] However, for oleosins, such a behavior seems to be unlikely. First, the strong hydrophobicity suggests an aggregation to micelles, which would be stabilized in the subphase by the two hydrophilic tails of each oleosin. In addition, recent work showed the persistence of this transition after the tryptic digestion of the oleosins,[34] which indicates a phospholipid triggered effect.

The time that elapses during introduction of the oleosomes into the aqueous subphase and rupture depends on the parameters of the subphase, e.g., pH-value and ionic strength as well as amount of oleosomes injected. The denser the packing of the oleosomes at the air−water interface, the faster the rupture.

Additionally, the higher the ionic strength and the closer the pH to the isoelectric point, the higher is the "end surface pressure". This behavior can be explained by the charge of the oleosins. At the isoelectric point, no charges are present and the oleosins do not repel each other, leading to denser packing at the air−water interface and more saturated bindings, thus resulting in higher surface pressure. At higher ionic strength the charges of the oleosins are screened much better, which also results in denser packing at the air−water interface.

Regarding the free oleosins, we propose four possible arrangements:

(a) A denaturation of the oleosins at the air−water interface via unfolding of the hydrophobic hairpin.
(b) A clustering of the hydrophobic parts of several oleosins and possibly diffusion into the bulk after a critical size and weight has been reached.
(c) Insertion of an intact oleosin into a monolayer of phospholipids.[24]
(d) Insertion of an intact oleosin into an oil droplet.

The last two points are strengthened by observations in the literature[27] that oleosin aggregates cannot compete with the high surface activity of the triacylglycerides and phospholipids. The adsorption of oleosins at the interface and its conformational changes will be further investigated by spectroscopic techniques at the air−water and oil−water interface.

The formation of a network like film of protein−lipid complexes[38] with presumably entangled oleosins (pH 5−8, oleosome concentration ≥0.8, ≥5 h time before compression) strongly influences the surface film behavior: it prevents diffusion of surface active substances into the subphase and constrains the mobility of the film, which is of great interest for stabilizing interfaces.

■ ASSOCIATED CONTENT

Ⓦ Web-Enhanced Features

Movies showing events that occur immediately after addition of oleosomes into the subphase (movie I.avi-LINK), the same events for not buffered or under-buffered systems (movie II.avi-LINK), and additional "bursting events" (movie III.avi-LINK),

■ AUTHOR INFORMATION

Corresponding Author

*Telephone: +49 6131 379548. Fax: +49 6131 379100. E-mail: waschatko@mpip-mainz.mpg.de.

Notes

The authors declare no competing financial interest.

■ ACKNOWLEDGMENTS

The authors thank Christine Peter, Mara Jochum, Christoph Globisch, Markus Deserno, Johannes Franz, and Sania Maurer for fruitful discussions, David Baßler, Wanja Wiese, and Torsten Stühn for video editing, and Sandra Ritz for the use of SDS−PAGE equipment.

■ REFERENCES

(1) Griffin, W. C. *J. Soc. Cosmet. Chem.* **1949**, *1*, 311.
(2) Pearce, K. N.; Kinsella, J. E. *J. Agric. Food Chem.* **1978**, *26* (3), 716−723.
(3) Corsi, A.; Milchev, A.; Rostiashvili, V. G.; Vilgis, T. A. *Food Hydrocolloid* **2007**, *21* (5−6), 870−878.
(4) Ettelaie, R.; Akinshina, A.; Maurer, S. *Soft Matter* **2012**, *8* (29), 3582−3597.
(5) Martinet, V.; Saulnier, P.; Beaumal, V.; Courthaudon, J.-L.; Anton, M. *Colloids Surf., B* **2003**, *31*, 185−194.
(6) Patton, S.; Keenan, T. W. *Biochim. Biophys. Acta* **1975**, *415*, 273−309.
(7) Huang, A. H. C. *Annu. Rev. Plant Biol.* **1992**, *43* (1), 177−200.
(8) Hevonoja, T.; Pentikäinen, M. O.; Hyvönen, M. T.; Kovanen, P. T.; Ala-Korpela, M. *Biochim. Biophys. Acta—Mol. Cell Biol. Lipids* **2000**, *1488* (3), 189−210.
(9) Jolivet, P.; Boulard, C.; Beaumal, V.; Chardot, T.; Anton, M. *J. Agric. Food Chem.* **2006**, *54* (12), 4424−4429.
(10) Tzen, J. T. C.; Huang, A. H. C. *J. Cell. Biol.* **1992**, *117* (2), 327−335.
(11) Capuano, F.; Beaudoin, F.; Napier, J. A.; Shewry, P. R. *Biotechnol. Adv.* **2007**, *25* (2), 203−206.
(12) Li, M.; Murphy, D. J.; Lee, K.-H. K.; Wilson, R.; Smith, L. J.; Clark, D. C.; Sung, J.-Y. *J. Biol. Chem.* **2002**, *277* (40), 37888−37895.
(13) Alexander, L.; Sessions, R.; Clarke, A.; Tatham, A.; Shewry, P.; Napier, J. *Planta* **2002**, *214* (4), 546−551.
(14) Palacios, L.; Wang, T. *J. Am. Oil Chem. Soc.* **2005**, *82* (8), 571−578.

(15) Iwanaga, D.; Gray, D. A.; Fisk, I. D.; Decker, E. A.; Weiss, J.; McClements, D. J. *J. Agric. Food Chem.* **2007**, *55* (21), 8711−8716.
(16) Chen, Y.; Yamaguchi, S.; Ono, T. *J. Agric. Food Chem.* **2009**, *57* (9), 3831−3836.
(17) Towa, L.; Kapchie, V.; Hauck, C.; Wang, H.; Murphy, P. *J. Am. Oil Chem. Soc.* **2011**, *88* (5), 733−741.
(18) Chen, Y.; Ono, T. *J. Agric. Food Chem.* **2010**, *58* (12), 7402−7407.
(19) Watkins, J. C. *Biochim. Biophys. Acta—Lipids Lipid Metabolism* **1968**, *152* (2), 293−306.
(20) Blume, A. *Biochim. Biophys. Acta—Biomembr.* **1979**, *557* (1), 32−44.
(21) Albrecht, O.; Gruler, H.; Sackmann, E. *J. Colloid Interface Sci.* **1981**, *79* (2), 319−338.
(22) von Tscharner, V.; McConnell, H. M. *Biophys. J.* **1981**, *36* (2), 409−419.
(23) Möhwald, H. *Annu. Rev. Phys. Chem.* **1990**, *41* (1), 441−476.
(24) Millichip, M.; Tatham, A. S.; Jackson, F.; Griffiths, G.; Shewry, P. R.; Stobart, A. K. *Biochem. J.* **1996**, *314*, 333−337.
(25) Boniewicz-Szmyt, K.; Pogorzelski, S.; Mazurek, A. *Oceanologia* **2007**, *49* (3), 413−437.
(26) Lacey, D. J.; Wellner, N.; Beaudoin, F.; Napier, J. A.; Shewry, P. R. *Biochem. J.* **1998**, *334*, 469−477.
(27) Roux, É.; Baumberger, S.; Axelos, M. A. V.; Chardot, T. *J. Agric. Food Chem.* **2004**, *52* (16), 5245−5249.
(28) Kim, H.; Kim, S.-Y.; Han, N.; Tao, B. *Biotechnol. Bioprocess Eng.* **2007**, *12* (5), 542−547.
(29) Gohon, Y.; Vindigni, J.-D.; Pallier, A.; Wien, F.; Celia, H.; Giuliani, A.; Tribet, C.; Chardot, T.; Briozzo, P. *Biochim. Biophys. Acta—Biomembr.* **2011**, *1808* (3), 706−716.
(30) Bonsegna, S.; Bettini, S.; Pagano, R.; Zacheo, A.; Vergaro, V.; Giovinazzo, G.; Caminati, G.; Leporatti, S.; Valli, L.; Santino, A. *Appl. Biochem. Biotechnol.* **2011**, *163* (6), 792−802.
(31) Beaglehole, D. *Rev. Sci. Instrum.* **1988**, *59* (12), 2557−2559.
(32) Henon, S.; Meunier, J. *Rev. Sci. Instrum.* **1991**, *62* (4), 936−939.
(33) Hoenig, D.; Moebius, D. *J. Phys. Chem.* **1991**, *95* (12), 4590−4592.
(34) Hönig, D.; Möbius, D. *Thin Solid Films* **1992**, *210−211* (Part 1, (0)), 64−68.
(35) Waschatko, G.; Junghans, A.; Vilgis, T. A. *Faraday Discuss.* **2012**, DOI: 10.1039/C2FD20036H.
(36) Kaganer, V. M.; Möhwald, H.; Dutta, P. *Rev. Mod. Phys.* **1999**, *71* (3), 779−819.
(37) Ahrens, H.; Bækmark, T. R.; Merkel, R.; Schmitt, J.; Graf, K.; Raiteri, R.; Helm, C. A. Hydrophilic/Hydrophobic Nanostripes in Lipopolymer Monolayers. *ChemPhysChem* **2000**, *1* (2), 101−106.
(38) Dauphas, S.; Beaumal, V.; Riaublanc, A.; Anton, M. *J. Agric. Food Chem.* **2006**, *54* (10), 3733−3737.

PUBLIKATIONEN

2 Waschatko, G.; Junghans, A.; Vilgis, T. A., Soy milk oleosome behaviour at the air-water interface. *Faraday Discussion* 2012, 158 (0), 157-169.

Faraday Discussions Vol 158

Soft Matter approaches to Structured Foods

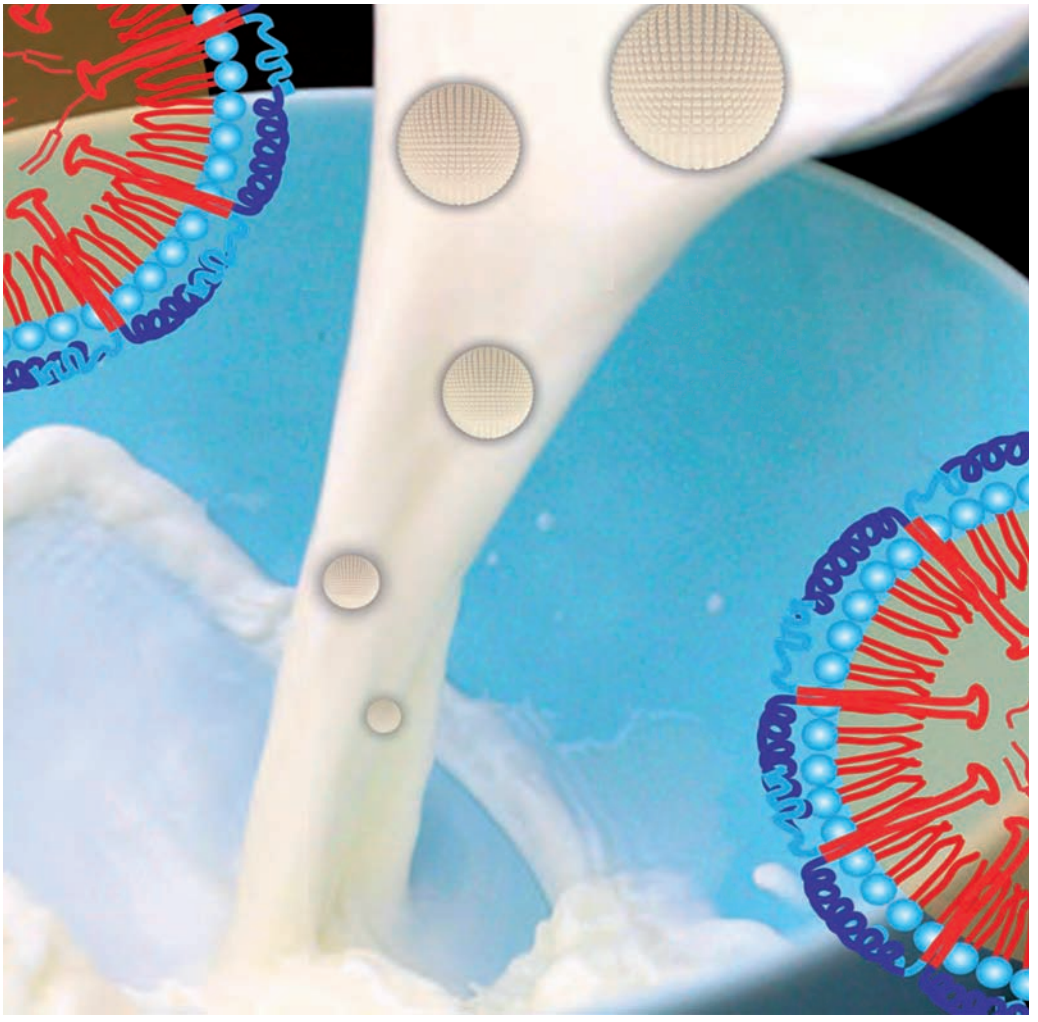

RSC Publishing

Soy milk oleosome behaviour at the air–water interface

Gustav Waschatko,*[ab] Ann Junghans[a] and Thomas A. Vilgis[a]

Received 24th February 2012, Accepted 24th April 2012
DOI: 10.1039/c2fd20036h

Soy milk is a highly stable emulsion mainly due to the presence of oleosomes, which are oil bodies and function as lipid storage organelles in plants, *e.g.*, in seeds. Oleosomes are micelle-like structures with an outer phospholipid monolayer, an interior filled with triacylglycerides (TAGs), and oleosins anchored hairpin-like into the structure with their hydrophilic parts remaining outside the oleosomes, completely covering their surface (K. Hsieh and A. H. C. Huang, *Plant Physiol.*, 2004, **136**, 3427-3434). Oleosins are alkaline proteins of 15–26 kDa (K. Hsieh and A. H. C. Huang, *Plant Physiol.*, 2004, **136**, 3427–3434) which are expressed during seed development and maturation and play a major role in the stability of oil bodies. Additionally, the oil bodies of seeds seem to have the highest impact on coalescence, probably due to the required protection against environmental stress during dormancy and germination compared to, *e.g.*, vertebrates' lipoproteins. Surface pressure investigations and Brewster angle microscopy of oleosomes purified from raw soy milk were executed to reveal their diffusion to the air–water interface, rupture, adsorption and structural modification over time at different subphase conditions. Destroying the surface portions of the oleosins by tryptic digestion induced coalescence of oleosomes (J. Tzen and A. Huang, *J. Cell. Biol.*, 1992, **117**, 327–335) and revealed severe changes in their adsorption kinetics. Such investigations will help to determine the effects behind oleosome stability and are necessary for a better understanding of the principal function of oleosins and their interactions with phospholipids.

Introduction

Evolution has developed different native structures to solubilise oil in water as small droplets: lipoproteins in vertebrates' circulatory systems (HDL, LDL, chylomicrons), fat globules in mammalian milk and oleosomes or oil bodies (OB) in plant seeds.[3,4] Their apparent similarity is based on the fact that nature has a limited amount of natural emulsifiers, *i.e.*, phospholipids and proteins. However, on closer examination the lipid droplets produced in animals are totally different with regard to their surface proteins compared to plant oleosomes. One very high mass apolipoprotein, *i.e.*, Hen Apolipoprotein B (UniProtKB: Q197X2) in egg yolk with its 4631 amino acids wound around the whole particle is located more or less closely to the surface made of phospholipids.[5,6] Thus it significantly constrains the dynamics of the phospholipids in the domains close to the proteins. The positive effect of the apolipoproteins is therefore obvious, they yield more stable droplets compared to "classical" emulsions where only phospholipids are used. Nevertheless, oleosomes appear

[a]*Max Planck Institute for Polymer Research, Ackermannweg 10, 55128 Mainz, Germany. E-mail: waschatko@mpip-mainz.mpg.de; Fax: +49 6131 379100; Tel: +496131 379548*
[b]*Institut für Pharmazie und Biochemie, Johannes Gutenberg-Universität Mainz, Johann-Joachim-Becher-Weg 30, 55128 Mainz, Germany*

even more stable than LDL-particles, for example from egg-yolks. In accordance, soy lecithin gives more stable emulsions than egg lecithin.[7] The reason is a very different arrangement of stabilizing proteins, probably due to the required protection of the oil bodies of seeds against environmental stress during dormancy and germination. Even so, the usage of intact oil bodies in food products and food processing, even cooking (*e.g.*, desserts, instant drinks, salad dressing) does not take place yet, especially not in the western world, whereas egg yolk, cream and other dairy products are very common in food emulsions. On the other hand, for the triacylglycerides (TAGs) and the phospholipids (soy lecithin), the two main components of the oil bodies, the situation is reversed: compared to animal fat sources, their usage and popularity is higher. More and more animal fat is replaced by vegetable oil and soy lecithin is the main emulsifier of processed food, for example in chocolate, bakery products, desserts, margarine or creams. Food manufacturers could easily profit from the pre-existing natural protection[8] of intact oleosomes to improve the stability of their products like dressings, sauces or desserts during storage and utilization. Neither emulsifiers nor homogenisation processes are needed, when oleosomes are used in those food systems.

Furthermore, the extraction process of oleosomes *via* flotation–centrifugation is of interest in two different research areas:

First, extracting oil from oil seeds with solvents like hexane is still the primary method in the food industry. However, safety and environmental requirements promote aqueous extraction processes, which can already be done on a pilot plant scale.[9] The use of enzymes like cellulase or pectinase to open the seeds cell wall[10] raises the yield of oleosomes. Moreover, disruption of oleosomes with proteases can improve the quantity and quality of the free oil.[11] Showing that a simple trypsin treatment is able to break open the otherwise extremely stable oil bodies is an important step in the direction of safer, more efficient and more environmentally friendly oil extraction. Secondly, oleosomes are attractive for genetic engineering and biotechnology, where they are used as plant expression systems for recombinant proteins or peptides, *e.g.*, antibodies or vaccines. The protein–oleosin fusions are enriched in the seed oil bodies, which are easy to harvest *via* flotation–centrifugation, and after cleavage eukaryotic proteins without potential contamination of animal pathogens are obtained.[8] As the oil content of soybeans is around 20% there is a high amount of oleosomes and oleosins available from the soybean crops.

Simply put, oleosomes can be viewed as micelle-like structures with an outer phospholipid monolayer, an interior filled with TAGs, and associated proteins, the so called oleosins (Fig. 1).[4] Oleosins are alkaline proteins of 15–26 kDa which are expressed during seed development and maturation and are assumed to play a major role in the stability of oil bodies.[2] These oleosins are different to the apolipoproteins in LDL-particles, because they are not just located on the surface, but most likely anchored with their central hydrophobic stretch deep in the oil-phase. (Fig. 1) This location of the hydrophobic domain is commonly accepted as well as a proline knot forming a 180° turn of a hairpin-like sequence.[13] The secondary structure of this longest hydrophobic sequence (about 70 amino acids) known to date can either be antiparallel β-sheets[14] or α-helical.[15] The N- and C-terminal domains are more hydrophilic (*e.g.*, amphipathic α-helix[2]), most probably remain umbrella-like outside the oleosome, and are less conserved among the plant species.

To investigate the impact of the individual compounds on the interfacial behaviour of the oleosomes further purification processes such as isolation of native oleosins are necessary, but currently not yet available. Regarding the oleosome proteins, the use of proteases provides analogous insight into their impact, such as the investigations of the low-density lipoproteins (LDL) in egg yolk by Dauphas *et al.*[16] As such enzymes completely destroy the functionality of the oleosins (*e.g.*, phospholipid shielding, binding of phospholipids, water solubility, surface charge).

To better understand the nature of the oleosomes, systematic experiments have been performed. First, oleosomes are purified at pH 11 similar to a procedure

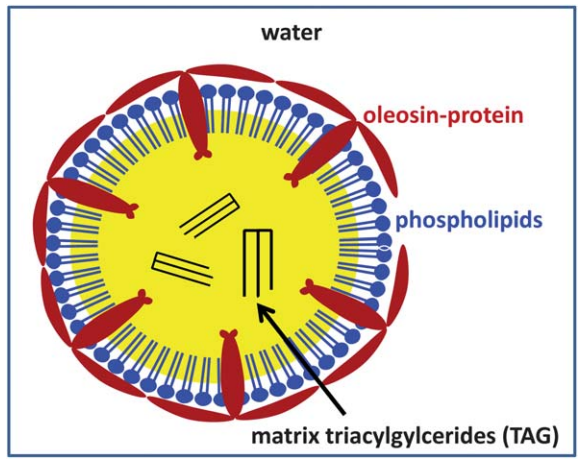

Fig. 1 2D-Model of a soybean oleosome in bulk water (depiction adapted from Huang[12]). The oleosins (red) are located at the oil–water interface of the intact oleosome. They penetrate the surface phospholipids (blue) into the oil matrix (yellow) with their hydrophobic hairpins forming a proline knot at the 180° turn. This central hydrophobic stretch is flanked by the different hydrophilic N- and C-terminal domains, interacting with the charged headgroups of the phospholipids and the surrounding water. Oleosomes are very stable against coalescence in bulk water, but break-up at interfaces, liberating their internal constituents.

introduced by Chen and Ono (2010).[17] Next, untreated and trypsin digested oleosomes are observed at the air–water interface of a film balance. This procedure allows the study of their stability and the behaviour of the three different constituents, *i.e.*, oleosins, phospholipids and TAGs. This method offers two basic observations. First, the kinetics, which show the instability and the "destruction" of the oleosomes at the air–water interface. The second issue is the behaviour of the oleosomes and their constituents under pressure (isotherms). Consequently, we can expect several physical scenarios: First of all, oil bodies immersed in the subphase will rise to the surface. Some oleosomes may stay intact and agglomerate at the interface. Others break up into a phase of triacylglycerides, phospholipids and oleosins. The oil spreads on the surface as film or droplets. The phospholipids separate from the oil droplets and either go to the air–water interface or form micelles in the subphase. The oleosins denature partially and form aggregates. Of course, these processes depend on many parameters, such as pH-value and ionic strength, especially when proteins are involved, since their behaviour depends strongly on the present charge defined by their amino acids exposed to the watery environment.

Thus, when the oleosomes are (partially) destroyed at the air–water interface four different components with competing interactions rule the physical picture at compression of the barriers of the film balance: TAGs, phospholipids, partially denatured or enzymatically cut oleosins, and still intact oil bodies, which will have different contributions to the pressure-surface dependence. Depending on their concentration, phospholipids will form different phases at the surface (see for example ref. 18–22), TAGs will partially wet the interface, oleosins may form micelles by clustering their hydrophobic parts (originally placed in the oil core) into collapsed, dense cores surrounded by the hydrophilic part (N-and C- terminal domains). These ideas and scenarios are depicted in Fig. 2 for intact and trypsin digested oleosomes on a pH 8 subphase.

Previous publications (Bonsegna *et al.*[23]) showed that Brewster angle microscopy (BAM) is the method of choice for visualising areas of different brightness due to different molecular density and/or refractive index in a thin interfacial layer and it has long been used to study for example lipids, proteins and mixed systems at the

air–water interface.[24–27] This technique is indeed a very useful tool in the characterization of the interfacial behaviour of oleosomes as marking them is not necessary for visualisation. Also, the surface pressure is recorded simultaneously to the BAM micrographs, so the changes in surface tension can be directly correlated with the surface active components seen by BAM.

In a previous paper,[28] oleosomes purified from soybeans have been studied at the air–water interface at different subphase conditions to determine the effects behind oleosome stability. Here, we repeat those experiments using trypsin digested oleosomes.

Soybean oleosomes are highly robust micelle-like structures and provide extremely stable emulsions, preventing coalescence much better than egg lecithin. Before being able to use those naturally occurring emulsifiers in food applications, their compatibility with the human digestive system must be studied as proteins are the allergic components in food. Allergies occur when proteins or fragments of proteins are resistant to digestion, cannot be broken down in the digestive process and are tagged by immunoglobulin E, which triggers an immune response. To prevent food intolerances or allergic reactions the successful digestion and metabolism of all components needs to be guaranteed.

Additionally, such investigations are necessary for a better understanding of the principal function and structure of oleosins (*i.e.*, phospholipid binding sites on oleosins). They provide information on the mode of action of the digestive enzyme trypsin, and are of interest for food technique applications or carriers. The trypsin cleavage sites are located only on the hydrophilic part of oleosins, with the greater portion on the C-terminus.[29] The measurement depicted in Fig. 2 suggests a detailed scenario of the different physical processes occurring to the oleosome's components at the air–water interface. As already described, oleosomes contain three thermodynamically competing components: non-polar TAGs, phospholipids and oleosins. The oleosins are of special interest, since they consist of a long hydrophobic part and two mainly hydrophilic ends. Their secondary structure accounts for the high stability of the oleosomes by stretching its hydrophobic part into the oil droplets

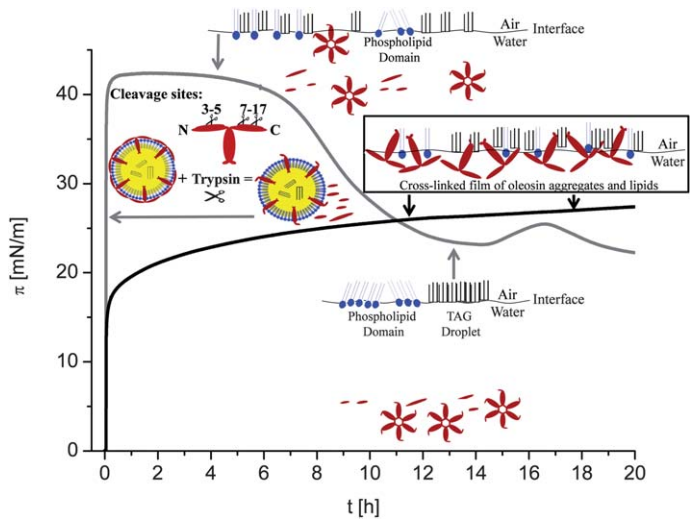

Fig. 2 Time evolution of the surface pressure and summary of the corresponding scenarios at the air–water interface for untreated (black) and trypsin digested (grey) oleosomes. The figure shows typical measurements of the time evolution of the pressure at open barriers at pH 8. Possible scenarios of the oil bodies when exposed to an air–water interface are sketched for illustration (oleosome depiction adapted from Huang[12]).

and arranging their hydrophilic ends into the continuous water phase. When the oleosins are partly digested by trypsin the hydrophilic part becomes cut in various places, leaving a small polar part attached to the hydrophobic sequence at the N-terminal domain. The remaining long hydrophobic parts of the oleosins turn to the surface, aggregate, collapse and form globules of mainly hydrophobic chains in the subphase, which are stabilized and held in the water phase by the short polar tails. The trypsin digested oleosins release most of the phospholipids which rise to the air–water interface quickly and increase the pressure. The TAGs form droplets and arrange themselves into domains of TAG droplets at the air–water interface. The fundamental difference between the digested and the non-digested case is shown in Fig. 2 by a significant difference in the development of the pressure with time. In the non-digestive case, a different arrangement of the components at the subphase and interface develops. The non-digested oleosins keep the oil bodies intact until they reach the air–water interface, then they burst and liberate oleosins, TAGs and phospholipids as indicated in Fig. 2.

Material and methods

For all preparation steps, ultra-pure water, filtered with a Millipore device (Billerica, MA/USA) was used and all experiments were carried out at room temperature.

Oleosome purification

Isolation of soybean oleosomes was performed by a modified aqueous flotation–centrifugation method proposed by Chen and Ono.[17] Dried soybeans from a local supermarket (Davert) were soaked in deionised water at 4 °C for at least 20 h. Then water was added to obtain a 10% soybean-to-water ratio and the mixture was ground in a Vorwerk Thermomix TM31 at a speed of 10 200 rpm for 90 s. The resulting slurry was filtered through two layers of Kimtech science precision wipes 21 × 11 cm (Kimberly Clark) to obtain raw soy milk. 25% sucrose (w/w) was added to the raw soy milk and the pH was adjusted to 11.0 with 1 mol l^{-1} NaOH (AVS Titrinorm, Prolabo/VWR) solution. The solution was filled into six 50 ml centrifuge tubes (Roth), which were centrifuged in a Thermo Heraeus Multifuge X1R with 15 000 × g at 4 °C for at least 5 h. The resulting floating fractions (creamlayer, fat pat, oleosomes) were lifted with a small spoon and resuspended in 45 ml of 20% (w/w) sucrose in deionised water (pH 11) in a new centrifuge tube. This washing step (15 000 × g, 4 °C, 5 h) was performed twice. The resulting oleosomes were collected and dispersed in 20 ml of deionised water and dialyzed over night with Thermo Scientific Slide-A-Lyzer G2 Dialysis Cassettes (20 K MWCO).

Sodium dodecyl sulfate-polyacrylamide gel electrophoresis (SDS-PAGE)

The SDS-PAGE was performed with the invitrogen NuPAGE®-System. NuPAGE® MES-Running Buffer and a 10% NuPAGE® Novex® Bis-Tris Mini Gel were applied according to the manufacturer's instructions but without heating the samples, instead they were incubated overnight with the NuPage®LDS Sample Buffer and the NuPage®LDS Reducing Agent.

For the visualization of the protein bands Coomassie® G-250 SimplyBlue™ SafeStain (invitrogen) was used. After staining for 1 h, the polyacrylamide gel was destained twice with ultrapure water for 1 h and subsequently overnight.

Trypsin digestion

1 mg trypsin from porcine pancreas (Serva Electrophoresis GmbH, Tryptic activity: ≥ 50 U g^{-1} (Ph. Eur.) or 4699 FIP-U g^{-1}) was added to 1 ml of dialysed

oleosomes (85% water content) and was incubated at 25 °C for 1 h in a HLC ThermoMixer MKR 13.

Buffer

For buffered subphases the following chemicals were used:

Phosphoric acid, ACS reagent, (Sigma-Aldrich, Munich, Germany, ≥85 wt. % in H_2O), acetic acid (Sigma-Aldrich, Munich, Germany, ≥99.8%) and monosodium phosphate (Fluka, Munich, Germany, ≥99%). For varying the ionic strength, the molarity was kept constant and adjusted by adding the required amount of sodium chloride (Prolabo/VWR, Darmstadt, Germany, min. 99.5%).

Film balance

The surface pressure was measured as a function of time (kinetics) and surface area (isotherms) on a Nima (Biolin Scientific, Västra Frölunda, Sweden) BAM Trough (available area at completely opened barriers = 715 cm^2), with symmetric Delrin twin barriers. The trough was equipped with a surface pressure sensor that uses the Wilhelmy plate technique to determine the change in surface tension of the air–water interface in the presence of surfactant molecules. In general, measurements were repeated at least 3 times for any given set of parameters with a very good agreement between the different measurements.

Kinetics

The surface pressure was recorded as a function of time at a fixed surface area. If not denoted otherwise, 22 μl suspension of oleosomes in water were inserted into the subphase with a pipette (Eppendorf, Hamburg, Germany). Preliminary experiments have shown that no agitation was necessary to enable proper mixing of oleosomes in the subphase. The total volume of the trough was 500 ml.

Isotherms

Immediately after oleosome injection or subsequent after a kinetic, the surface pressure was recorded as a function of area, hence monitoring the changes in surface tension upon compressing. If not denoted otherwise, the barrier compression speed was 30 $cm^2\ min^{-1}$.

Brewster angle microscopy

All BAM micrographs were taken on a EP^3-BAM (Nanofilm Göttingen, Germany) with a lateral resolution of approx. 1 μm. The size of the micrographs was 600 × 500 μm and images were not processed in any way except for background correction carried out with the provided software. Simultaneously, the surface pressure was recorded.

Results and discussion

Oleosome purification, characterization and trypsin digestion

The dialyzed oleosomes used for all experiments had a water content of 85%. Their mean diameter of 300–350 nm was measured at room temperature and diluted in water by means of Dynamic Light Scattering (DLS) with a Nicomp particle sizer (model 380, PSS Santa Barbara, California) at a scattering angle of 90° (data not shown). The coomassie stained SDS-PAGE (Fig. 3) confirmed three proteins of 15–16, 17–18 and 23–24 kDa corresponding to the size of the four soybean oleosins known in protein databases (UniProtKB: Isoforms P29530 and P29531 23–2 kDa, C3VHQ8: 17–18 kDa, C6SZ13: 15–16 kDa).

This confirms that pH 11 extraction removed the unspecifically bound soybean storage proteins (glycinin and β-conglycinin), and potential allergenic proteins (such as Gly m Bd 30 K),[17] that exist in raw soy milk, from the surface of the oleosomes as shown in the SDS-PAGE.

Compared to other soybean oleosome purifications,[8] the oleosomes used here showed a very sharp aggregation behaviour between pH 4.4 and 5.7 (data not shown).

All four oleosins were digested during the trypsin treatment independently of the amount of protease used. The maximum remaining tryptic fragments were below approximately 8 kDa, including the hydrophobic hairpin and the proline knot motif.[2]

Film balance

Independent of the subphase condition, an increase in surface pressure from 0 mN m^{-1} to approx. 12 mN m^{-1} is observable immediately after oleosome injection together with the diffusion of round, very bright 3D particles in the size of the lateral resolution (approx. 1 μm) of the BAM to the air–water interface. With time, a further increase of surface pressure—whereby the gradient is dependent on subphase conditions such as pH, ionic strength *etc.*—can be monitored as well as a partial aggregation of the particles visible by BAM. When the area is decreased by compression, the shape of the subsequent isotherm depends on the subphase conditions as well as the time between injection and compression, but usually one to two transitions are observable: Liquid-expanded (LE) to coexistence of liquid-expanded/liquid-condensed (LE/LC) and/or LE/LC to liquid-condensed (LC). In accordance, the BAM micrographs show a two-phase system that is growing in intensity, and hence in optical density, with decreasing area and increasing surface pressure. In summary, intact oleosome behaviour at the air–water interface is driven by the charge of the oleosins.[28]

Trypsin digestion

Trypsin is a specific serine protease found in the digestive system of many vertebrates, where it hydrolyses proteins. It cleaves proteins at the carboxyl side of the basic amino acids lysine and arginine. This means the oleosins found in soybean oleosomes have 21–22 cleavage sites for the long and 10 for the short oleosins, with the main part located at the hydrophilic C-terminal domain (Fig. 2).[29]

When intact oleosomes were digested with trypsin, pronounced differences compared to native oleosomes were visible in the phase behaviour and BAM micrographs at the air–water interface.

After injection of the same amount of oleosome solution, trypsin digested oleosomes show a much higher increase in surface pressure (between 38 and 43 mN m^{-1}, depending on pH), whereas untreated, intact oleosomes only reach values between 24 and 27 mN m^{-1} after the same waiting time. (Fig. 4A)

This is a strong indication that trypsin cleaves the outer heads of the oleosins and hence destroys the stability of the oleosomes to a large extent, which leads to the breakage of the oil bodies. Their constituents become released and redistribute themselves in the subphase and air–water interface. As the surface pressure after injection is still considerably higher than the maximum observed for intact oleosomes after presumed breakage we assume that binding sites between the oleosins and phospholipids are destroyed during trypsin cleavage, leading to more free phospholipids.

Fig. 4A shows the pH-dependence of the surface pressure for intact as well as trypsin digested oleosomes. For intact oleosomes, lower surface pressure values are recorded at pH-values different from the isoelectric point (pI = pH 5), due to higher repulsion of the oleosins carrying a net charge. The pH-dependence of trypsin digested oleosomes is different. Here, the lowest surface pressure is recorded at pH 5.

As the charged terminal domains of the oleosin were cut by trypsin only a weak pH-dependency could be expected for such systems, because of the loss of almost all acidic and basic amino acids.[29] However, it is known from the literature[30] that the interfacial tension of the lipid membrane is dependent upon the hydrogen ion concentration of the surrounding solution. This connection explains the slightly lower surface pressure values at pH 5, as the interfacial tension of phosphatidylethanolamine, one of the main components of the present phospholipids,[31] peaks at pH 4, and shows lower values at pH 2 and 8.

This also explains the appearance of branched, starlike domains, that occur at pH 2 and pH 8 for trypsin digested oleosomes (Fig. 3B, 4, 5). Due to the high packing density, lipids cannot repel each other as much as necessary, which results in domain formation as this is energetically more favourable. The driving force for domain shape formation is the free energy $F = F_{el} + F_L$.[32] Here F_{el} is the free energy of the electrostatic repulsion and F_L the contribution from the line tension of the quasi two dimensional droplets perimeter. In the absence of charged headgroups (at the pI), the minimum energy domain shape is determined entirely by the short-range interaction line tension that favours circular structures. The isoelectric point of

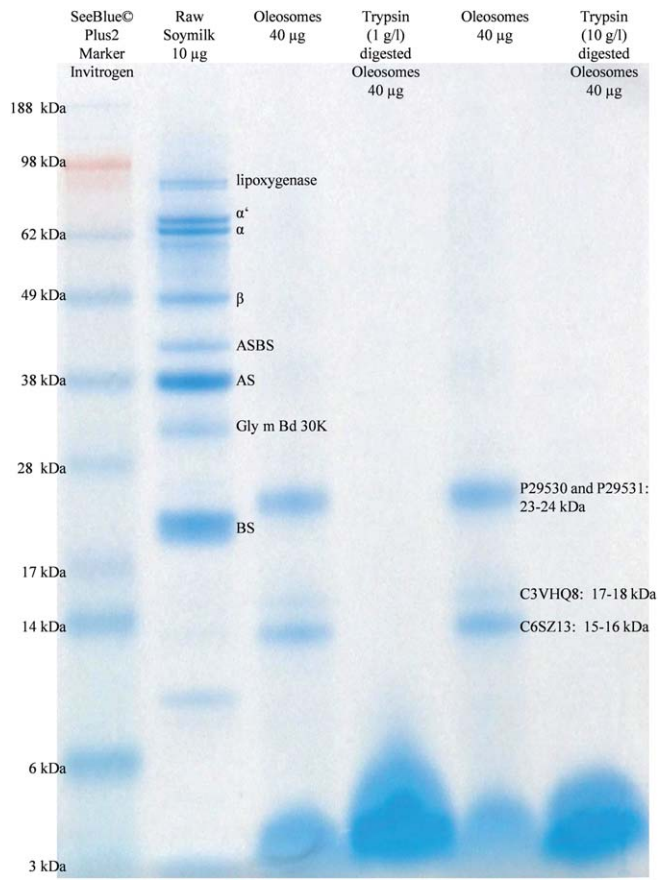

Fig. 3 Commassie stained SDS-PAGE gel of purified soybean oleosomes before and after digestion with trypsin. The raw soy milk shows the subunits of soybean storage proteins glycinin (AS: acidic subunit, BS: basic subunit) and β-conglycinin (α, α′, β). Oleosomes were trypsin digested with 1 mg ml^{-1} and 10 mg ml^{-1} of protease at 25 °C for 1 h in a ThermoMixer. The tryptic fragments were below 8 kDa.

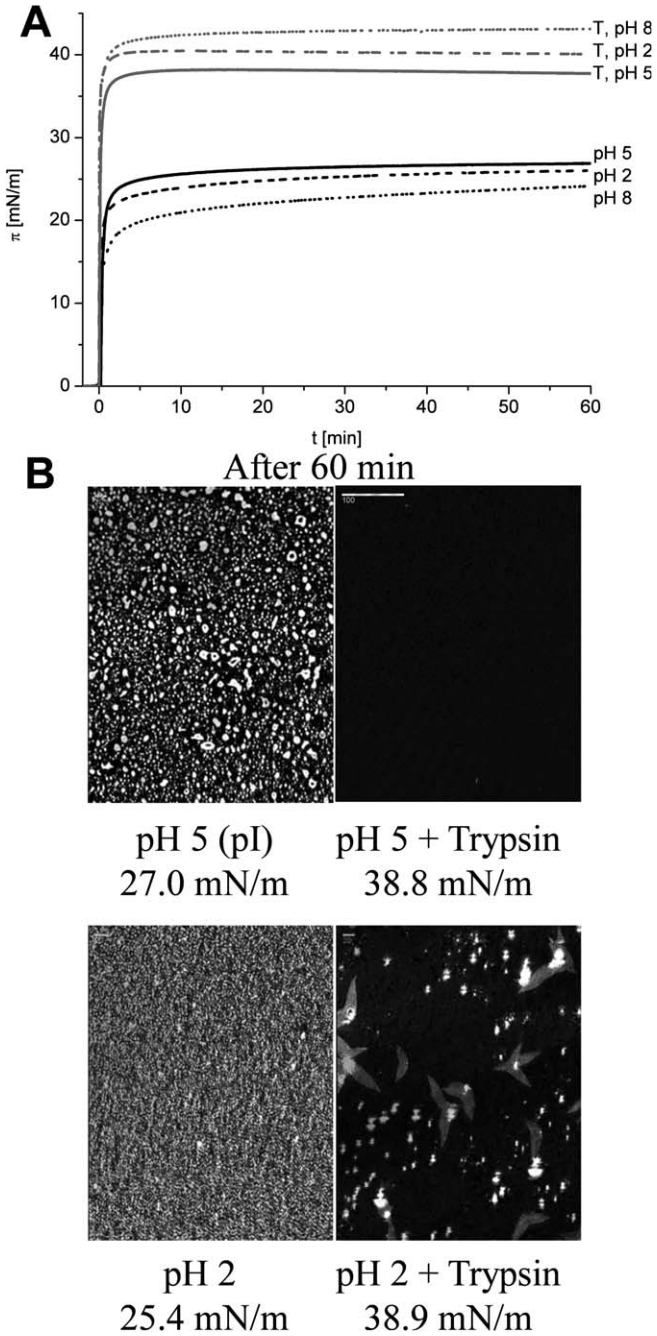

Fig. 4 (A) Measurement of surface pressure as a function of time at defined area at different pH (I = 5 mM). For intact oleosomes (black) at pH-values different from the isoelectric point (pH 5) lower surface pressure values are recorded due to higher repulsion of the oleosins. Trypsin digested oleosomes (grey) show higher surface pressure values and different pH dependencies. (B) BAM micrographs of soybean oleosomes at different pH after 60 min. At pH-values above and below the isoelectric point, repulsion between the charged oleosins occurs, leading to smaller aggregates for untreated oleosomes. Trypsin digested oleosomes show star-shaped phospholipid domains at pH 2 and small round lipid domains at pH 5. Conditions: 22 μl (6.6 mg l^{-1}) OB, pH 2: phosphoric acid, pH 5: acidic acid, pH 8: monosodium phosphate, all with 5 mM buffer concentration and I = 5 mM.

phosphatidylethanolamine is at pH 5.5[33] which leads to higher electrostatic repulsion at pH 2 and 8 between the lipids compared to pH 5, hence the long-range electrostatic dipolar repulsion F_{el} dominates, which leads to elongated, irregular structures.

The long-time development, shown in Fig. 5A, is also different for digested and intact oleosomes. For the latter, the surface pressure as well as the aggregate density

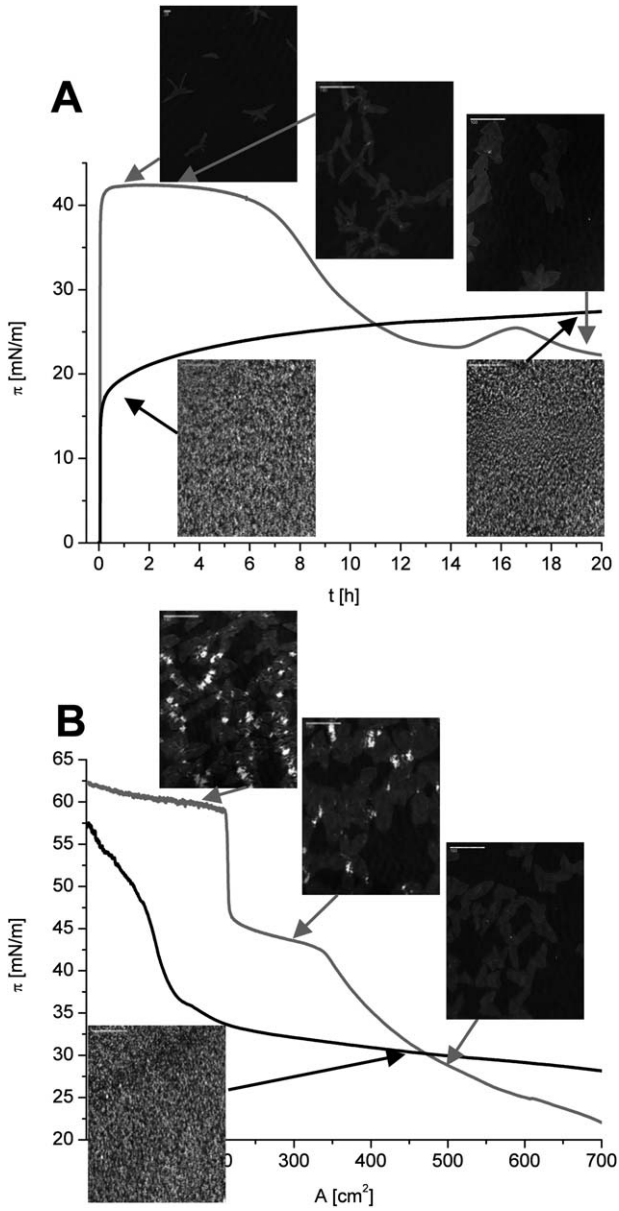

Fig. 5 (A) Measurement of surface pressure as a function of time at defined area at pH 8 (I = 5 mM) of intact (black) and trypsin digested oleosomes (grey). Trypsin digested oleosomes show star-shaped phospholipid domains and "drops of grease" which cause a decrease in surface pressure. (B) Compression (v_B = 30 cm^2 min^{-1}) isotherm of intact (black) and trypsin digested (grey) soybean oleosomes. Conditions: 22 μl OB (6.6 mg l^{-1}), 5 mM Tris, pH 8.

increase with time, presumably due to the breakup of the oleosomes. The situation is reversed when trypsin digested oleosomes are present. The surface pressure is then decreasing. These observations probably result from the faster aggregation of the longest tryptic fragments (<8 kDa, Fig. 3), including basically the hydrophobic hairpin of the oleosins. The remaining protein chains in water could be largely considered as unstructured random copolymers which tend to collapse. Several chains form dense, globular aggregates. Under these circumstances the size of the aggregates (*i.e.*, the number of chains involved) is determined by a balance of the surface tension of the aggregates, their bulk energy, and the interactions between the (polar) hydrophilic tails, which are distributed on the surface of the aggregate. The size of such aggregates diminishes with the polarity of the remaining short hydrophilic tail of the N-terminus. This also explains the occurrence of larger protein aggregates, *e.g.*, visible in Fig. 4B (pH 2) that are more likely to diffuse into the subphase due to their weight and less amphiphilic nature. Additionally, also here, a dependence on pH is noticeable: Close to the isoelectric point of phosphatidylethanolamine, where a presumably homogeneous film of phospholipids is present, no protein aggregates are visible. At pH 2, where domain formation occurs, large aggregates are observable in the first hours due to available interfacial space.

The setting of oleosins leaves only phospholipids and triglycerides at the air–water interface which continue to phase separate as the oleosins, which functioned as emulsifiers, start to sink. This can be seen in the growing of the phospholipid domains (Fig. 5A + 6A) and the appearance of circular TAG oil droplets (Fig. 6B). Those oil droplets coalesce with time (see flower-like structures in Fig. 5B), leading to bigger droplets with bigger area-to-perimeter ratio, which results in fewer binding sites and hence lower surface pressure.

These assumptions are further strengthened by the compression isotherms in Fig. 5B: In the isotherm of intact oleosomes only one distinct transition can be observed, whereas trypsin digested oleosomes show two transitions and a collapse at 60 mN m^{-1} that are very similar to phospholipid phase behaviour. Also the domains that are visible at high surface pressure (above 40 mN m^{-1}) reappear and increase in size during compression, confirming our hypothesis that these are indeed phospholipid domains that reform due to the decreasing area.

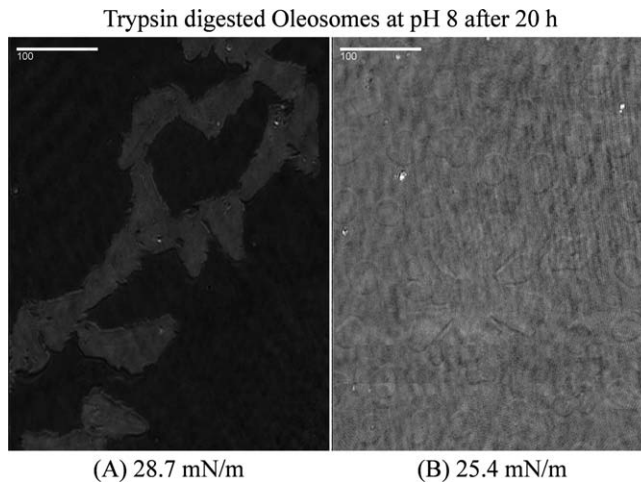

Fig. 6 BAM micrographs of trypsin digested soybean oleosomes at pH 8 after 20 h. (A) Left picture (100% brightness and contrast) shows irregular grown phospholipid domains. (B) The right picture (brightness and contrast +40%) shows TAG oil droplets and flower-like structures. Conditions: 22 µl (6.6 mg l^{-1}) OB, 5 mM Tris, pH 8, $I = 5$ mM.

Additionally, for the untreated oleosomes a highly viscous film is formed during the waiting time, which suggests a denaturation of oleosins and the formation of a protein-network.[28] Trypsin digested oleosins, due to the loss of the hydrophilic part, are no longer able to form this viscous detachable film after compression.

Conclusions

The combination of surface pressure measurements and simultaneous Brewster angle microscopy is used to reveal the behaviour at the air–water interface of trypsin digested oleosomes compared to untreated ones.

In principle, oleosomes are micelle-like structures with an outer phospholipid monolayer and an interior filled with triglycerides, but with oleosins sticking hairpin-like in the structure, with the hydrophilic parts remaining outside the oleosomes. After injection into the aqueous subphase, intact oleosomes diffuse immediately to the air–water interface due to flotation and their amphiphilic nature, which is visible in the steep increase in surface pressure and the bright, micrometer sized particles at the air–water interface during this diffusion. Rupture and subsequent coalescence take place when the packing of oleosomes exceed a crucial level and oil bodies come too close together. This rupture can be seen in an additional increase in surface pressure and increase in aggregate size visible by BAM.

Trypsin is a serine protease able to hydrolyse proteins. We assume that trypsin cleaves the N-and C-terminal domains of the oleosins, thereby destroying the stability of the oil bodies. This is supported by the increased surface activity compared to intact oleosomes, after injection into an aqueous subphase. Since the jump in surface pressure after injection of trypsin digested oleosomes into the subphase is much higher than the maximum measured for the same amount of untreated oleosomes we believe that the trypsin cleaved oleosins lead to different complexes with the phospholipids at the air–water interface. Binding sites between them are not available anymore, resulting in a large number of free phospholipids and a further decrease of the water surface tension. Furthermore, as inferred from the faster decrease in surface pressure, trypsin digested oleosomes presumably form larger protein aggregates and growing lipid domains. In general, the air–water interface after the injection of trypsin digested oleosomes is dominated by their phospholipids, showing star-shaped domains and collapse during compression, and their TAGs (circular oil droplets).

Soybean oleosomes are highly robust micelle-like structures and provide extremely stable emulsions but before their use in food applications their compatibility with the human digestive system has to be studied as proteins are the most common allergic component in food. Oleosomes consist of triacylglycerides and phospholipids, which can be emulsified and enzymatically digested, and oleosins. We could show that oleosins can be cleaved by trypsin, which is one indication that they can be safely used in food industries. Additionally, such investigations are requisites to better understand the principal function and structure of oleosins (*i.e.*, phospholipid binding sites on oleosins), investigate their usability as plant expression system for recombinant proteins or peptides and provide information on the mode of action of the digestive enzyme trypsin.

Moreover, the use of proteases like trypsin yields a higher release of phospholipids (lecithin) and oil (TAGs) from the oleosomes during this safe and environmentally friendly aqueous oil extraction process.

Acknowledgements

The authors like to thank Markus Deserno, Johannes Franz, Sania Maurer, Christine Peter and Birgitta Schiedt for fruitful discussions and Sandra Ritz for the use of SDS-PAGE equipment.

References

1 K. Hsieh and A. H. C. Huang, *Plant Physiol.*, 2004, **136**, 3427–3434.
2 J. Tzen and A. Huang, *J. Cell Biol.*, 1992, **117**, 327–335.
3 V. Martinet, P. Saulnier, V. Beaumal, J.-L. Courthaudon and M. Anton, *Colloids Surf., B*, 2003, **31**, 185–194.
4 A. H. C. Huang, in *Annu. Rev. Plant Physiol. Plant Mol. Biol.*, 1992, vol. 43, pp. 177–200.
5 T. Hevonoja, M. O. Pentikäinen, M. T. Hyvönen, P. T. Kovanen and M. Ala-Korpela, *Biochim. Biophys. Acta, Mol. Cell Biol. Lipids*, 2000, **1488**, 189–210.
6 P. Jolivet, C. Boulard, V. Beaumal, T. Chardot and M. Anton, *J. Agric. Food Chem.*, 2006, **54**, 4424–4429.
7 L. Palacios and T. Wang, *J. Am. Oil Chem. Soc.*, 2005, **82**, 571–578.
8 D. Iwanaga, D. A. Gray, I. D. Fisk, E. A. Decker, J. Weiss and D. J. McClements, *J. Agric. Food Chem.*, 2007, **55**, 8711–8716.
9 L. Towa, V. Kapchie, C. Hauck, H. Wang and P. Murphy, *J. Am. Oil Chem. Soc.*, 2011, **88**, 733–741.
10 V. N. Kapchie, D. Wei, C. Hauck and P. A. Murphy, *J. Agric. Food Chem.*, 2008, **56**, 1766–1771.
11 L. Towa, V. Kapchie, G. Wang, C. Hauck, T. Wang and P. Murphy, *J. Am. Oil Chem. Soc.*, 2011, **88**, 1581–1591.
12 A. H. C. Huang, *Plant Physiol.*, 1996, **110**, 1055–1061.
13 F. Capuano, F. Beaudoin, J. A. Napier and P. R. Shewry, *Biotechnol. Adv.*, 2007, **25**, 203–206.
14 D. J. Murphy, J. N. Keen, J. N. O'Sullivan, D. M. Y. Au, E.-W. Edwards, P. J. Jackson, I. Cummins, T. Gibbons, C. H. Shaw and A. J. Ryan, *Biochim. Biophys. Acta, Gene Struct. Expression*, 1991, **1088**, 86–94.
15 L. Alexander, R. Sessions, A. Clarke, A. Tatham, P. Shewry and J. Napier, *Planta*, 2002, **214**, 546–551.
16 S. Dauphas, V. Beaumal, A. Riaublanc and M. Anton, *J. Agric. Food Chem.*, 2006, **54**, 3733–3737.
17 Y. Chen and T. Ono, *J. Agric. Food Chem.*, 2010, **58**, 7402–7407.
18 J. C. Watkins, *Biochim. Biophys. Acta, Lipids Lipid Metab.*, 1968, **152**, 293–306.
19 B. Alfred, *Biochim. Biophys. Acta, Biomembr.*, 1979, **557**, 32–44.
20 O. Albrecht, H. Gruler and E. Sackmann, *J. Colloid Interface Sci.*, 1981, **79**, 319–338.
21 V. von Tscharner and H. M. McConnell, *Biophys. J.*, 1981, **36**, 409–419.
22 H. Möhwald, *Annu. Rev. Phys. Chem.*, 1990, **41**, 441–476.
23 S. Bonsegna, S. Bettini, R. Pagano, A. Zacheo, V. Vergaro, G. Giovinazzo, G. Caminati, S. Leporatti, L. Valli and A. Santino, *Appl. Biochem. Biotechnol.*, 2011, **163**, 792–802.
24 D. Beaglehole, *Rev. Sci. Instrum.*, 1988, **59**, 2557–2559.
25 S. Henon and J. Meunier, *Rev. Sci. Instrum.*, 1991, **62**, 936–939.
26 D. Hoenig and D. Möbius, *J. Phys. Chem.*, 1991, **95**, 4590–4592.
27 D. Hönig and D. Möbius, *Thin Solid Films*, 1992, **210–211**(Part 1), 64–68.
28 G. Waschatko, A. Junghans and T. A. Vilgis, *J. Phys. Chem. B*, 2012, accepted.
29 E. Gasteiger, C. Hoogland, A. Gattiker, S. e. Duvaud, M. R. Wilkins, R. D. Appel and A. Bairoch, ed. J. M. Walker, Humana Press, 2005, pp. 571–607.
30 A. D. Petelska and Z. A. Figaszewski, *Biochim. Biophys. Acta, Biomembr.*, 2002, **1567**, 79–86.
31 J. M. Garcia, L. C. Quintero and M. Mancha, *Phytochemistry*, 1988, **27**, 3083–3087.
32 H. M. McConnell, *Annu. Rev. Phys. Chem.*, 1991, **42**, 171–195.
33 M. C. Phillips and D. Chapman, *Biochim. Biophys. Acta, Biomembr.*, 1968, **163**, 301–313.

PUBLIKATIONEN

3 Maurer, S.; Waschatko, G.; Schach, D.; Schiedt, B.; Dahl, J.; Weidner, T.; Bonn, M.; Vilgis, T. A., The role of intact oleosin for the stabilization of oleosomes. *The Journal of Physical Chemistry B, submitted*

The role of intact oleosin for the stabilization of oleosomes

Journal:	*The Journal of Physical Chemistry*
Manuscript ID:	Draft
Manuscript Type:	Article
Date Submitted by the Author:	n/a
Complete List of Authors:	Maurer, Sania; Max Planck Institute for Polymer Research, Waschatko, Gustav; Max Planck Institute for Polymer Research, ; Johannes Gutenberg University Mainz, Institute of Pharmacy and Biochemistry Schach, Denise; Max Planck Institute for Polymer Research, Schiedt, Birgitta; Max Planck Institute for Polymer Research, Weidner, Tobias; Max Planck Institute for Polymer Research, Bonn, Mischa; Max Planck Institute for Polymer Research, Molecular spectroscopy Vilgis, Thomas; Max Planck Institut fur Polymerforschung, Dahl, Jakob; Max Planck Institute for Polymer Research, ; Massachusetts Institute of Technology, Departement of Chemistry

The role of intact oleosin for the stabilization of oleosomes

Sania Maurer [†,‡,], Gustav Waschatko [††,‡], Denise Schach [‡], Birgitta Schiedt, Jakob Dahl [§], Tobias Weidner, Mischa Bonn, Thomas A. Vilgis*

‡: Those authors contributed equally to this work

Max Planck Institute for Polymer Research, Ackermannweg 10, 55128 Mainz, Germany

† Department of Food Biotechnology and Food Process Engineering, Berlin University of Technology, Königin-Luise-Str. 22, 14195 Berlin, Germany

†† Institute of Pharmacy und Biochemistry, Johannes Gutenberg University Mainz, Johann-Joachim-Becher-Weg 30, 55128 Mainz, Germany

§Department of Chemistry, Massachusetts Institute of Technology, 77 Massachusetts Avenue, Cambridge, 02139 Massachusetts, USA

*Corresponding author:

Sania Maurer

Max Planck Institute for Polymer Research, Ackermannweg 10, 55128 Mainz, Germany

Phone: +49 6131 379149

Fax: +49 6131 379100

maurer@mpip-mainz.mpg.de

KEYWORDS

Oil bodies, Emulsion, Air-water interface, SFG, FTIR, Digestion

ABSTRACT

The universal mechanism of plant lipid storage relies on the formation of oleosomes or oil bodies, enclosing oil, *i.e.*, triacylglycerides, in small subcellular droplets. Particularly plant seeds are rich in this pre-emulsified oil to provide a sufficient energy reservoir for growing. The triacylglyceride core of the oleosomes is surrounded by a phospholipid monolayer containing densely packed oleosin-proteins. The oleosins are anchored to the oleosome with their hydrophobic hairpin in the oil phase while the hydrophilic termini remain outside. These specialized proteins are expressed during seed development and maturation and play a major role in the stabilization of oleosomes. To better understand the importance of oleosins for oleosome stabilization we studied the molecular structure in correlation with changing macroscopic properties of soybean oleosomes during the process of partial digestion. Tryptic digestion of soybean oleosins reveals their function in their native environment, which is the stabilization of an oil-water interface and when reaching an air-water interface. The surface charge and the associated aggregation of oleosomes are governed by proteins before and by phospholipids after digestion. Cleavage of the hydrophilic oleosin parts is accompanied by the loss of secondary structures as evidenced by Fourier-transform infrared and sum frequency generation spectra on the one hand, and weakening of emulsifying properties on the other hand.

INTRODUCTION

The fascination of plant oleosomes is based on their unique structure and their unusual interactions. The oil particles are stabilized by a monolayer of phospholipids and proteins (oleosins) which contain a long hydrophobic domain ranging deeply into the droplets. Their *C*- and *N*-terminals are mostly composed of hydrophilic amino acids providing a pH-dependent net charge. The terminals of the domains are less conserved across the plant species and length and sequence can vary significantly.[1-3] An ensemble of oleosomes forms thus natural, stable emulsions stabilized by steric and electrostatic repulsion of oleosins supported by their interactions with different zwitterionic phospholipids.[4, 5] Within the natural diversity of proteins, known to stabilize interfaces, such as hydrophobins or apolipoproteins, only oleosins are reminiscent of a chain surfactant as it can be seen by their amphiphilic structure.[6] The challenging tasks are to understand the structure and interfacial behavior of the protein in detail. In a previous paper[7], we have already discussed the behavior of oleosomes at the air-water interface, which is driven by the oleosins net charge.

In this paper we use another approach for the structural analysis of oleosomes: by enzymatic digestion the hydrophilic domains of the oleosomes are cut, which changes intra- and intermolecular interactions and structure simultaneously.

Oleosomes are expressed during seed development and maturation. By these subcellular organelles, nature developed a suitable system to store and preserve lipids as an energy source for plant growth.[3] In the last two decades, the cosmetic, pharmaceutical and food industry discovered those oleosomes to benefit from their stable structure by using them as pre-emulsified additive or carrier of valuable (bioactive) ingredients.[8]

Plant sources from which oleosomes can be extracted are diverse. Soybeans are the most important protein and oil source for millions of people and become increasingly important for nutritional and health and care products due to their valuable compounds. In this study, we determine the secondary structure of soybean oleosins for the first time. To extract the oleosomes from soybeans, we have used a modified gentle flotation-centrifugation method at pH 11 developed by Chen and Ono[9]. The centrifugation method yields intact oleosomes free of storage proteins which might affect the pH-dependent charge and aggregation behavior of oleosomes and the secondary structure analysis of soybean oleosins. Additionally, allergenic soy proteins are removed by this method. To study the folding of the oleosins at the oil-water interface of oleosomes and after bursting at the air-water interface, we have treated the oleosomes by enzymatic digestion.

The trypsin from porcine pancreas used in this work exhibits proteolytic and lipolytic activity, both also taking place in plants during seed germination, as well as in the human gastro-intestinal tract. Lipolysis and proteolysis of oleosomes[10, 11] most likely interfere with each other in physiological processes. On the one hand, proteolysis cleaves the outer domains of the oleosins, which is the barrier preventing coalescence and a potential anchor for lipases.[10] On the other hand lipases hydrolyze the TAG into FFAs, mono- and diglycerides (MG and DG) on a lipid droplet interface.[12]

Studies by Waschatko *et al.*[7] revealed that digestion also affects the behavior of the oleosomes at air-water interfaces. It could be shown by film balance measurements and Brewster angle microscopy (BAM) that intact oleosomes burst and spread when reaching the air-water interface. The composition of the interfacial layer formed from ruptured oleosomes is now further investigated with sum frequency generation (SFG), a spectroscopy used to probe molecular

vibrations which are exclusively generated at the interface. For further verification, drop-shape analysis is introduced to show the diffusion driven surface behavior of oleosomes.

In general, the secondary structure of oleosins has been extensively investigated and controversially debated. First the structure of several oleosins was predicted by molecular modeling of the amino acid sequences and structural similarities to well-understood animal apolipoproteins.[13] Murphy *et al.*[13] concluded that the central hydrophobic sequence appears as β-strand but also a hairpin of anti-parallel α-helices connected by a proline knot was proposed for this domain. For the *N*- and *C*-terminal regions of the protein, amphiphilic α-helical structures exposed to the cytosol were suggested. Later, it was predicted that the terminal regions of different oleosins are highly variable and no specific structure appears to be preferential.[3]

Based on secondary structure analysis by means of circular dichroism (CD) and FTIR spectroscopy the protein structure of oleosins from different sources such as peanut[14], rapeseed[2, 15], sunflower[15-17], and safflower[16] was probed. To this end, several studies were done on purified oleosins in aqueous solutions[2, 14, 15] whereas others stabilized purified oleosins in mixed micelles[17, 18] or even probed the structural features of oleosin in its natural environment to avoid possible denaturation[4, 16]. Secondary structure content of native oleosin was compared to samples of which partial proteolysis was applied to the exposed terminals. This study suggested the central protein segment was mostly α-helical, while the termini appeared to have mostly random structure.[16]

The main concern with these studies is that the harsh conditions (*e.g.,* solvents, chaotropes) used for the isolation of oleosins from their native environment and the extraction procedures (*e.g.,* pH, mechanical stress) employed to remove residual seed storage proteins from the

oleosomes may have resulted in significant alterations of secondary structure and protein composition at the oleosome surface.

Enzymatic digestion of oleosomes has already been applied to investigate the stability of oleosomes, revealing that oleosomes are mainly stabilized via steric hindrance and electrostatic repulsion of the oleosins.[3] Drop size, zeta-potential and rheological measurements of oleosomes free of any storage proteins have been employed in this study to verify the exclusive stabilizing effect of oleosins.

By the combination of a non-destructive extraction method, non-invasive physical methodologies providing information on different length scales, as well as the exploitation of enzymatic digestion we could finally reveal in this study the structure-function relation of oleosins at the natural oil-water interface of an oleosome.

MATERIAL AND METHODS

For all preparation steps, ultra-pure water, filtered with a Millipore device (Billerica, MA/USA) was used. For oleosome digestion, trypsin NB from porcine pancreas (Cat. No. 37294, tryptic activity: ≥ 50 µkat/g (Ph.Eur.), Serva, Germany) was used, which contains mainly trypsin, but also minor contents of chymotrypsin, elastase, and non-proteolytic activity, which is usually lipolytic. Proteolytic activity was proven by SDS-PAGE, lipolytic activity by Thin Layer Chromatography (TLC) with soybean oil emulsions. Solvents were purchased from Sigma Aldrich (Steinheim, Germany). The used buffers and salts are described in previous publications.[7, 19] The control emulsion for FTIR Spectroscopy contained 0.75 % lecithin (Serva, Heidelberg, Germany) and 15 % soybean oil (Sojola, Hamburg, Germany) emulsified in ultra-pure water with an IKA® T18 basic Ultra Turrax (15.600 rpm, 1 min).

Oleosome isolation and purification

Isolation of soybean oleosomes was performed by a modified aqueous flotation-centrifugation method proposed by Chen and Ono[9]. Briefly, dried soybeans (Davert) bought from a local supermarket were soaked in deionized water at 4 °C for at least 20 h. After this, soaked beans were separated from the excessive water and fresh water was added to obtain a 10 % soybean-to-water ratio. The mixture was grounded in a Vorwerk Thermomix TM31 at a speed of 10 200 rpm for 90 s. Raw soy milk was obtained by filtering the resulting slurry through two layers of Kimtech science precision wipes 21x11 cm (Kimberly Clark). To remove residual storage proteins, 25 % sucrose (w/w) was added to the soy milk and the pH was adjusted to 11.0 with 1 mol l^{-1} NaOH solution. Divided into portions of 50 ml each, the solution was centrifuged (15 000 g, 4 °C) for at least 5 h. The resulting cream layer was taken off with a spoon, resuspended in a 20 % sucrose-solution of pH 11.0 and anew centrifuged. The washing step was performed twice. The resulting oleosomes were collected, dispersed in 50 ml of deionized water and dialyzed in a cellulose tube (MWCO: 12,000 - 14,000, b = 45 mm, wall thickness = 20 μm) from ZelluTrans (Roth, Karlsruhe, Germany) to remove the sucrose used for the purification of the oleosomes.

Trypsin digestion

1 mg of trypsin from porcine pancreas was added to 1 ml of dialyzed, isolated, intact oleosomes (85 % water content). The tryptic digestion was performed at 25 °C for 1 h at 500 rpm in a HLC ThermoMixer MKR 13.

FTIR Spectroscopy

The FTIR spectra were recorded on a Bruker Vertex 70 equipped with a DLaTGS detector in transmission mode. All spectra were recorded at room temperature. A transmission cell with a

CaF_2 window was used. Each spectrum was averaged for 40 scans at a resolution of 2 cm^{-1}. As a background reference the bare CaF_2 window was used and the sample chamber was purged with dry air for ten min. After purification the soy oleosome emulsions of either native or trypsin-digested oleosomes were centrifuged for 30 min to again separate the aqueous phase from the oleosome cream layer. 20 mg of the oleosome cream layer was spread on one of the CaF_2 windows and dried overnight under a stream of dry air to remove any excess water. Before the measurement the chamber was purged for 10 min with dry air. The spectra of aqueous emulsions consisting of water, soy oil and soy lecithin with and without trypsin were compared to the native and digested oleosome spectra. These negative samples were prepared and dried on the transmission windows in the same way as the native oleosomes. The exact peak positions were identified by the minimum positions in the second derivatives. The derivative spectra were obtained using the Savitzky-Golay algorithm with a degree of 2 and a width of 9 points using the software package OPUS. A linear baseline correction was applied to the spectra. The amide I region was fitted with a sum of profiles consisting of 50 % Lorentzian shape and 50 % Gaussian shape[20] using the Levenberg-Marquardt algorithm[21]. The resonance positions inferred from the second derivative spectra were fixed and the full width at half maximum (FWHM) as well as the band area were determined. For better comparison, the spectrum of the trypsin-digested oleosomes was multiplied by a factor of 4.5 in the figures. Bands were assigned to secondary structure according to literature,[16, 22, 23] which allowed us to quantify the relative contributions of different structural components to the overall structure. We note that we did not calibrate this procedure, and that the numbers obtained for the relative contributions of different structural components should therefore not be considered absolute. The resonance positions are reported with an error margin of ± 2 cm^{-1}.

SFG Spectroscopy

For the sum frequency generation (SFG) experiments we used broadband infrared pulses (FWHM of ~200 cm^{-1}) generated by an OPG/OPA (TOPAS, Light Conversion) which was pumped by ~2 W average power of 800 nm pulses from a Spitfire Ace (Spectra Physics) amplified laser system (1 kHz, ~40 fs FWHM). In addition, ~0.5 W of the laser output passes through an etalon that generates a narrow band visible pulse (FWHM bandwidth of ~15 cm^{-1}) to provide the spectral resolution of the experiment. The broadband infrared pulse (~3.5 μJ) provided a spectral window of 200 cm^{-1}, centred around 1700 cm^{-1} in the amide I region. A trough (3 x 80 x 40 mm) was filled with 6 ml of 5 mM PBS buffer (pH 7). 26.7 μl of native or digested aqueous oleosome solutions (1440 mg/l) were injected into the subphase to yield a total concentration of about 6.4 mg/l (surface pressure measurements at different oleosome concentrations, including this one, are described in a previous work[19]). The samples were allowed to equilibrate for 20 min before the SFG measurements. The visible and infrared beams were spatially and temporally overlapped at the solution surface. The incident angles of the visible (VIS) and infrared (IR) beam were ~35° and ~40° with respect to the surface normal. The VIS beam was focused down to a diameter of approximate 400 μm. The SFG light was spectrally dispersed by a monochromator and detected by an Electron-Multiplied Charge Coupled Device (EMCCD, Andor Technologies). Spectra were recorded using p-polarized SFG, VIS, and IR beams with 600 s of acquisition time. The spectra were then corrected for the background and normalized with a reference spectrum generated by the non-resonant SFG signal of a silver surface. The background signal was also recorded with 600 s of acquisition time while blocking the IR pulse. Lorentzian band shapes were fitted to the spectra according to the relation

$$I \propto \left|\chi^{(2)}\right|^2 \propto \left|A_{NR}e^{-i\phi_{NR}} + \sum_n \frac{A_n}{\omega_n - \omega_{IR} - i\Gamma_n}\right|^2$$

in a manner that was consistent with the imaginary part of the susceptibility $|\chi^{(2)}|$ obtained using the maximum entropy method (MEM), which is a numerical method to retrieve the phase-information in spectra.[24]

Droplet Size Distribution

The cumulative volume distribution (Q_3 (%)), defined as average volume of droplets that are equal to or smaller than a specific droplet size x, of native and trypsin-digested oleosomes dispersed in buffer solutions of varying pH value were analyzed by using a laser diffraction analyzer (Horiba LA-950, Retsch Technology, Germany). For the measurement, the oleosomes were diluted as appropriate with buffer solution to avoid multiple scattering effects. The Sauter mean diameter $d_{32} = 6\,V_d/A_d$, where V_d which is the volume of the droplet and A_d the droplet area, was determined as the characteristic average droplet size. The diffractive data were calculated by using a predefined optical model for liquid disperse formulations of small droplets ($\leq$ 10 µm) according to Mie-theory. As the refractive index of oleosomes is not yet known and could not be readily determined due to the constituents' inhomogeneity, the imaginary and real part of the refractive indices (n) where estimated according to known parameters of soybean oil (n = 1.47)[25] and common proteins (*e.g.,* casein, lactoglobulin, lysozyme) with refractive indices ranging from 1.594 to 1.630 as given in literature[26]. Test trials where the measured scattering intensities were compared to the calculated ones (variance $\chi^2 = 0.45$) verified appropriate indices of 1.6 (real part) and 0 (imaginary part). The ionic strength of the oleosome-buffer solution was kept constant at 10 mM and the measurements were conducted at 25 °C. Droplet size distributions were measured in triplicate using three different samples.

The droplet size distribution of emulsions prepared from native and digested oleosomes was also examined by laser diffraction. Here, the same procedure as described above was conducted. The measurements were conducted in duplicate using two different samples.

Zeta-potential

Dispersions of native and trypsin-digested oleosomes were diluted using buffer solutions (10 mM sodium chloride, varying pH) to avoid multiple scattering effects. Diluted oleosome dispersions were filled into the capillary of a sample cell, which was then placed into the chamber of a Zetasizer Nano ZS (Malvern, Germany). The zeta-potential was measured on basis of Laser Doppler Anemometry (LDA) and deduced from the electrophoretic mobility of the droplets according to the Helmholtz-Smoluchowski equation (1). By applying an external electric field, the charged disperse droplets move with different velocity detected by laser light scattering. Based on this approximation and the assumption that oleosomes are spherical with a smooth surface, the zeta-potential ζ is derived from the shear viscosity η, the velocity ν, the external electrical field E, and the dielectric constant ε.[27]

$$\zeta = 4\pi\eta v/E\varepsilon \quad (1)$$

Measurements were conducted in duplicate from two freshly prepared samples at 25 °C.

Interfacial Activity

The dynamic properties of native and digested oleosome layers at the air-water interface were investigated by applying axisymmetric drop shape analysis (ADSA). An automated drop tensiometer OCA20 (Dataphysics GmbH, Germany) was used to determine the interfacial surface pressure of native and trypsin-digested oleosomes dispersed in different solutions of varying pH (2, 5.3, 8) and at constant ionic strength (10 mM, NaCl). A high speed frame grabber (200 frames per 15 min) recorded shape changes of the pendant drop. Static measurements were

conducted in a temperature controlled chamber (T = 22.8 ± 0.2 °C). To prevent evaporation and changes in the drop volume due to air current, the syringe placed in the automated dosing system was enclosed with a cuvette, which was filled with a few drops of water and tightly sealed with Parafilm® to ensure constant humidity. The drop was formed with a dosage rate of 5 µl/s at the tip of a stainless steel hydrophobized capillary. The injected drop volume of varying concentrations (15.6 – 1560 mg/l) of native and trypsin-digested oleosome dispersions was 15 ± 0.3 µl. To assure that the drop volume could equilibrate for each measurement equally, a waiting time of 30 s after the drop formation was taken before the measurements were started. Changes in drop shape were monitored for 600 s. A software belonging to the drop tensiometer OCA20 was used to fit the Gaussian-Laplace equation of capillary to the experimental drop shape coordinates and thus to be able to determine the interfacial tension.[28] By subtracting the obtained surface tension of the pendant drop from the surface tension of pure water (σ_0 = 72.65 mN/m at 22.8 °C), the surface pressure (in mN/m) can be calculated according to $\pi = \sigma_0 - \sigma$ and is plotted against the time. Measurements were conducted at least in duplicate.

Rheology of Emulsions

50 g soybean oil was slowly added to 25 ml of a 23.3 % soybean oleosome dispersion (native and digested) in 5 mM Tris/NaCl (I = 5 mM) pH 8 buffer and homogenized with an IKA® T18 basic Ultra Turrax (15.600 rpm, 4 min). Rheological measurements of the emulsions were performed directly after preparation.

A Bohlin Gemini 200 with a coaxial cylinder measuring system (inner diameter 25 mm, outer diameter 27.5 mm) was used to determine the viscosity of 12 g emulsion depending on shear rate employing the Searle method. The shear rate $\dot{\gamma}$ was varied from 0.0002-400 1/s. The measurement time for each point was 5 s. A shear rate dependent delay time t_d (equilibration time

between measurement points) was used, with $t_d = 120$ s for the lowest shear rate. $t_d(\dot{\gamma})$ was calculated in the following way:

$t_d(\dot{\gamma}) = 120\ s\ \frac{0.0002\ 1/s}{\dot{\gamma}}$. An upwards shear rate ramp was followed by a downwards one to check for hysteresis effects. All measurements were performed at 25 °C.

RESULTS AND DISCUSSION

Oleosome Purification, Digestion and Characterization

The efficiency of the purification with regard to the removal of the storage proteins has been verified by SDS-PAGE. Additionally, the total nitrogen content of isolated soybean oleosomes was measured with the Dumas method, revealing a protein content of 4.4 to 5.8 % (calculated factor for the conversion of total nitrogen content to protein content for soybean oleosins was 5.9). After digestion with commercial trypsin only protein fragments smaller than 6 kDa are visible in the SDS-PAGE (Figure 1), due to the proteolytic activity of trypsin, chymotrypsin and elastases. Furthermore, the electrophoretic separation of the commercial trypsin (lane 1) displayed proteins with molecular weights between 38 and 62 kDa, which is in accordance with the size of pancreatic lipases, *e.g.,* P00591 (porcine pancreatic triacylglycerol lipase, 50 kDa).

TLC with mobile phase A of Soxhlet extraction residues of native oleosomes showed phospholipids (R_f = 0.2–0.5)[29], which are not extractable with pentane, thereby confirming that they had been bound to the intact oleosin proteins[5]. Hydrolysis products of TAG were detected at R_f = 0 for MG, R_f = 0.3 for DG and R_f = 0.5 for FFA (mobile phase B).[30]

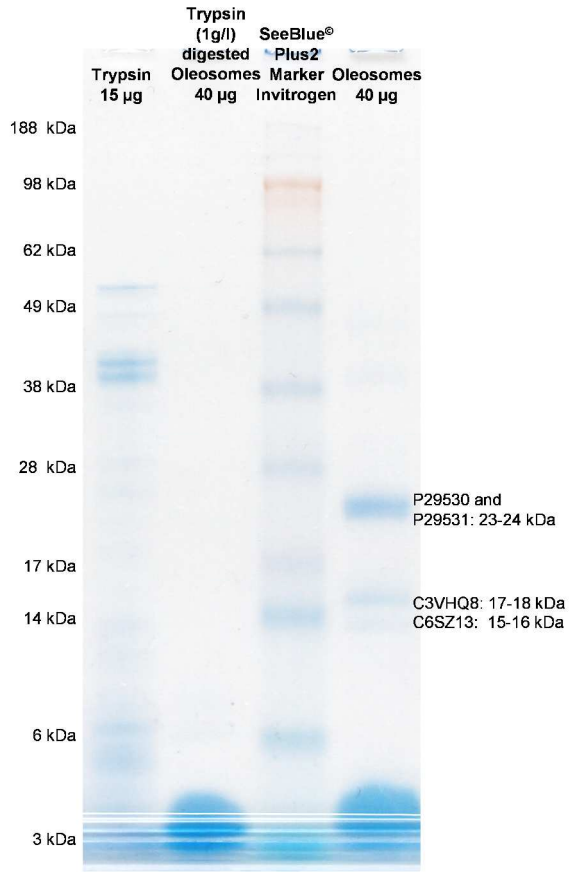

Fig. 1 Commassie stained SDS-PAGE gel of purified soybean oleosomes before and after digestion with trypsin. Oleosomes were digested with 1 mg/ml of commercial trypsin at 25 °C for 1 h in a ThermoMixer. The trypsin lane (15 µg) shows high molecular weight proteins between 38 and 62 kDa, like pancreatic lipase.

FTIR Spectroscopy

FTIR spectroscopy was applied to estimate the secondary structure contents of native and trypsin-digested oleosomes. Since trypsin was shown to cleave the hydrophilic from the hydrophobic part at lysine and arginine, comparison of spectra from native and protease treated oleosomes can yield information about the secondary structures of the two protein regions. The native samples contain secondary structure elements of all protein parts, whereas the spectra of trypsin-digested oleosomes contain only structural elements of the remaining central

hydrophobic part. To exclude water bands we dried all samples on CaF_2 windows before the measurements. The spectra of native and digested oleosomes as well as dried aqueous soy oil/lecithin emulsions have common bands around 2800-3050 cm^{-1}, 1456 cm^{-1} and 1200-1100 cm^{-1} (data not shown) which have been attributed to C–H stretch, C–H deformation and C–O bonding vibrational modes of the TAGs, respectively.[16] Moreover, all spectra show a prominent band near 1745 cm^{-1}, which we assigned to the carbonyl stretch vibration of TAG esters[16] (see Figure 2).

By comparing spectra of native oleosomes with soy oil/lecithin samples, we could identify bands referring to lipid molecules such as TAG. The oil/lecithin control samples were also treated with commercial trypsin to check whether the enzymes or lipid digestion products generate additional bands (see Figure 2, upper solid trace). A strong additional band around 1714 cm^{-1} was detected, which also appeared in the spectra of digested oleosomes (see Figure 2, lower solid trace). The band did not appear in samples treated with trypsin (Cat. No. 37291, Serva, Heidelberg, Germany) of higher purity without lipolytic activity. Hence we assign this band to the carboxyl group (fatty acids) carbonyl stretching (see Table 1). From this observation we can conclude that the commercial trypsin we applied to the samples of the shown spectra contains not only pancreatic proteases but also lipases. This could be a general issue when working with commercial pancreatic proteases. The spectra of the control samples exhibit a very weak band around 1650 cm^{-1} which might be attributed to amide I vibrational modes of residual proteins in the control emulsion. However, this weak band does not seem to increase after digestion, indicating no additional protein input from enzymes. In the spectra of all oleosome samples broad absorption bands were found in the amide I region centered around 1656 cm^{-1} (Figure 3, solid trace) and in the amide II region around 1550 cm^{-1} indicating protein content.

Second derivative analysis (data not shown) was employed to determine the exact band positions for the secondary structure analysis. The spectrum of native oleosomes exhibits a strong signal around 1656 cm^{-1}. The second derivative indicates that this signal might consist of two contributions, one at 1657 cm^{-1} and one at 1653 cm^{-1}. In D_2O (data not shown) the band at 1657 cm^{-1} remains whereas the band at 1653 cm^{-1} shifts to 1645 cm^{-1} as expected for unordered structures[31]. The band at 1657 cm^{-1} can be assigned to α-helical structures, accounting for 47 % of the total amide intensity, and the band at 1653 cm^{-1} to unordered structures (see Table 1). Shoulders on both sides of the main absorbance were found at 1624, 1634 and 1682 cm^{-1} which we attributed to β-sheet structures. These modes represent 31 % of the amide content, which is in line with findings of Lacey *et al*[16]. A further band that arises at 1673 cm^{-1} with a content of 5 % is expected to originate from β-turns.

To determine the structural content of the remaining parts after digestion we have analyzed the amide I bands in spectra of trypsin-digested oleosomes (Figure 3, dashed trace). In these experiments we used trypsin without lipolytic activity to avoid spectral confusion with lipid-based digestion products. When comparing the spectrum of the native oleosomes with digested oleosomes, it becomes apparent that the overall band shapes strongly differ, in agreement with previous observations by Lacey *et al.*[16]. In the second derivative spectrum the central absorbance around 1656 cm^{-1} no longer consists of two bands and is narrower, although weak shoulders on both sides of the central band are visible. This 1656 cm^{-1} band - which is assigned to α-helical structures - accounts for 73 % of the total amide intensity. There is no significant amount of random structures present in these samples. Contributions attributed to β-sheet structures are also less pronounced (27 % of the total amide intensity). The predominance of α-helical structures after protease treatment has been observed before and shows the hydrophobic oil soluble oleosin

domains have significantly more of an α-helix than a β-sheet structure. The cleaved hydrophilic protein fraction - which has been removed from the emulsion after protease treatment by centrifugation - consequently seems to be dominated by random coils and β-sheets.

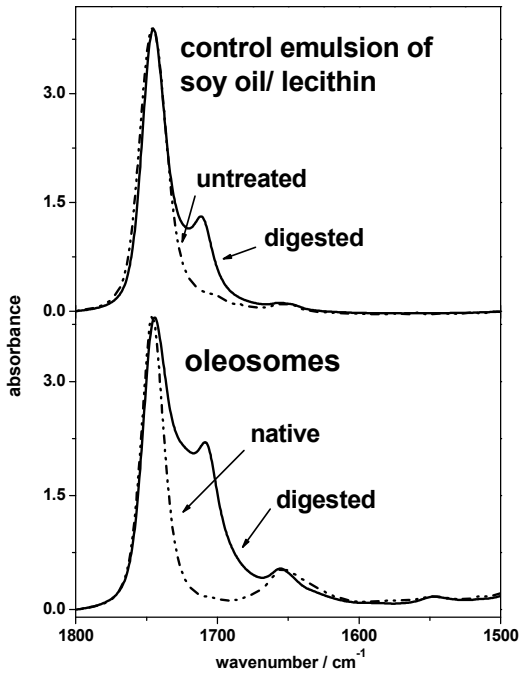

Fig. 2 Absorbance spectra of native (lower dashed trace) and trypsin-digested (containing lipases) soybean oleosomes (lower solid trace) compared to absorbance spectra of untreated (upper dashed trace) and trypsin treated soy oil lecithin emulsions (upper solid trace).

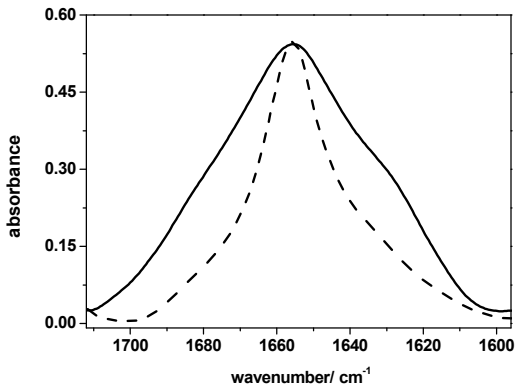

Fig. 3 Absorbance spectra in the amide I region of native (solid trace) and trypsin-digested (low lipase activity) soybean oleosomes (dashed trace).

Table 1 Parameters resulting from band fit of FTIR spectra in the amide I region for native and digested soybean oleosomes (A) shown in Figure 2 and 3 and tentative assignment of fitted bands to secondary structures according to literature[16, 22, 23]. In comparison: parameters reported in Lacey *et al.*[16] which have been obtained from FTIR spectra of native and protease digested safflower (B) and sunflower oleosins (C). Below (dashed line) assignment of bands to carbonyl stretching modes of lipid content is reported

A. Soybean				**B. Safflower**		**C. Sunflower**	
Band / cm^{-1}	FWHM/ cm^{-1}	Area / %	Tentative assignment	Band / cm^{-1}	Area / %	Band / cm^{-1}	Area / %
Native							
1624	18	6	Intermolecular β-sheet	1618	9	1621	6
1634	24	13	Antip. β-sheet / β-sheet	1628 / 1641	5 / 26	1628 /1639	4 / 22
1653	30	17	random coil				
1657	34	47	α-helix	1657	50	1654	33
1673	31	5	β-turns	1671	6	1668	23
1682	26	12	β-sheet	1682	3	1678	2
-	-	-	β-sheet /β-turns	1690	1	1687	10
1746	-	-	carbonyl stretch of ester	-	-	-	-
Digested							
-	-	-	-	1618	6	1617	7
1633	25	21	Antip. β-sheet / β-sheet	1629 / 1641	5 / 20	1632 / 1640	13 / 8
1656	22	73	α-helix	1656	60	1655	59
			β-turns	1670	5	1667	11
1680	14	6	β-sheet	1680	4	1681	2
1714	-	-	carbonyl stretch of carboxyl group	-	-	-	-
1746	-	-	carbonyl stretch of ester	-	-	-	-

Droplet Size Analysis and Zeta-potential

For the incorporation of oleosomes into food matrices, cosmetic formulations and drugs, the optimal conditions for their stability should be known. Conditions during processing, storage,

consumption, and digestion can have an impact on the physical and chemical stability of oleosomes. To evaluate such factors, interactions and stability of colloidal droplets can be determined by measuring the droplet size (Sauter mean diameter d_{32} (μm)), cumulative volume distribution Q_3 (vol (%)) and the zeta-potential ζ (mV). Reflecting the colloidal structure of oleosomes, oleosomes are micellar spherical droplets with a lipid core that is surrounded by a monolayer of PL and completely covered by the umbrella-like oleosins. Due to the different side chains of the amino acids located at the oleosome surface, the net surface charge distribution depends on the type and concentration of ions present in solution.[32]

Droplet size measurements in a pH range of 2 to 4.3 and 5.7 to 8 revealed that oleosome droplets are relatively small (70 vol % of droplets with $d < 0.3$ μm) (Figure 4A and B). However, at their isoelectric point (pI ≈ 5.3) 90 vol % of oleosomes form aggregates larger than 5 μm. At pH values not very far from the pI, the mean droplet size of 0.3 μm (pH 4.5 and 5.7) is only slightly higher than for oleosomes ($d_{32} = 0.2 \pm 0.2$ μm) at low (pH 2 – 4) or high (6 – 8) pH values (Fig. 4A). Although the effect of the pH on the mean droplet size is marginal, 40 vol % of colloidal oleosomes are larger than 0.3 μm at pH 4.56, which is also the case for 30 vol % at pH 4 and 20 vol % at pH 5.7 (Figure 4B) revealing a higher tendency to aggregate for pH values close to the pI. In general, the further away the pH is from the pI the more the oleosomes repel each other. Close to the pI, the remaining Coulombic (electrostatic) repulsion is not sufficiently strong to overcome attraction interactions (*e.g.,* hydrophobic and van der Waals) and aggregation occurs.

In contrast to similar studies reported in the literature[33] that revealed formation of larger aggregates in a broad pH range of 3 to 6, in our case the pH range in which the oleosomes are unstable is relatively narrow (pH 4.7 ($d_{32} = 2.0$ μm) to pH 5.5 ($d_{32} = 6.5$ μm)) (Figure 4A). This

discrepancy might result from different purification procedures during the aqueous extraction process. The centrifugation of oleosomes at pH 11 provided a better separation from residual storage proteins. Creaming stability tests of oleosomes containing some remaining residues of storage proteins showed a pronounced shift of the pI to around pH 4 and a significantly broader pH range within which the oleosomes aggregate.[9, 33]

The digestion of the oleosomes causes a loss of structural integrity that result in a different droplet size distribution that is affected by pH differently than it is for intact oleosomes.

In the pH range of 4.2 to 8, the average mean droplet size is with < 0.3 µm comparable to the average droplet size of native oleosomes in the high acidic (pH 2 – 4) and high alkaline (pH 5.7 – 8) region. However, the volume distribution is, in contrast to intact oleosomes, relatively inhomogeneous, as 20 (pH 5.3) to 40 vol % (pH 4) of the droplets are significantly larger than 5 µm (Figure 4C). In the very acidic region (pH 2 and 3), droplets of digested oleosomes form aggregates of average size of 3.0 µm (Figure 4A) and almost 50 % of those are larger than 5.0 µm (Figure 4C).

With regard to the multicomponent mixture of protein fragments and lipids (TAGs, PLs, FFA, MG, and DG) in the dispersion after the digestion, it is difficult to evaluate the effects contributing to the increase in droplet size in the acidic region and the broadening of the droplet size distribution. The shift in the highest peak of the mean droplet size in dependence of the pH (Figure 4A) is probably caused by the cleavage of the hydrophilic and charged protein parts from the oleosome surface. The cleavage of the proteins alters the electrical charge distribution of the oleosome surfaces, which is predominately based on the different zwitterionic properties of the polar head groups of the PL and FFA. Zeta-potential measurements provided in the following as well as observations during creaming stability tests indicate that oleosomes with PL monolayers

coalesce but protein-covered oleosomes form flocculates at critical pH values. Besides the change of the electrical layer of the oleosomes, the cleavage of proteins also removes the steric barrier against destabilization.

To better understand the destabilizing phenomenon, the zeta-potential was analyzed to quantify the electric double layer of the intact and digested oleosomes relevant for the evaluation of colloidal interaction and colloidal stabilization. The zeta-potential for native oleosomes changes from +32 ± 1.2 mV at pH 2 to -24 ± 1.6 mV at pH 8 intersecting the zero line at pH 5 which is consistent with the pI of the oleosin (Figure 5). This typical behavior for proteins adsorbed at oil droplets[34] indicates that oleosins remain at the oleosome surface despite the relatively harsh conditions during the extraction and purification procedure.

A different behavior is observed for digested oleosomes. The zeta-potential in the acidic region is almost the same as for intact oleosomes (+30 mV) but becomes 0 mV at pH 3.2 and shifts to more negative values (-75 ± 3.3 mV at pH 8) in the alkaline region. This pH dependency of the zeta-potential is consistent with that of so-called parental emulsions stabilized with PLs and FFAs[35], here particularly driven by phosphatidylcholine, the most occurring phospholipid in oleosomes[36]. The higher magnitude of negatively charged phosphate head groups of PLs, *i.e.,*phosphatidylethanolamine[37] and phosphatidylserine, in the alkaline region might attribute to the more negative values, but, as shown in the droplet size distribution (Figure 4C), the higher negative charges seem not to be sufficient to overcome attraction forces and coalescence might have occurred. Although native oleosomes are stable already from a zeta potential of approximately 15 mV on, it has to be taken into account that they are additionally sterically stabilized by the native oleosins on their interface. On the other hand, for digested oleosomes, even a low probability to approach each other as expected for intermediate zeta-potentials might

lead to coalescence due to the lower stability of their interface. Only at high zeta-potentials (-75 mV at pH 8) the probability for collisions is sufficiently reduced to stabilize the droplets. In order to investigate further the relation between zeta-potential and coalescence in the digested oleosomes system, comparative measurements with PL stabilized emulsions exhibiting similar sizes and droplet volume fractions are planned.

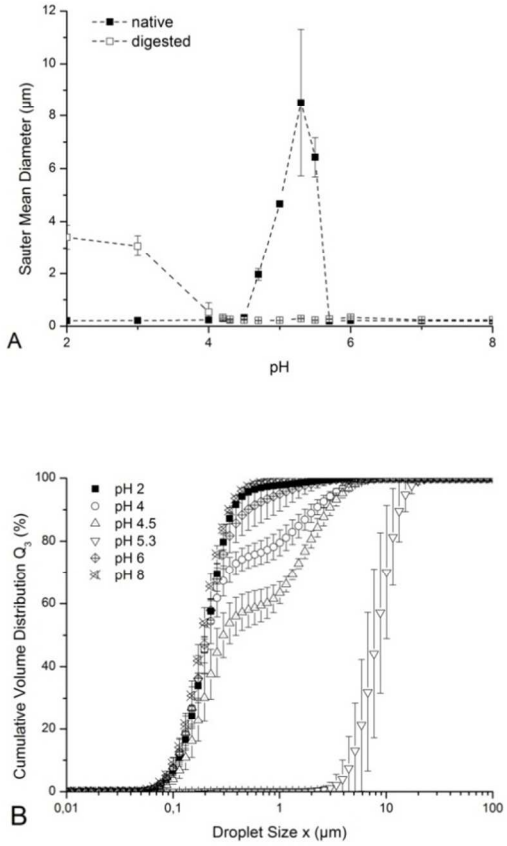

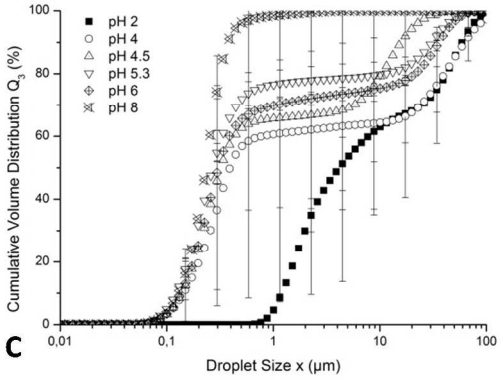

Fig. 4 Sauter mean diameter (µm) of native and trypsin-digested oleosomes in dependence of the pH (A). Cumulative volume distribution Q_3 (%) plotted against the droplet size (µm) of native (B) and digested oleosomes (C) (with representative arrow bars).

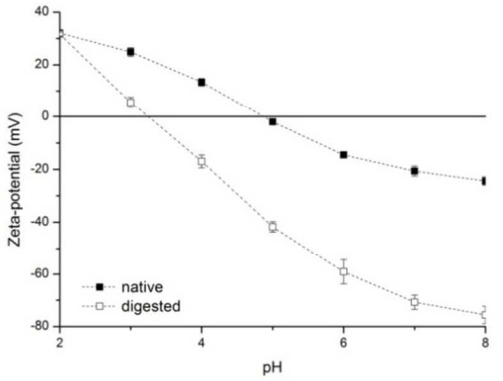

Fig. 5 Zeta-potential (mV) of native and digested oleosomes measured in dependence of pH.

SFG-Spectroscopy

Sum frequency generation spectroscopy was employed to probe the secondary structure of native and digested oleosomes at the air-water interface, after rupture of the vesicles at the interface. Figure 6 shows spectra of the amide I region. The spectrum of native oleosomes after rupture exhibits a distinct strong band at 1747 cm^{-1} and a weaker band at 1664 cm^{-1} (Figure 6 upper trace). The strong 1747 cm^{-1} band is also present in the FTIR spectra hence we assigned it

to the carbonyl stretch mode of TAG (Table 2). The band at 1664 cm^{-1} can be attributed to amide I protein modes. Referring to previous reports of amide I band assignments we tentatively assigned this signal to β-turns and/or symmetric stretch of parallel β-sheet structures.[38, 39] The α-helical oleosin segments are not visible in the spectra. The absence of helical structure in the spectra can be explained by two scenarios: (i) The α-helical structures are not present at the interface or (ii) the net SFG signal is cancelled out because of anti-parallel α-helical orientations. SFG is a coherent technique and signals from groups having opposite orientations are not detected in the far field. Since the presence of both α-helices and β-sheets is evident from the FTIR analysis and because of the consistent interpretation of the hydrophobic part as an antiparallel α-helix structure in the literature, we conclude that the latter possibility is far more likely here.

For digested oleosomes the amide I band is completely absent (Figure 6, lower trace). This observation is in line with our results obtained from FTIR spectroscopy. The protein fractions facing the water have been cleaved by proteases. We cannot make a statement about whether the hydrophobic antiparallel domains (antiparallel α-helices) aggregate or dissolve in lipid domains at the air-water interface.[19] Furthermore, a small but distinct shift of the carbonyl stretching mode related to the TAG esters is observed. Analysis of this signal by means of the Maximum Entropy Method (MEM) exhibited two signals with opposite phase, *i.e.,* opposite orientations. By this means we can identify two bands, the remaining band at 1747 and an additional one at 1719 cm^{-1}. We tentatively assign the additional signal to the carbonyl stretching mode of FFA obtained after cleavage of the TAGs by lipase. This result is again in agreement with the observation made using FTIR spectroscopy. Deviating from the results obtained from FTIR spectroscopy the signal of this band in the SFG spectra seems to be much stronger than the signal

from residual intact TAG, which decreases significantly whereas this band in FTIR spectra remains strong. There seems to be a difference in composition after spreading of oleosomes constituents after their rupture at the air-water interface compared to the bulk emulsion. This can be explained by the higher surface concentration of FFA (due to TAG hydrolysis) and PL (due to digestion of binding sites to oleosins), which are both forming monolayers and domains at the air-water interface, visible with Brewster angle microscopy[7].

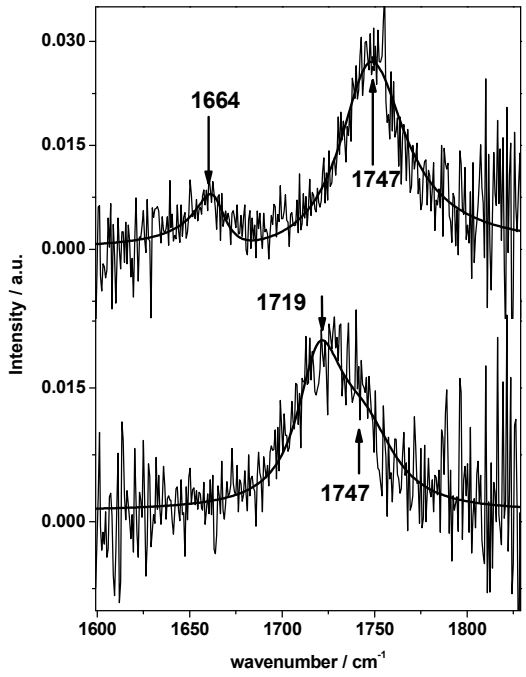

Fig. 6. SFG spectra measured under ppp polarization conditions and band fit of native (upper trace) and digested soybean oleosomes (lower trace) 1200 s after injection of oleosomes. Conditions: 6.4 mg/l oleosomes in 5 mM phosphate buffer, pH 7.

Table 2 Parameters resulting from band fit of SFG spectra for native and digested soy oleosomes under ppp polarization conditions (Figure 6). Asterisks assign the parameters which were fixed during the fitting procedure (A_{NR} – amplitude of non-resonant signal, Φ_{NP} – phase of non-

resonant signal, ω_n – frequency of resonant signal, Γ_n – FWHM of resonant signal, A_n – amplitude of resonant signal)

	A_{NR}	Φ_{NP}	ω_n/cm^{-1}	Γ_n / cm^{-1}	A_n / a.u.	Tentative assignment
native	-0.01	2.80	1663.84	26.66	0.84	ß-sheet structures
			1746.70	42.93	3.44	carbonyl stretch of ester
digested	0.03	*2.80	1719.23	34.74	3.44	carbonyl stretch of carboxyl group
			*1746.70	*42.93	-3.08	carbonyl stretch of ester

Interfacial Behavior

The interfacial behavior of intact and digested oleosomes was investigated by axisymmetric drop shape analysis (ADSA). In previous studies[7, 19] we investigated the adsorption mechanisms and behavior of oleosomes at the interface by using a film balance but the analysis by ADSA additionally allows us to detect very fast diffusion processes at the beginning of the kinetics under relatively stable measurement conditions. Here, the diffusion of oleosomes to the air-water interface is passive while buoyancy forces have been the driving forces in the case of film balance measurements. Together with the information from molecular spectroscopy at the air-water interface (SFG) representative kinetics of intact and digested oleosomes (78 mg/l, pH 2) recorded with ADSA (Figure 7) are discussed.

As soon as sufficient oleosomes have diffused from the bulk phase to the lower interphase, rupture of oleosomes and release of their components occur and the surface pressure steeply increases. The lag-time, the sharp increase and then the kink in the surface pressure development can be explained by typical PL monolayer behavior[40], comparable to a Langmuir (trough) isotherm. During the lag-time oleosomes burst at the air-water interface and release parts of their PL (native oleosomes) and PL and FFA (digested oleosomes), which spread on the surface of the droplet in a gaseous phase going step by step in a coexistence with liquid expanded phase. When more oleosomes diffuse to the surface and/or are disrupted the initial free surface is diminished

(decreasing the area per molecule) and the monolayer of PL and FFA proceed into the liquid expanded phase (sharp increase). The leveling-off of the surface pressure after the kink indicates a depletion of oleosomes in the bulk phase as all oleosomes have diffused to the interface. For the intact oleosomes, where great amounts of oleosin-lipid conjugates[19] fill in the surface, after the kink the free PL can be considered to be in the condensed + liquid expanded phase coexistence[40]. For the digested oleosomes the final surface pressure (28.5 mN/m) is considerably higher than for native ones (13.3 mN/m), which is induced by the enzymatic cutting-off of oleosin-PL-binding sites leading to the release of more free PL and FFA after rupture, but with a dominating influence of the PL on the surface pressure[41]. However, FFAs are detected in SFG spectra (Figure 6), which were recorded 20 min after the injection of oleosomes. Additionally there are indications in literature[42] that adsorption of special proteins (with an affinity to PL-monolayers) can change PL head and tail interactions, leading to less tilted aliphatic chains in the condensed phase and increasing the lipid packing efficiency.

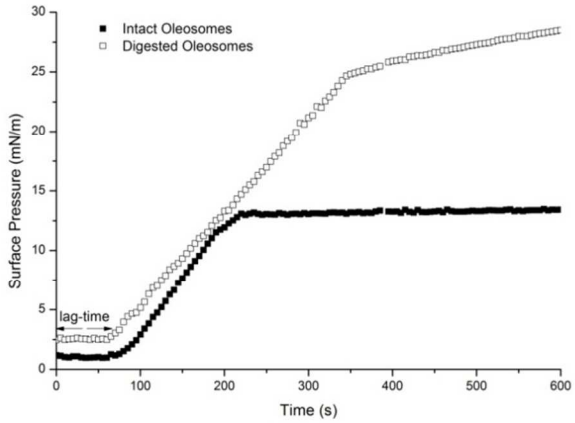

Fig. 7 Surface pressure (mN/m) of 78 mg/l of intact and digested oleosomes diluted in a buffer solution of pH 2.

Rheology of Emulsions

The macroscopic emulsifying properties and their molecular origin (also of interest with regard to a possible use of whole oleosomes as emulsifiers in food) were probed by preparing emulsions from native (emulsion N) and digested oleosomes (emulsion D) and measuring their shear rate dependent viscosities. The molecular changes of the enzymatic digestion on the surface of the oleosomes determine the interactions between them and are apparent in macroscopic properties, such as the rheological behavior. Emulsion N as well as D show a shear thinning behavior (Figure 8A). However, the viscosity of emulsion N is about three orders of magnitude higher than that of emulsion D. A plot of shear stress versus shear rate for increasing and decreasing shear rates shows almost no hysteresis (Figure 8B), meaning that no substantial irreversible structural breakdown occurred for higher shear rates [43]. On the other hand emulsion N has a yield stress of about 10 Pa, whereas emulsion D does not exhibit any yield stress.

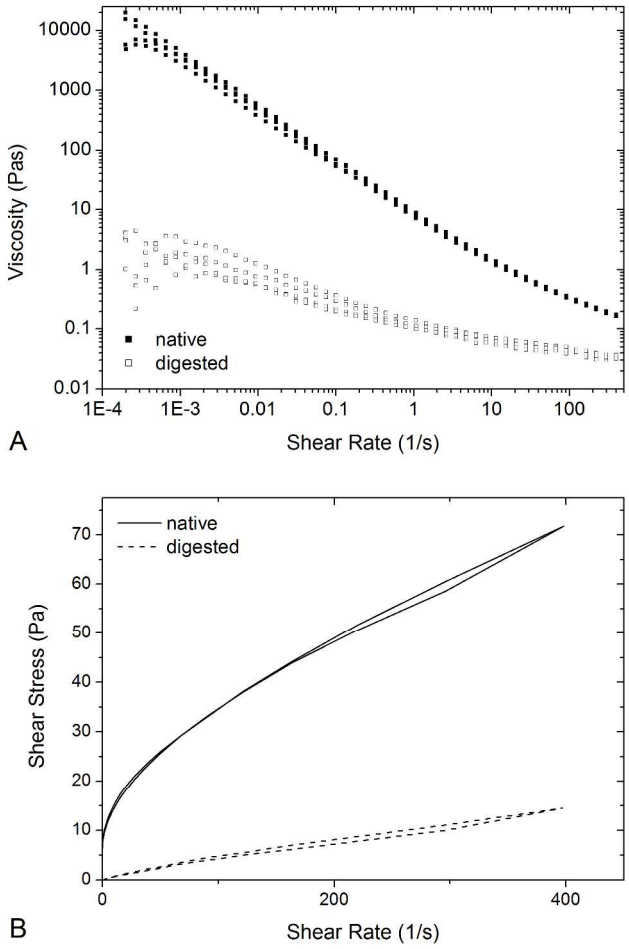

Fig. 8 Viscosity (A) and shear stress (B) versus shear rate for emulsions prepared from native and digested oleosomes. 50 g soybean oil was added in small portions to 25 ml of a 23.3 % soybean oleosome in 5 mM Tris/NaCl (I = 5 mM) pH 8 buffer and homogenized with an ultra turrax (15.600 rpm, 4 min).

The viscosity of an emulsion strongly depends on the volume fraction of the dispersed phase and for concentrated emulsions ($\phi > 0.6$) on the droplet size[44] - with larger droplets leading to lower viscosities - and their size distribution[45]. The oil volume fraction here is 0.75 in both cases (estimated using a density of 0.93 kg/l for soybean oil and assuming the volumes of the oleosomes to be made up almost exclusively of oil), therefore a difference in droplet sizes would be expected to have an influence on the viscosity. Laser diffraction measurements (Figures 9)

indeed show a different droplet size distribution of emulsions N and D. In general, droplets of emulsion D are larger than of emulsion N, with Sauter mean diameters of 35.9 ± 0.1 µm and 14.0 ± 0.1, respectively.

Additionally, the cumulative volume distribution of emulsion D is bimodal, as a volume fraction of approx. 2 % of the droplets is smaller than 2.5 µm, while all droplets of emulsion N are larger than 3 µm.

The resulting drop size of an emulsion is determined by the equilibrium between drop breakage and drop-drop coalescence[46]. Roughly speaking, drop breakage is determined by the ratio of shear forces occurring during emulsification to the Laplace pressure ($2\sigma/R$) of the droplets. The shear forces having an impact on the droplet breakup are equal for the two emulsions compared here due to the identical emulsification process. However, the surface tension can be lowered more by the components present in digested oleosomes (Figure 7) leading to a lower Laplace pressure, therefore a smaller droplet size could be expected for emulsions from digested oleosomes. On the other hand, the stability against coalescence is expected to be lower for emulsion D, due to the more fluid interfacial layer and missing steric stabilizing effects from native oleosins, thus leading to larger droplets.

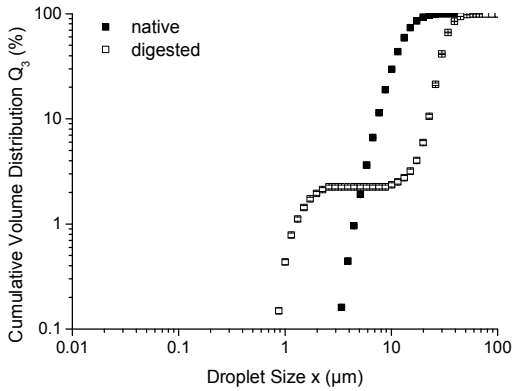

Fig. 9 Cumulative volume distribution of emulsions prepared from native and digested oleosomes.

The droplet size distribution suggests a lower stability against coalescence for droplets between 2 and 10 µm for emulsion D.

At high volume fractions of the dispersed phase as used here, the droplets get deformed by contact with their neighbors[43], leading to a strong increase in the elastic modulus of emulsions[47]. This deformation occurs above a critical volume fraction, which is larger for droplets with an uniform size distribution than for those with a broader one, as for the latter the smallest droplets can fit in between the larger ones[45]. This leads to a reduction in viscosity for more polydisperse emulsions[48] at the same volume fraction.

Yield stress occurs if the droplets are so densely packed that they have to deform first before they can move past each other. The force needed for deforming the droplets therefore depends on the volume fraction and size distribution of the droplets (how much they are deformed by their neighbors) as well as on the deformability of the droplet itself. The different droplet size distributions of the two different emulsions could already explain a higher yield stress for emulsion N. But additionally, for the latter also a stronger elastic layer at the interface is expected due to the presence of proteins which can interact with each other. On the other hand, the FFAs and PLs present in emulsions from digested oleosomes are not able to interact and lead to easily deformable droplets.

Further investigations of droplet size distribution as well as stress and strain dependent rheological investigations of emulsions at different pH and emulsifier concentration are planned to further elucidate the underlying mechanisms of oleosomes' emulsifying capacities.

CONCLUSIONS

SFG measurements were performed to obtain information of the surface composition and the secondary structure of oleosins after rupture of native and digested oleosomes at the air-water interface. For the interpretation of bands these spectra have been complemented with FTIR spectra. Since SFG cannot be applied to interfaces in emulsions we approached this problem as in previous studies[7, 19] in which the behavior of soybean oleosomes at the air-water interface was investigated. As observed in FTIR spectra, SFG spectra of native oleosomes spread on the water surface yield a characteristic band generated by carbonyl stretch modes of esters (PLs amd TAGs). An additional band in the amide I region indicated protein secondary structures, most likely β-sheets and/or –turns. SFG spectra of the interfacial layer derived from digested oleosomes do not contain any amide I bands. This is due to the loss of non-parallel secondary structure elements during digestion which is in line with our findings based on FTIR spectroscopy. Contrary to the FTIR spectra, the SFG spectra do not exhibit any bands in the frequency region expected for α-helical structures, neither for native nor for protease treated samples. This is most probably due to the fact that the hydrophobic α-helical part is folded in an antiparallel manner to which the SFG spectroscopy is blind. However, we cannot exclude that the hydrophobic protein parts diffuse apart from the interface which would also result in the lack of signals. The composition of the interfacial layer after digestion is dominated by PLs and FFAs as well as acylglycerides which are products of the lipase digestion.

These findings are new and show explicitly how the surface of oleosomes is affected by trypsin and lipase digestion which is not accessible with common methods such as CD and FTIR spectroscopy.

Time dependent surface pressure measurements provide a lag-time with constant surface pressure followed by a strong increase and finally levels off. This process is most likely determined by the rupturing kinetics of oleosomes at the interface as well as phase transitions occurring in the interfacial layer of the droplet. PL phase transitions leading to regions with different rates of increase of surface pressure are likely to occur, if more and more oleosomes release their surface active components which spread out on the interface. The plateau in the surface tension curve may also be related to the depletion of oleosomes in the bulk phase. The behavior of whole oleosomes at the air-water interface should be compared to studies performed with purified oleosins[49, 50], which however have to face the problem of insolubility of the oleosins and aggregation of those in water.

Oleosin degradation decreases the stabilization of oleosome emulsions which is reflected by the increasing distribution of the oleosome size, decreasing elasticity of the droplets interfacial layer and changing interaction between droplets. As a consequence of digestion which obviously comes along with changes in the molecular content and structure of the oleosome surface, the zeta-potential and aggregation behavior of oleosomes change as the steric stabilization by the oleosin disappears and coalescence of the oil droplet is likely to occur.

This study could further prove the expected role of intact oleosin on the stabilization of oleosomes. Moreover it points out the drastic changes in the physical character of oleosomes when the hydrophilic terminals are cleaved by means of tryptic digestion. This correlation is of course essential when lipids need to be accessed and consumed in plants during seed germination or in the mammalian gastro-intestinal digestion. With regard to oil refinery of edible oils, enzyme assisted-aqueous extraction, which is ecological and environmental more friendly and

healthier than the common solvent extraction, can achieve higher oil yields when extracting oil from isolated oleosomes[51].

It is conceivable to make use of stabilizing proteins, such as oleosins or modified oleosin-derivatives on the basis of the described mechanism in order to stabilize drug or bioactive ingredient containing emulsions, while accessibility, depending on where the according proteolysis occurs, is maintained. With particular respect to biodegradability, which is a general issue when dealing with emulsions used for biomedical, biotechnological and food applications, it seems even more obvious to exploit the nature of these proteins. Similar as it is the case for membrane proteins, a suitable solubilization and reconstitution remains to be developed. The present study might inspire and provide useful information towards this possible development.

ACKNOWLEDGMENTS

We thank Michael Schleeger and Ellen Backus for fruitful discussions regarding IR and SFG spectra interpretation. Additionally, many thanks are given to Prof. Dr. Ing. Heike Schuchmann and Philipp Stähle from the Karlsruher Institute for Technology (KIT, Germany) where we could use the Horiba LA-950 for the droplet size measurements, as well as to Prof. Dr. Stephan Drusch and Frederic Tamm from the Technical University of Berlin who provided the pendant drop tensiometer.

REFERENCES

1. Huang, A. H. C., Oil Bodies and Oleosins in Seeds. *Annu. Rev. Plant Biol.* **1992,** 43, 177-200.
2. Li, M.; Smith, L. J.; Clark, D. C.; Wilson, R.; Murphy, D. J., Secondary structures of a new class of lipid body proteins from oilseeds. *J. Biol. Chem.* **1992,** 267, (12), 8245-53.
3. Tzen, J. T. C.; Huang, A. H. C., Surface-Structure and Properties of Plant Seed Oil Bodies. *J.Cell Biol.* **1992,** 117, (2), 327-335.
4. Alexander, L. G.; Sessions, R. B.; Clarke, A. R.; Tatham, A. S.; Shewry, P. R.; Napier, J. A., Characterization and modelling of the hydrophobic domain of a sunflower oleosin. *Planta* **2002,** 214, (4), 546-551.

5. Purkrtova, Z.; Jolivet, P.; Miquel, M.; Chardot, T., Structure and function of seed lipid body-associated proteins. *C. R. Biol.* **2008,** 331, (10), 746-754.
6. Vargo, K. B.; Parthasarathy, R.; Hammer, D. A., Self-assembly of tunable protein suprastructures from recombinant oleosin. *Proc. Natl. Acad. Sci.* **2012,** 109, (29), 11657-11662.
7. Waschatko, G.; Junghans, A.; Vilgis, T. A., Soy milk oleosome behaviour at the air-water interface. *Faraday Disc.* **2012,** 158, 157-169.
8. Bhatla, S. C., Kaushik, C., Yadav, M. K., Use of oil bodies and oleosins in recombination protein production and other biotechnological applications. *Biotechnol. Adv.* **2010,** 29, 293-300.
9. Chen, Y., Ono, T., Simple extraction method of non-allergenic intact soybean oil bodies that thermally stable in an aqueous medium. *J. Agric. Food Chem.* **2010,** 58, 7402-7407.
10. Beisson, F.; Ferté, N.; Bruley, S.; Voultoury, R.; Verger, R.; Arondel, V., Oil-bodies as substrates for lipolytic enzymes. *Biochim. Biophys. Acta (BBA) - Mol. Cell Biol. Lip.* **2001,** 1531, (1–2), 47-58.
11. Allen, D. K.; Tao, B. Y., Kinetic characterization of enhanced lipase activity on oil bodies. *Bioprocess Biosys. Eng.* **2007,** 30, (4), 271-279.
12. Day, J. P. R.; Rago, G.; Domke, K. F.; Velikov, K. P.; Bonn, M., Label-Free Imaging of Lipophilic Bioactive Molecules during Lipid Digestion by Multiplex Coherent Anti-Stokes Raman Scattering Microspectroscopy. *J. Am. Chem. Soc.* **2010,** 132, (24), 8433-8439.
13. Murphy, D. J.; Keen, J. N.; Osullivan, J. N.; Au, D. M. Y.; Edwards, E. W.; Jackson, P. J.; Cummins, I.; Gibbons, T.; Shaw, C. H.; Ryan, A. J., A Class of Amphipathic Proteins Associated with Lipid Storage Bodies in Plants - Possible Similarities with Animal Serum Apolipoproteins. *Biochim Biophys Acta* **1991,** 1088, (1), 86-94.
14. Jacks, T.; Hensarling, T.; Neucere, J.; Yatsu, L.; Barker, R., Isolation and physicochemical characterization of the half-unit membranes of oilseed lipid bodies. *J. Am. Oil Chem. Soc.* **1990,** 67, (6), 353-361.
15. Li, M.; Keddie, J. S.; Smith, L. J.; Clark, D. C.; Murphy, D. J., Expression and characterization of the N-terminal domain of an oleosin protein from sunflower. *J. Biol. Chem.* **1993,** 268, (23), 17504-12.
16. Lacey, D. J.; Wellner, N.; Beaudoin, F.; Napier, J. A.; Shewry, P. R., Secondary structure of oleosins in oil bodies isolated from seeds of safflower (Carthamus tinctorius L.) and sunflower (Helianthus annuus L.). *Biochem. J.* **1998,** 334, 469-477.
17. Millchip, M., Tatham, A. S., Jackson, F., Griffiths, G., Shewry, P. R., Stobart, A. K., Purifiaction and charaterization of oil bodies (oleosomes) and oil-body boundary proteins (oleosins) from the developing cotyledons of sunflower (Helianthus annus L.). *Biochem. J.* **1996,** 314, 333-337.
18. Gohon, Y.; Vindigni, J. D.; Pallier, A.; Wien, F.; Celia, H.; Giuliani, A.; Tribet, C.; Chardot, T.; Briozzo, P., High water solubility and fold in amphipols of proteins with large hydrophobic regions: Oleosins and caleosin from seed lipid bodies. *Biochim. Biophys. Acta-Biomembr.* **2011,** 1808, (3), 706-716.
19. Waschatko, G.; Schiedt, B.; Vilgis, T. A.; Junghans, A., Soybean Oleosomes Behavior at the Air-Water Interface. *J. Phys. Chem. B* **2012,** 116, (35), 10832-10841.
20. Arrondo, J. L. R.; Goñi, F. M., Structure and dynamics of membrane proteins as studied by infrared spectroscopy. *Progress Biophys. Mol. Biol.* **1999,** 72, (4), 367-405.
21. Marquardt, D. W., An Algorithm for Least-Squares Estimation of Nonlinear Parameters. *J. Soc. Ind. Appl. Math.* **1963,** 11, (2), 431-441.

22. Byler, D. M.; Susi, H., Examination of the Secondary Structure of Proteins by Deconvolved Ftir Spectra. *Biopolymers* **1986,** 25, (3), 469-487.
23. Susi, H.; Byler, D. M., Resolution-enhanced Fourier transform infrared spectroscopy of enzymes. *Methods in Enzymol.* **1986,** 130, 290-311.
24. Sovago, M.; Vartiainen, E.; Bonn, M., Determining Absolute Molecular Orientation at Interfaces: A Phase Retrieval Approach for Sum Frequency Generation Spectroscopy. *J. Phys. Chem. C* **2009,** 113, (15), 6100-6106.
25. Zeleny, L., Neustadt, M. H. , Rapid determination of soybean-oil content and of iodine number of soybean oil. In Agriculture, D. o., Ed. U.S. Departement of Agriculture: 1940; Vol. 748, p 23.
26. McMeekin Thomas, L.; Groves Merton, L.; Hipp Norbert, J., Refractive Indices of Amino Acids, Proteins, and Related Substances. In *Amino Acids and Serum Proteins*, AMERICAN CHEMICAL SOCIETY: 1964; Vol. 44, pp 54-66.
27. Attard, P.; Antelmi, D.; Larson, I., Comparison of the Zeta Potential with the Diffuse Layer Potential from Charge Titration. *Langmuir* **2000,** 16, (4), 1542-1552.
28. Cheng, P.; Li, D.; Boruvka, L.; Rotenberg, Y.; Neumann, A. W., Automation of axisymmetric drop shape analysis for measurements of interfacial tensions and contact angles. *Colloids Surf.* **1990,** 43, (2), 151-167.
29. Samoto, M.; Maebuchi, M.; Miyazaki, C.; Kugitani, H.; Kohno, M.; Hirotsuka, M.; Kito, M., Abundant proteins associated with lecithin in soy protein isolate. *Food Chem.* **2007,** 102, (1), 317-322.
30. Vinarov, Z.; Petkova, Y.; Tcholakova, S.; Denkov, N.; Stoyanov, S.; Pelan, E.; Lips, A., Effects of Emulsifier Charge and Concentration on Pancreatic Lipolysis. 1. In the Absence of Bile Salts. *Langmuir* **2012,** 28, (21), 8127-8139.
31. Haris, P. I.; Severcan, F., FTIR spectroscopic characterization of protein structure in aqueous and non-aqueous media. *J. Mol. Catal. B: Enzym.***1999,** 7, 207-221.
32. Nylander, T.; Arnebrant, T.; Bos, M.; Wilde, P., Protein/Emulsifier Interactions

In *Food Emul. Appl.*, Hasenhuettl, G. L.; Hartel, R. W., Eds. Springer New York: 2008; pp 89-171.
33. Iwanaga, D.; Gray, D. A.; Fisk, I. D.; Decker, E. A.; Weiss, J.; McClements, D. J., Extraction and Characterization of Oil Bodies from Soy Beans: A Natural Source of Pre-Emulsified Soybean Oil. *J. Agric. Food Chem.* **2007,** 55, (21), 8711-8716.
34. Guzey, D.; Kim, H. J.; McClements, D. J., Factors influencing the production of o/w emulsions stabilized by β-lactoglobulin–pectin membranes. *Food Hydrocolloids* **2004,** 18, (6), 967-975.
35. Wabel, C., Influence of lecithin on structure and stability of parenteral fat emulsions. *PhD Thesis. Friedrich-Alexander-University, Erlangen-Nürnberg, Germany.* **1998**.
36. Garcia, J. M.; Quintero, L. C.; Mancha, M., Oil bodies and lipid synthesis in developing soybean seeds. *Phytochem.* **1988,** 27, (10), 3083-3087.
37. Petelska, A. D.; Figaszewski, Z. A., Interfacial tension of bilayer lipid membrane formed from phosphatidylethanolamine. *Biochim. Biophys. Acta - Biomembr.* **2002,** 1567, (SUPPL.), 79-86.
38. Fu, L.; Ma, G.; Yan, E. C. Y., In Situ Misfolding of Human Islet Amyloid Polypeptide at Interfaces Probed by Vibrational Sum Frequency Generation. *J. Am. Chem. Soc.* **2010,** 132, (15), 5405-5412.

39. Nguyen, K. T.; King, J. T.; Chen, Z., Orientation Determination of Interfacial β-Sheet Structures in Situ. *J. Phys. Chem. B* **2010,** 114, (25), 8291-8300.
40. Kaganer, V. M.; Möhwald, H.; Dutta, P., Structure and phase transitions in Langmuir monolayers. *Rev. Mod. Phys.* **1999,** 71, (3), 779-819.
41. Levy, M. Y.; Benita, S.; Baszkin, A., Interactions of a non-ionic surfactant with mixed phospholipid—oleic acid monolayers. Studies under dynamic conditions. *Colloids Surf.* **1991,** 59, (0), 225-241.
42. Dahmen-Levison, U.; Brezesinski, G.; Möhwald, H., Specific adsorption of PLA2 at monolayers. *Thin Solid Films* **1998,** 327–329, (0), 616-620.
43. Rosenthal, A. J., *Food texture : measur. percep.*. Aspen Publishers: Gaithersburg [Maryland], 1999.
44. Pal, R., Shear viscosity behavior of emulsions of two immiscible liquids. *J. Colloid Interf. Sci.* **2000,** 225, (2), 359-366.
45. Lacasse, M.-D.; Grest, G. S.; Levine, D.; Mason, T. G.; Weitz, D. A., Model for the Elasticity of Compressed Emulsions. *Phys. Rev. Lett.* **1996,** 76, (18), 3448-3451.
46. Tcholakova, S.; Denkov, N. D.; Danner, T., Role of Surfactant Type and Concentration for the Mean Drop Size during Emulsification in Turbulent Flow. *Langmuir* **2004,** 20, (18), 7444-7458.
47. Mason, T. G.; Bibette, J.; Weitz, D. A., Elasticity of Compressed Emulsions. *Phys. Rev. Lett.* **1995,** 75, (10), 2051-2054.
48. Mason, T. G.; Rai, P. K., Shear-induced elastification of concentrated emulsions probed by sinusoidal amplitude variation rheometry. *J. Rheol.* **2003,** 47, (2), 513-533.
49. Roux, É.; Baumberger, S.; Axelos, M. A. V.; Chardot, T., Oleosins of Arabidopsis thaliana: Expression in Escherichia coli, Purification, and Functional Properties. *J. Agri. Food Chem.* **2004,** 52, (16), 5245-5249.
50. Nikiforidis, C. V.; Ampatzidis, C.; Lalou, S.; Scholten, E.; Karapantsios, T. D.; Kiosseoglou, V., Purified oleosins at air-water interfaces. *Soft Matter* **2013**.
51. Towa, L.; Kapchie, V.; Hauck, C.; Murphy, P., Enzyme-Assisted Aqueous Extraction of Oil from Isolated Oleosomes of Soybean Flour. *J. Am. Oil Chem. Soc.* **2010,** 87, (3), 347-354.

TABLE OF CONTENT ONLY

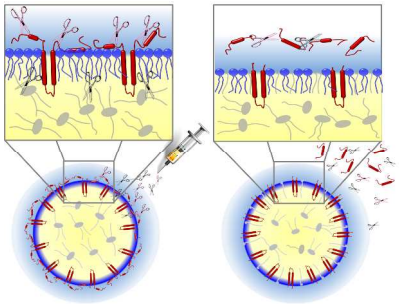

TOC: Depiction of enzymatic digestion of soybean oleosomes. Proteases cleave the oleosin-proteins and pancreatic lipases hydrolyse the TAGs at the oil-water interface of an oleosome